


 Cite this: *RSC Adv.*, 2020, **10**, 13316

## Super tough poly(lactic acid) blends: a comprehensive review

Xipo Zhao, \* Huan Hu, Xin Wang, Xiaolei Yu, Weiyi Zhou and Shaoxian Peng\*

Poly(lactic acid) or poly(lactide) (PLA) is a renewable, bio-based, and biodegradable aliphatic thermoplastic polyester that is considered a promising alternative to petrochemical-derived polymers in a wide range of commodity and engineering applications. However, PLA is inherently brittle, with less than 10% elongation at break and a relatively poor impact strength, which limit its use in some specific areas. Therefore, enhancing the toughness of PLA has been widely explored in academic and industrial fields over the last two decades. This work aims to summarize and organize the current development in super tough PLA fabricated via polymer blending. The miscibility and compatibility of PLA-based blends, and the methods and approaches for compatibilized PLA blends are briefly discussed. Recent advances in PLA modified with various polymers for improving the toughness of PLA are also summarized and elucidated systematically in this review. Various polymers used in toughening PLA are discussed and organized: elastomers, such as petroleum-based traditional polyurethanes (PUs), bio-based elastomers, and biodegradable polyester elastomers; glycidyl ester compatibilizers and their copolymers/elastomers, such as poly(ethylene-co-glycidyl methacrylate) (EGMA), poly(ethylene-*n*-butylene-acrylate-co-glycidyl methacrylate) (EBA-GMA); rubber; petroleum-based traditional plastics, such as PE and PP; and various biodegradable polymers, such as poly(butylene adipate-co-terephthalate) (PBAT), polycaprolactone (PCL), poly(butylene succinate) (PBS), and natural macromolecules, especially starch. The high tensile toughness and high impact strength of PLA-based blends are briefly outlined, while the super tough PLA-based blends with impact strength exceeding 50 kJ m<sup>-2</sup> are elucidated in detail. The toughening strategies and approaches of PLA based super tough blends are summarized and analyzed. The relationship of the properties of PLA-based blends and their morphological parameters, including particle size, interparticle distance, and phase morphologies, are presented.

 Received 25th February 2020  
 Accepted 21st March 2020

 DOI: 10.1039/d0ra01801e  
[rsc.li/rsc-advances](http://rsc.li/rsc-advances)

### 1. Introduction

Environment, economic, and safety challenges have prompted scientists and producers to partially substitute petrochemical-based polymers with biodegradable materials. The materials science community has been striving for decades to generate biodegradable plastics to substitute or complement conventional synthetic plastics exclusively based on petroleum feedstock.<sup>1-3</sup> Biodegradable polymers,<sup>4-6</sup> especially those derived from renewable resources, have been widely considered in solving environmental problems and resource crises associated with traditional petroleum-based polymers.

Poly(lactic acid) or poly(lactide) (PLA)<sup>7-11</sup> is a renewable, bio-based, and biodegradable aliphatic thermoplastic polyester that has been researched for its use in several applications over the last two decades. PLA can be considered a promising alternative to petrochemical-derived polymers in a wide range of commodity and engineering applications.<sup>7,8,12</sup> PLA is also one of

the most investigated sustainable polymers because of its numerous advantages, such as biodegradability, biocompatibility, compostability, good mechanical properties, and processability. PLA has broad application prospects in the fields of disposable products, such as food packaging, tableware, water cups, nurseries, and electronic product buffer packaging, to effectively prevent and alleviate environmental problems, such as “white pollution”, caused by currently available non-biodegradable petroleum-based plastics. Furthermore, PLA is a leading biomaterial for numerous applications in medicine.<sup>10</sup> Therefore, vigorously promoting the application of biodegradable materials represented by PLA is an important measure to achieve sustainable green development.

However, PLA is inherently brittle, with less than 10% elongation at break and relatively poor impact strength, thereby limiting its use in some specific areas.<sup>13</sup> Although its tensile strength and elastic modulus are comparable with those of poly(ethylene terephthalate) (PET) and polystyrene (PS), the poor toughness of PLA limits its use in wide industrial and medical applications that require plastic deformation at high stress levels.<sup>14,15</sup>

*Huber Provincial Key Laboratory of Green Materials for Light Industry, Collaborative Innovation Center of Green Light-weight Materials and Processing, Hubei University of Technology, Wuhan 430068, China. E-mail: xpzhao123@163.com; psxbb@126.com*



For decades, enhancing the toughness of PLA has extensively promoted in academic and industrial fields.<sup>16–19</sup> PLA should be enhanced to improve its performance and achieve balanced mechanical properties so that it becomes a suitable alternative to low-cost and flexible conventional petroleum-based polymers for a wide range of applications. Research efforts have been devoted to enhancing PLA. Various strategies and technologies, including modifying PLA with plasticizers, blending with other polymers, copolymerizing chemicals, and incorporating fillers, have been applied to toughen PLA.<sup>20</sup> In contrast to chemical copolymerization, polymer blending with a carefully selected component is an efficient and cost-effective method of improving the toughness of PLA.<sup>17–19</sup>

Polymer blending<sup>21,22</sup> is an economical and convenient strategy for developing new polymeric materials, combining the advantages of numerous existing polymers. The properties of the resulting polymer blends are also tunable by changing components and compositions of blend. Therefore, many flexible or elastic polymers have been blended with PLA to enhance its toughness. In early studies, flexible or elastic polymers are usually produced from petroleum resources, and they include non-biodegradable polymers, such as polyethylene (PE),<sup>23</sup> acrylonitrile–butadiene–styrene (ABS) copolymer,<sup>24,25</sup> polyurethanes (PU),<sup>26,27</sup> and poly(ethylene-*co*-glycidyl methacrylate) (EGMA),<sup>28,29</sup> and biodegradable polymers, such as polycaprolactone (PCL).<sup>30,31</sup> Considering that the use of petroleum-based species to toughen PLA partially compromises sustainability, increasing attention has been given to toughening PLA with renewable polymers. Some bio-based materials of natural rubber, bio-elastomers obtained from some plant oils and their derivatives, polyamide 11 (PA11),<sup>32,33</sup> and biodegradable materials, such as poly(butylene adipate-*co*-terephthalate) (PBAT),<sup>34–36</sup> poly(butylene succinate) (PBS),<sup>37,38</sup> starch,<sup>39</sup> and cellulose,<sup>40</sup> are extensively used to modify PLA without losing its sustainability. Blending PLA with a flexible or elastic polymer, which exhibits fine morphology and suitable compatibility of blends, can provide an alternative method to considerably improve its tensile toughness and impact toughness simultaneously.

Some of these polymers show high toughening efficiency, and super-tough PLA blends with an impact strength of higher than  $530 \text{ J m}^{-1}$  are achieved occasionally.<sup>41</sup> The resulting PLA blends with drastically improved impact strength are referred to as super toughened PLA. The term “super tough” is first proposed by Wu<sup>42,43</sup> for convenience to denote polymer blends with a notched impact strength of higher than 10 ft per lb or  $530 \text{ J m}^{-1}$  (energy lost per unit width, North American standard), which is approximately equal to  $53 \text{ kJ m}^{-2}$  (energy lost per unit cross-sectional area, European standard) depending on the dimension of a sample.

PLA-based polymer blends, especially those with a high toughness performance, have been developed quickly, and remarkable achievements have been attained. Over the last two decades, several papers have summarized various aspects of PLA materials, including compatibilization methods and strategies, phase behavior and phase morphologies, and relationship of structure–performances.<sup>44–55</sup> Hirt *et al.*<sup>17</sup> reported

various bulk and surface-modification strategies used to date and their basic principles, drawbacks, and achievements. Wang *et al.*<sup>47</sup> summarized the relationship between the crystalline structure and properties of PLA. Other studies have also outlined some strategies for manipulating crystallization toward high-performance PLA materials. Zeng *et al.*<sup>48</sup> systematically presented various strategies that compatibilized PLA blends with different polymers.

Langer *et al.*<sup>49</sup> elaborated the mechanical and physical properties that affect the stability, processability, immiscibility, and potential suitability of PLA and other polymers for specific applications. Other studies have discussed strategies regarding component and plasticizer blending, nucleation agent addition, and PLA modifications and nanoformulations. He *et al.*<sup>50</sup> presented recent advancements in the synthesis of PLA-based block/graft copolymers with complex architectures, such as star- and comb-shaped blocks and various PLA-grafted structures. A stereocomplexation strategy can be used with these copolymers to prepare a variety of new materials with novel chemical functionalities, bioactivities, and smart (responsive to external stimulus) properties. Zeng *et al.*<sup>52</sup> aimed to review the progress in toughening PLA with renewable polymers, including plant oils and their derivatives, natural rubber, bio-based aliphatic polyesters, microbial polyesters, and bio-elastomers. Hamad *et al.*<sup>53</sup> discussed the miscibility and compatibilization strategies of polymer blends and the preparations and characterization of PLA blends. Alias and Ismail *et al.*<sup>54</sup> provided general information regarding the progress in PLA toughening by an elastomer. Nofar *et al.*<sup>55</sup> reviewed the investigations related to PLA-based blends and compared the composition/processing–morphology–property relationships developed for various applications.

However, few of these articles have elaborated the efforts toward achieving PLA-based polymeric materials with super toughness. Comprehensive papers that exclusively report the progress in toughening PLA with super toughness are lacking. Therefore, research progress in super tough PLA materials should be recognized to show insights into PLA blends and to guide future investigations on the toughness and ductility modification of PLA.

Given that the preparation of super tough PLA and a series of significant outputs have been achieved over the last decade, detailed information about super tough PLA blends should be summarized and analyzed. Therefore, current developments in super tough PLA fabricated *via* polymer blending methods are described and summarized in the present review. Various polymers used in toughening PLA are discussed and organized systematically. The following materials have also been described: elastomers, such as petroleum-based traditional polyurethanes (PUs), bio-based elastomers, and biodegradable polyester elastomers; glycidyl ester compatibilizers and their copolymers/elastomers, such as poly(ethylene-*co*-glycidyl methacrylate) (EGMA), poly(ethylene-*n*-butylene-acrylate-*co*-glycidyl methacrylate) (EBA-GMA); rubber; petroleum-based traditional plastics, such as PE and PP; and various biodegradable polymers, such as PBS, PBAT, PCL, and natural macromolecules, especially starch. Toughening PLA to achieve



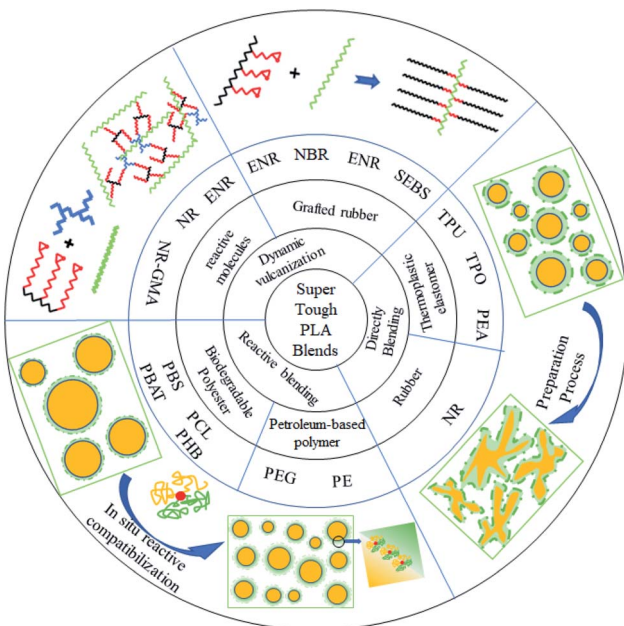


Fig. 1 The summarized approaches and toughening strategies for super tough PLA-based blends.

super tough blends is reviewed. Properties such as high toughness, especially super toughness of PLA-based polymer blends are presented. The high tensile toughness and high impact strength of PLA-based blends are briefly outlined, while the super tough PLA-based blends with impact strength exceeding  $50 \text{ kJ m}^{-2}$  are elucidated in detail. The toughening strategies and approaches of PLA based super tough blends are summarized and analyzed, as presented in Fig. 1. The relationships of the performance of PLA-based polymer blends with their compatibility and phase structures, such as phase morphologies, dispersed phase parameters of particle size, and interparticle distance, are also outlined and discussed.

### 1.1. Miscibility/compatibility of polymer blends and chain structures

The carbonyl group in the molecular structure of PLA presents a coplanar rigid structure with adjacent oxygen atoms. The PLA molecular chain segment is difficult to rotate, and the carbon atom of the carbonyl group is close to the adjacent carbon atom, resulting in a semi-rigid PLA molecular chain.<sup>44</sup> The critical entanglement molecular weight ([Me];  $8300 \text{ g mol}^{-1}$ ) of PLA is higher than that of PC ( $1780 \text{ g mol}^{-1}$ ),<sup>56,57</sup> and the degree of the molecular chain entanglement of the former is relatively smaller than that of the latter. Therefore, the macroscopic properties of PLA show negligible deformation and less energy absorbed under an external force. PLA materials are brittle and hard with low elongation at break. Given that PLA is a brittle material, the key to toughening PLA is to achieve the combination of strength and ductility. Improving ductility (elongation at break) is usually easy, but remarkably enhancing the impact strength of a PLA material is difficult.

**1.1.1. Definition of toughness.** Toughness mainly emphasizes the ability of a material to absorb energy before failure during stress.<sup>58,59</sup> Generally, it can be classified as tensile toughness and impact toughness. Tensile toughness describes the ability to absorb tensile fracture energy during stretching, whereas impact toughness indicates the ability to absorb impact energy.<sup>51</sup> Toughening<sup>60,61</sup> mainly refers to the ability of a material to absorb external energy as much as possible during failure and increase its failure energy ( $G$ ) in eqn (1):

$$G = G_y + G_c + G_s \quad (1)$$

In comparison with yield energy ( $G_y$ ) and crazing energy ( $G_c$ ), fracture surface energy ( $G_s$ ) of polymer materials can be disregarded because of its minimal contribution to the toughness of materials. Toughening mainly increases energy absorption in two aspects. (1) The number of crazes increases during the stress process, leading to an increase in  $G_c$ . (2) A material undergoes plastic deformation (shear yield) to obtain a large  $G_y$ . An increase in material toughness is limited because of the crazes produced by force, and the toughness of a material cannot be improved sharply. Toughness can be remarkably enhanced when a material undergoes plastic deformation during stress, resulting in the rapid increase of the toughness of a material.

**1.1.2. Relationship of toughness and molecular structure.** The toughness of a material<sup>52</sup> is the result of the combination of the effects of internal structures (internal factor) and external conditions (external factor). External factors include temperature, humidity, material geometry, notched or unnotched, notch mode, loading, mode, and fracture behavior. The intrinsic molecular structure of materials is mainly characterized by chemical structures, chain structures, chain entanglement, and phase behavior. Wu<sup>42,43,62,63</sup> qualitatively explained and introduced the fracture behavior of materials in terms of microstructure and molecular parameters. Wu<sup>42,63</sup> indicated that entanglement density ( $V_e$ ) and characteristic ratio ( $C_\infty$ ) are the two most important parameters that determine whether the fracture behavior of a material is crazing or shear yield. Crazing stress and yield stress are proportional to  $V_e^{1/2}$  and  $C_\infty$ , respectively.

In the binary blends of typical rubber-toughened brittle polymers, the fracture behavior of blends is determined by the phase behavior of the rubber phase and the chain parameters of the brittle polymers. The super-tough blends can be obtained when  $V_e$  of a brittle polymer is  $0.1 \text{ mmol cm}^{-3}$ . The considerable fracture energy of materials can be absorbed due to the occurrence of massive combined crazing and shear yield of a matrix at this entanglement density. For PLA-based blends with different compositions, super toughening is generally predicted to occur in the range of  $0.12\text{--}0.14 \text{ mmol cm}^{-3}$ .<sup>64,65</sup>

Wu<sup>63</sup> studied the relationship of toughening efficiency with phase morphology, particle size, and chain parameters and found that the optimum particle size decreases obviously as  $V_e$  of brittle polymers/rubber blends increases when  $V_e$  is less than  $0.15 \text{ mmol cm}^{-3}$  and  $C_\infty$  is greater than 7.5. Wu<sup>63</sup> also reviewed the detailed summary and analysis of these parameters. The



phase behavior (phase structure, dispersed phase size, and particle size distribution) of PLA-based blends is introduced in detail in Section 7.

**1.1.3. Miscibility and compatibility of polymer blends.** PLA needs to be toughened because of its small elongation at break (10%) and low impact strength (2.5 kJ m<sup>-2</sup>) to further broaden the application field of a PLA material. The strategies for toughening PLA mainly include blending, copolymerization, plasticization, and composite modification. Among these strategies, blending with flexible or elastic polymers is the simplest and most effective. However, preparing PLA blends with high toughness through simple physical blending is difficult because of the inherent immiscibility, poor compatibility, and weak interfacial bonding of blend components. The interfacial compatibility and phase behavior of blends have a decisive influence on the properties of blends. The phase morphology of polymer blends is mainly controlled by the thermodynamics and kinetics of blending. Reviews and studies on the miscibility of polymer blends<sup>66,67</sup> are few, so our review only makes a simple analysis and introduction.

From the thermodynamics perspective, miscibility is a property involved in interactions between blend components at a molecular or nanoscale level.<sup>68,69</sup> A homogeneous system with molecular dispersion and thermodynamic stability can be formed at any mixing ratio. Polymer macromolecules are uniformly dispersed at a molecular or chain level, and miscibility affects the phase morphology and phase behavior of the blends. Compatibility considers the final properties of the blends. A phase interfacial interaction exists in polymer components.<sup>70</sup> Hence, blends with the desired physical and mechanical properties can be obtained with uniform distribution and homogeneity of the dispersed phase and fine phase particles. The final properties can be achieved by the combined action of the intrinsic properties of blend components and the phase behavior and phase morphology of blends. The miscibility of polymer blends can be described by the Gibbs free energy ( $\Delta G$ ) eqn (2):<sup>53,71,72</sup>

$$\Delta G = \Delta G - T\Delta S \quad (2)$$

Polymer blends are miscible when  $\Delta G$  of a mixture is negative. When special interactions, such as strong ion interaction, relatively weak hydrogen bonding, ion-dipole, dipole-dipole, and donor-acceptor interaction, exist between polymers, exothermic heat may be present during mixing, and  $\Delta G$  can be negative. However, only weak van der Waals forces exist in most polymer components, and the interfacial tension between the components is high, which is the cause of the poor miscibility of most polymers.

Given the complexity of the chain structure of polymer materials, Flory-Huggins formula (eqn (3)) with many parameters is used to describe the miscibility of polymer blends.

$$\Delta G_{\text{mix}} = kTV \left[ \frac{\varphi_1}{V_1} \ln \varphi_1 + \frac{\varphi_2}{V_2} \ln \varphi_2 \right] + \varphi_1 \varphi_2 \chi_{12} kTV / v_r \quad (3)$$

The miscibility of blends is evaluated using the Flory-Huggins formula; the interaction parameter  $\chi_{12}$  is one of the key

parameters.<sup>73</sup> The miscibility and compatibility of blends can also be predicted on the basis of the interaction parameter  $\chi_{12}$  as follows eqn (4):

$$\chi_{12} = \frac{V_r}{RT} (\delta_1 - \delta_2)^2 \quad (4)$$

The closer to 0 the interaction parameter  $\chi_{12}$  is, the better the miscibility of the blend components will be. Interaction parameters are determined by the molecular structure of polymers and do not change with the blending ratio or processing conditions. Given the complexity of the macromolecular chain movement of polymers and the low diffusion ability between polymers, the application of equilibrium thermodynamics in polymer blends is limited. The compatibility and relationship of structure-properties should be determined in terms of thermodynamic and kinetic parameters.

Zhong and Al-Saigh *et al.*<sup>74</sup> examined the miscibility and compatibility of PLA/amylopectin (AP) blends, and the results of thermodynamic calculations and phase morphologies indicate that interaction parameters are also related to blend composition. The phase diagram of a binary polymer blend shows the miscibility of a polymer blend as a function of temperature and composition. The transition of blend from immiscibility to miscibility can be determined on the basis of the results of this diagram. Li and Woo *et al.*<sup>75</sup> reported similar findings on PLA/poly(methyl methacrylate) (PMMA) blends and investigated the effects of composition on the miscibility and compatibility of blends. The immiscibility-miscibility transition behavior of PLA/PMMA blends changes with composition. They also obtained an upper critical solution temperature of 255 °C of miscibility for PLA/PMMA blends (70/30, w/w). In another work, Li and Woo *et al.*<sup>76</sup> further investigated the immiscibility-miscibility transition behavior of PLA/PMMA blends and observed that the phase separation at a low temperature becomes miscible at a high temperature. Stoclet *et al.*<sup>77</sup> conducted a similar work on PLA/PA11 blends. The effects of the blend ratio and viscosities of the two components on the compatibility and morphological characteristics of PLA/PA11 binary blends in the whole range of composition have been reported. The scanning electron microscope (SEM) images of cryofractured blends show that PLA/PA11 blends containing 20 wt% or 40 wt% PLA have good compatibility. Their co-continuous morphologies are formed in PLA/PA11 blends as the PLA content increases to 50–60 wt%. At high contents of PLA (60–80 wt%), PLA/PA11 blends display two different morphologies, namely, thread-like and globule-like morphologies. The morphologies that form in binary blends are discussed on the basis of the composition, the viscosities of components, and the interfacial surface free energy.

The thermodynamical miscibility and phase morphologies of blends are mainly influenced by the interactions among chain segments, interfacial tension, and kinetics of blending. The interfacial tension between blends can be reduced *via* compatibilization, and the properties of polymers can be improved by changing the ratio of blends, the viscosity ratio of blends, and processing parameters, such as processing strategy,



temperature, and time. The combination with compatibilization for reducing the interfacial tension between blends, the blend ratio, viscosity ratio of blends, and processing parameters, such as processing strategy, temperature, and time, can control the phase morphology and improve the mechanical performance of polymer blends.

### 1.2. Methods and approaches for compatibilized blends

Given the poor compatibility of most polymers, the compatibility of PLA-based blends should be improved through compatibilization to obtain high-performance PLA-based blends. Similar to toughening of other brittle polymers, blending with flexible or elastic polymer is a practical, common, and effective strategy to enhance the impact toughness of PLA.

The improvement of interfacial compatibility between a PLA matrix and flexible or elastic polymers is a key to preparing high-performance PLA-based blends. The approaches and strategies used for compatibilized PLA are also described in related reviews,<sup>48</sup> and only a few brief explanations are given. The compatibilizers of PLA blends mainly include non-reactive compatibilizers, reactive polymer compatibilizers or active small molecular substances, and *in situ* formed block copolymers or graft copolymers. Zeng *et al.*<sup>48,52</sup> reviewed the common principles and characteristics of compatibilization for polymer blends. The compatibilizers whether physical compatibilizers, non-functional polymers, or highly reactive substances utilized as compatibilizers for a PLA blend system should be miscible with one component of a blend or reactive with functional groups in other components. Hence, interfacial tension is reduced, leading to an increase in dispersibility, and the interfacial adhesion between the components of PLA blends improves.<sup>53,71</sup> In general, directly adding block or graft copolymers and block or graft copolymers generated by *in situ* reactive blending is the most effective way and toughening efficiency to improve the compatibility of incompatible blends.

A compatibilizer is dispersed at the two-phase interface of blends during blending under the action of shear force, thereby reducing the interfacial tension of the blend system and the size of dispersed phase, to stabilize the formed fine phase morphology. The aggregation of dispersed phase particles is prevented, and the morphological characteristics of the dispersed phase are stabilized *via* interfacial compatibilization. The interfacial entanglement in the block components of compatibilizers can facilitate the transfer of stress from one phase to another *via* the dispersed phase as the stress concentration point and prevent destructive cracking caused by multiple crazing. Massive impact energy can effectively absorb through the generation of new surfaces during fracture. Additionally, the interfacial adhesion of polymer components is enhanced by improving interfacial compatibility. However, an excessively high interfacial bond of blends is not conducive to the improvement of impact properties. Matrix yield is delayed when interfacial adhesion is too strong, whereas premature interfacial failure is caused by a very weak interfacial adhesion. The combination of internal and debond cavitation is generated for suitable interfacial adhesion to induce peaceful cavitation and achieve shear

yielding without catastrophic crack propagation. Hence, the super toughness of PLA materials can be achieved.

### 1.3. Toughening mechanisms of PLA-based polymer blends

Merz<sup>78-80</sup> first proposed the microcrack toughening mechanisms of a typical rubber-toughened brittle polymer in 1956. After decades of research and development, shear yield,<sup>81-84</sup> multiple crazing,<sup>85-88</sup> and their combined toughening mechanism have been established. Shear yield is generally the main approach to absorb impact energy, which is an important parameter for brittle polymers to achieve high toughness.

The dispersed rubber particles can induce stress concentration when a blend is subjected to impact force. Multiple crazes dominate deformation if crazing that initiates stress is less than the yield stress. Shear yielding is the toughening mechanism characterized by craze initiating stress greater than yield stress. In addition, craze initiating stress is comparable with yield stress, and the combination of shear yielding and multiple crazing is the main toughening mechanism.<sup>51,52</sup>

The fracture process of glassy amorphous polymers, such as PS, is usually dominated by crazing. The main toughening mechanism of brittle crystalline materials, such as PA, is shear yield. PLA has two forms, namely, amorphous and semi-crystalline forms, due to the stereochemical structure of PLA and variations in processing parameters. Therefore, three different toughening mechanisms are described for PLA/flexible or elastic polymer blends.

## 2. Thermoplastic elastomer blend-toughened PLA materials

A thermoplastic elastomer (TPE) with excellent toughness and elasticity can deform considerably under weak stress. Therefore, TPE is an ideal choice and material for toughening PLA because of its flexibility and biocompatibility. The molecular structure of TPE includes plastic segments (hard segments) and rubber segments (soft segments), which form through tandem function and grafted copolymerization. Hard segments agglomerate into microzones (such as glass microzones or crystal microzones) to form the physical “cross-linking” between macromolecular chains, whereas soft segments are high-elastic segments with a remarkable strong chain movement ability.

PLA modified by TPE mainly includes a polyurethane thermoplastic elastomer (TPU), a polyolefin thermoplastic elastomer, a polyamide thermoplastic elastomer, new bio-based elastomers, and biodegradable elastomers prepared *via* bio-based monomers. The results of mechanical properties of highly tough PLA/elastomers blends are summarized in Table 1, and the super tough PLA/elastomers blends are shown in Table 2.

### 2.1. Preparation of PLA/elastomer blends *via* physical blending

PLA/elastomer blends with an elastomer effectively dispersed in PLA are prepared *via* direct physical blending. A PLA matrix and the dispersed phase of an elastomer are physically combined



Table 1 Mechanical performance results for highly toughened PLA/elastomer blends<sup>a</sup>

Comments	Impact strength/(kJ m <sup>-2</sup> )	Tensile strength/(MPa)	Elongation at break/(\%)	Ref.
PLA/TPO/TPO-PLA (80/20/5)	Good	34.6	107.2	91
PLA/PEA (90/10)	3.37	36.4	155.2	90
PLA/PUP (95/5)	—	~48	~240	101
PLA/TPU/PDI (80/20/0.5)	—	~40	200–300	102
PLA/TPEE/MDI (80/20/3)	—	38	280	103
PLA/TPEE/MDI (80/20/5)	—	36	340	
PLA/PLBSIS (60/40)	35.7	~40	324	110
PLA/TPU (85/15)	15	~40	168.9	111
PLA/copolyester (90/10)	6.12	33.4	358.7	112
PLA/copolyester (80/20)	9.96	30	251.5	
PLA/PELu-50/ADR (85/15/0.4)	~	43.8	340	113
PLA/Bio-TPU/L101 (90/10/0.1)	5.8	50	162	114
PLA/PAE (90/10)	—	40.9	194.6	115
PLA/PU (70/30)	315 J m <sup>-1</sup> (64)	31.5	363	116
PLA/COPUP (80/20)	154.0 J m <sup>-1</sup> (24.98)	45.15	229.14	117
PLA/COPUP (70/30)	269.6 J m <sup>-1</sup> (24.98)	37.28	377.46	
PLA/BE (bioelastomer)	10.3	~35	~200	118
PLA/COP-PU (95/5)	52.8 J m <sup>-1</sup> (33.9)	52.39	338	119
PLA/COP-PU (80/20)	222.9 J m <sup>-1</sup>	~35	>300	120

<sup>a</sup> The values in brackets ( ) are the impact strength corresponding to neat PLA.

through interfacial interaction. The elastomer is dispersed in the form of spherical particles. The toughness of PLA/elastomer blends can be improved through matrix shear yielding caused by interfacial debonding, and the dispersed elastomer particle acts as a stress concentration point to dissipate impact energy.

Huang *et al.*<sup>89</sup> succeeded in preparing PLA/TPU blends *via* melt blending. They indicated that spherical TPU particles disperse in the PLA matrix, and the matrix ligament thickness of PLA/TPU blends is below the critical value. With 30 wt% TPU, the elongation at break and notched Izod impact strength of the blend reach 602.5% and 40.7 kJ m<sup>-2</sup>, respectively, whereas tensile strength considerably decreases. Cramail *et al.*<sup>90</sup> used thermoplastic elastomer poly(ester-amide) synthesized from

fatty acid-based precursors as an impact modifier to prepare PLA with high toughness. Lee *et al.*<sup>91</sup> reported the effects of thermoplastic polyolefin elastomer-*graft*-polylactide (TPO-PLA) premade compatibilizer prepared by grafting PLA onto maleic anhydride-functionalized TPO (TPO-MAH) on the performance and microstructure of PLA/TPO blends. The interfacial adhesion of PLA/TPO blends enhances. The tensile toughness and notched Izod impact strength of compatibilized PLA/TPO blends also considerably improves.

Elastomers with different properties can be prepared by changing the ratio of the flexible and hard segments of the elastomer. Blending with different kinds of elastomers can control the structure and properties of PLA/elastomer blends

Table 2 Mechanical performance results for super toughened PLA/elastomer blends

Comments	Impact strength/(kJ m <sup>-2</sup> )	Tensile strength/(MPa)	Elongation at break/(\%)	Ref.
PLA/TPU (70/30)	40.7	36.8	602.5	89
PLA/TPU (70/30)	58	35	350	92
PLA/EAE (80/20)	59.5	57.8	104.1	93
PLA/PEBA (70/30)	60.5	36.8	335	94
				95
PLLA/PU/PDLA (70/30/2.5)	60	—	—	96
PLLA/TPU/PDLA (85/15/15)	>70	~45	—	97
PLA/PU/SiO <sub>2</sub> (85/15/5)	59.42	38.84	301.81	99
PLA/PU/PLA/PU/SiO <sub>2</sub> (85/15/6)	54.81	40.84	251.19	
PLA/TPU/CNT (70/30/2)	53.7	25.9	45.3	100
PLA/CPU (90/10)	407.6 J m <sup>-1</sup>	43.2	303.10%	107
PLA/CPU (80/20)	419 J m <sup>-1</sup>	~40	~220%	108
PLA/PU (70/30)	55.02	~44.9	516.45	109
PLA/LLDPE-TPV	586.6 J m <sup>-1</sup>	37.5	259.9	121
PLA/VUB (80/20)	575.9 J m <sup>-1</sup>	—	—	122
PLLA/VUB/PDLA (72/20/8)	659.9	—	—	



and prepare super tough PLA materials to achieve the super toughness of PLA blends. Ye *et al.*<sup>92</sup> used a TPU elastomer with high strength, toughness, and biocompatibility to prepare super tough PLA/TPU blends. These blends are partially miscible systems because of hydrogen bonding between the molecules of PLA and TPU. The spherical particles of TPU are dispersed homogeneously in a PLA matrix. The elongation at break and the notched impact strength of PLA/20 wt% TPU blend reach 350% and 25  $\text{kJ m}^{-2}$ , respectively.

Suttiruengwong *et al.*<sup>93</sup> prepared a series of PLA-based blends by using six different flexible copolymers, namely, acrylonitrile butadiene styrene (ABS) powder, biomax, PBAT, polyether block amide, ethylene-vinyl acetate (EVA), and ethylene acrylic elastomer (EAE). The toughening efficiency of EAE is higher than that of five other polymer materials. PLA/EAE blends exhibit super toughness; the elongation at break and notched impact strength increase to 59.5  $\text{kJ m}^{-2}$  and 104.1%, respectively. Tensile strength is as high as 57.8 MPa.

Dong *et al.*<sup>94,95</sup> studied the morphologies, microstructures, crystallization, and mechanical properties of PLA blends containing different contents of poly(ethylene oxide-*b*-amide-12) (PEBA). The blends are an immiscible system with evenly dispersed PEBA domains in the PLA matrix. The super tough PLA matrix produces an obvious shear yield in the blend during tensile and impact tests, thereby inducing energy dissipation and improving the toughness of PLA/PEBA blends, with elongation at break and impact strength increasing to 346% and 60.5  $\text{kJ m}^{-2}$ , respectively. The average particle size of PEBA in the blend and impact strength of PLA/PEBA blends were shown in Fig. 2. The effects of crystallization on the microstructure and the mechanical properties of the blends suggest that annealing crystallization treatment can improve the tensile strength of PLA/PEBA blends to some extent.<sup>94</sup>

Bai and Fu *et al.*<sup>96,97</sup> incorporated small amounts of poly(D-lactide) (PDLA) into thermoplastic polyurethane (TPU) toughened PLLA blends through melt-blending to fabricate super toughened and heat-resistant PLLA/elastomer blends to improve the strength and modulus of PLA/elastomer blends. The results indicate that introducing PDLA chains can readily interact with PLLA matrix chains and rapidly co-crystallize into stereocomplex crystallites (SC) in the PLA matrix of blend melts.

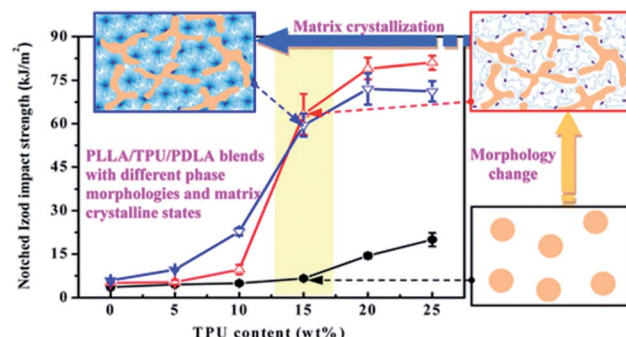


Fig. 3 The effect of TPU content on the impact strength and morphology evolution of PLLA/PU/PDLA blends. Ref. 97, copyright 2016. Reproduced with permission from American Chemical Society.

Thus, these SC crystallites can act as a highly efficient nucleating agent to significantly accelerate matrix crystallization and are beneficial to the preparation of PLLA blends with a highly crystallized PLLA matrix through conventional injection molding technology. SC crystallites can act as an efficient rheology modifier and induce the morphological change in the dispersed TPU phase from a typical sea-island structure to a unique network-like structure, as shown in Fig. 3 and 4. The impact strength of the PLLA/PU/PDLA blend (80/20/2.5) exceeds 70  $\text{kJ m}^{-2}$ , and the tensile strength remains around 45 MPa. The construction of SC crystallites in the matrix can be a simple and promising strategy for fabricating super toughened and heat-resistant PLLA/elastomer blends by simultaneously tuning phase morphology and matrix crystallization.

The interfacial compatibility and interfacial bonding of PLA matrix and elastomer components are improved by adding inorganic fillers into a PLA/elastomer blend system, and inorganic fillers are selectively dispersed at the dispersed phase and phase interface of the elastomer by taking advantage of the differences in the polarity of components. Bai and Fu *et al.*<sup>98</sup> used titanium dioxide ( $\text{TiO}_2$ ) nanoparticles to adjust the interfacial adhesion of PLA/poly(ether)urethane (PLA/PU) blends. Introducing  $\text{TiO}_2$  into these blends has no evident influence on phase morphology; however, the selective localization of  $\text{TiO}_2$  nanoparticles at the interface remarkably improves impact

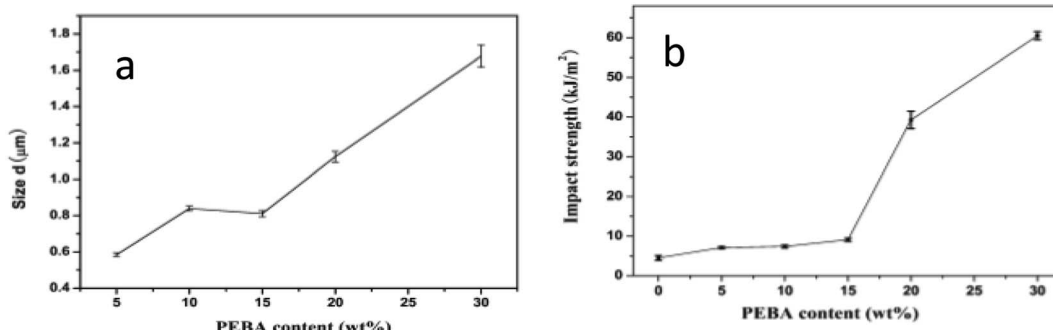


Fig. 2 The average particle size of PEBA in the blend (a) and impact strength of PLA/PEBA blends as a function of the content of PEBA (b). Ref. 94, copyright 2012. Reproduced with permission from John Wiley and Sons.



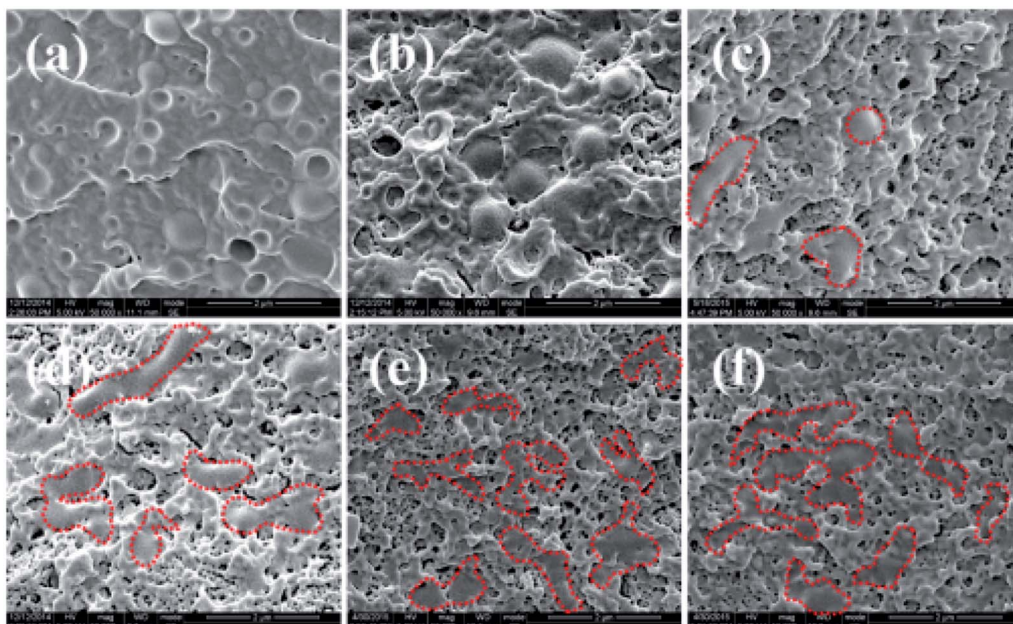


Fig. 4 SEM micrograph of cryofractured surfaces of the blends: (a) PLA/15TPU (b) PLA/15TPU/5PDLA (c) PLA/15TPU/10PDLA (d) PLA/15TPU/15PDLA (e) PLA/15TPU/20PDLA (f) PLA/15TPU/25PDLA. Ref. 97, copyright 2016. Reproduced with permission from American Chemical Society.

toughness. Bai and Fu *et al.*<sup>99</sup> also demonstrated that the inclusion of hydrophilic silica ( $\text{SiO}_2$ ) nanoparticles into PLA/PU blends can be applied to successfully prepare super toughened poly( $\text{L}$ -lactide) (PLLA) nanocomposites because hydrophilic silica ( $\text{SiO}_2$ ) nanoparticles have self-networking capability, thereby controlling the phase morphology and improving the interfacial compatibility of these nanocomposites. The selective localization of  $\text{SiO}_2$  nanoparticles in the PU phase and at the phase interface induces the morphological change from a common sea-island structure to a unique network-like structure constructed by discrete PU particles with irregular shapes. As the morphology evolution of blends is shown in Fig. 5. In addition, the synergistic effect between the self-networking of the interface-localized  $\text{SiO}_2$  and the enhanced elasticity of the  $\text{SiO}_2$ -localized PU phase leads to the formation of a network-like structure. The impact strength and elongation at break of PLLA/PU/ $\text{SiO}_2$  nanocomposites are  $59.42 \text{ kJ m}^{-2}$  and  $301.81\%$ , respectively. The morphological model of blend was constructed as seen in Fig. 6. Wang *et al.*<sup>100</sup> reported a similar work on super toughened PLLA/thermoplastic polyurethane (PLLA/TPU)/carbon nanotube (CNT) ternary nanocomposites. The results show that CNTs selectively localize in the TPU phase, leading to a morphological change from the sea-island morphology to the quasi-*co*-continuous morphology.

The direct physical blending of PLA with elastomer materials is a simple and effective way to improve the toughness of PLA. An elastomer is directly melted, blended with PLA, and dispersed by the shear force of a mixer or an extruder. The types of elastomer, dispersion, compatibility, and particle size of the dispersed phase in the PLA matrix have a decisive influence on the properties of PLA/elastomer blends.  $\text{SiO}_2$  and CNT are

added to a PLA/elastomer blend system to prepare nanocomposite materials and further improve the performance of PLA/elastomer blends. The enhancement effect of nanoparticles and the selective dispersion behavior among the components of these blends can enhance the interfacial compatibility of the blends and the dispersion behavior of the dispersed phase. The development of new high-strength and high-elasticity systems is also an important research direction for preparing high-

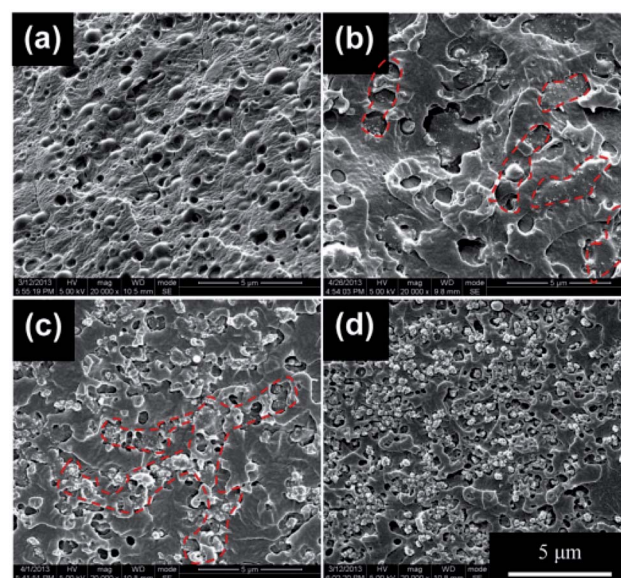


Fig. 5 SEM images of the cryofractured surfaces of PLA/15PU blend with various amounts of  $\text{SiO}_2$ : (a) 0 phr (b) 2.5 phr (c) 5 phr (d) 10 phr. Ref. 99, copyright 2014. Reproduced with permission from Elsevier.

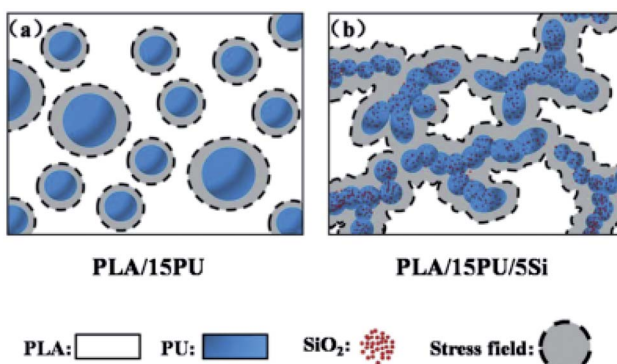


Fig. 6 Schematic representation of the deformation mechanisms of PLA/15PU blend with and without  $\text{SiO}_2$ : (a) PLA/15PU (b) PLA/15PU/5Si. Ref. 99, copyright 2014. Reproduced with permission from Elsevier.

performance PLA/TPE blends. Direct blending is simple and easy to achieve, but it has drawbacks, such as unsatisfactory compatibility between components, aggregation of dispersed elastomer particles, and uneven dispersion behavior, thereby affecting the structure and properties of materials and should be solved.

## 2.2. PLA/elastomer blends fabricated *via* reactive blending

Given the immiscibility of blending components, an elastomer dispersed phase easily aggregates and experiences difficulty in uniformly dispersing in a PLA matrix during blending. Therefore, the compatibility of blending components should be further improved. The functional groups of polymers can react at the phase interface and improve the compatibility of a PLA-based blending system by adding polymers or small molecules with reactive functional groups. For the elastomer-toughened PLA system, reactive blending can be carried out by adding a polyol component and an isocyanate component with a highly reactive elastomer or by adding the third component with high reactivity. The dispersed phase of a thermoplastic elastomer and the block or graft copolymer of PLA-elastomers are simultaneously generated. The presence of block or graft copolymer at the interface can reduce the interfacial tension and the size of the dispersed phase during melting. The *in situ* compatibilization of the PLA/elastomer blend system is achieved.<sup>71</sup>

Wu *et al.*<sup>101</sup> toughened PLA by melt blending with polyurethane prepolymer (PUP), thereby terminating with the isocyanate group and formed through the reaction between poly-1,4-butylene glycol adipate diol (PBA) and 4,4'-methylenedi-p-phenyl diisocyanate (MDI). The *in situ* interfacial compatibilization between PLA and elastomer is achieved through the reaction of PLA with PUP, and the tensile toughness of PLA materials considerably improves. Ozkoc *et al.*<sup>102</sup> and Yoon *et al.*<sup>103</sup> reported that 1,4 phenylene diisocyanate (PDI) and MDI are used as the compatibilizers of PLA/elastomer to achieve *in situ* reactive compatibilization, which significantly improves the tensile toughness of PLA blends; however, the impact toughness of PLA blends is not remarkably enhanced. Zhao *et al.*<sup>104-106</sup> investigated the structure-morphology-performance interrelationship of high strength and high toughness PLA/polyurethane elastomer (PUS) blends prepared through reactive blending. PUS is *in situ* formed *via* the reaction of polyester polyol (PPG) and toluene-2,4-diisocyanate (TDI), whereas block or graft copolymers are synthesized at the interface of blends through the isocyanate group that reacts with the hydroxyl group or carboxyl group of PLA. The interfacial adhesion of blends enhances, and the size of the dispersed phase decreases. The interfacial compatibility of PLA blends is quantitatively characterized *via* positron annihilation lifetime spectroscopy. The relationship between the free volume (the size and number of free volume cavities) and performance of PLA/PUS blends is established.

Zeng and Wang *et al.*<sup>107</sup> prepared ultra-tough PLA/CPU blends through a cross-linking reaction among polyethylene glycol (PEG), glycerol, and MDI. Aside from the isocyanate group of MDI participating in generating CPU, it also reacts with the end hydroxyl group or carboxyl group of PLA to improve the interface compatibility of PLA/CPU blends. The model of PLA/CPU blends was shown in Fig. 7. The morphological characteristics of the blend and the size of the dispersed phase of CPU are regulated by adjusting the amount of glycerin. The dispersed phase size of CPU in PLA/CPU (90/10, w/w) blends is about 0.7  $\mu\text{m}$  and can be used as the stress concentration point to obtain the matrix yield. The impact strength and elongation at break are 407.6  $\text{J m}^{-1}$  and 303.1%, respectively, which are 21 and 38 times those of pure PLA (16.9  $\text{J m}^{-1}$ , 8%), as seen in Fig. 8. The team<sup>108</sup> also prepared PLA blends with high toughness by reacting PLA with PEG and polyisocyanate.

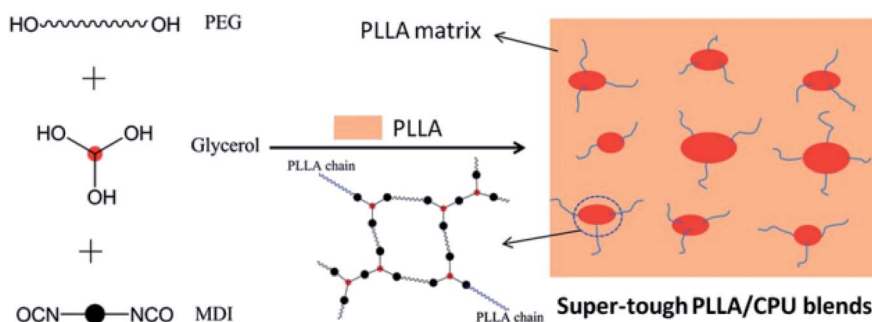


Fig. 7 Preparation of PLLA blends with crosslinked polyurethane formed by *in situ* polymerization. Ref. 107, copyright 2014. Reproduced with permission from Royal Society of Chemistry.



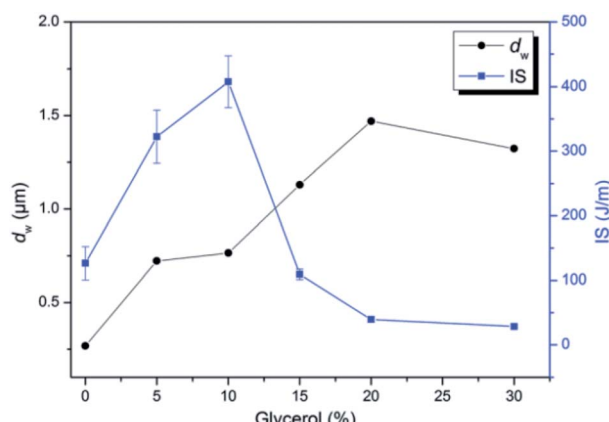


Fig. 8 The weight-average particle diameter ( $d_w$ ) and notched impact strength (IS) of PLLA/CPU blends as a function of glycerol content. Ref. 107, copyrights 2014. Reproduced with permission from Royal Society of Chemistry.

Qu *et al.*<sup>109</sup> blended PLA with polyurethane elastomer prepolymer (PUEP) terminated with an isocyanate group to prepare super-tough PLA blends *via* dynamic vulcanization. PUEP forms the dispersed phase of a PU elastomer, while PUEP reacts with the end group of PLA to generate copolymers as

a compatibilizer, thereby facilitating the dispersion of PU in the PLA matrix. The chemical routes of PLA reacted with PUEP and the phase morphological model of PLA/PU blends are represented in Fig. 9. The impact strength and elongation at break of PLA/PU (70/30, w/w) blend are up to 55.02 kJ m<sup>-2</sup> and 516.45%, which are 21 and 34.71 times those of pure PLA (2.55 kJ m<sup>-2</sup> and 14.88%), respectively (Fig. 10).

PU elastomer and PLA-elastomer copolymer are formed *in situ* because of the high reactivity of the isocyanate group ( $-N=C=O$ ) in the polyurethane component during reactive blending, thereby effectively improving the interfacial bonding of the blends and significantly improving the toughness of PLA/elastomer blends. Reactive blending and dynamic vulcanization are effective strategies for achieving the high toughness of PLA blends. The modulus and strength of the blending system should be further studied. Few studies on the addition of a high-strength third component and inorganic nanoparticles have been conducted.

### 2.3. Bio-based and biodegradable elastomer-modified PLA

A bio-based elastomer with green, environment-friendly, renewable, and biodegradable characteristics is a new type of elastomer that does not depend on petroleum and fossil resources. Toughening PLA *via* bio-based elastomers can

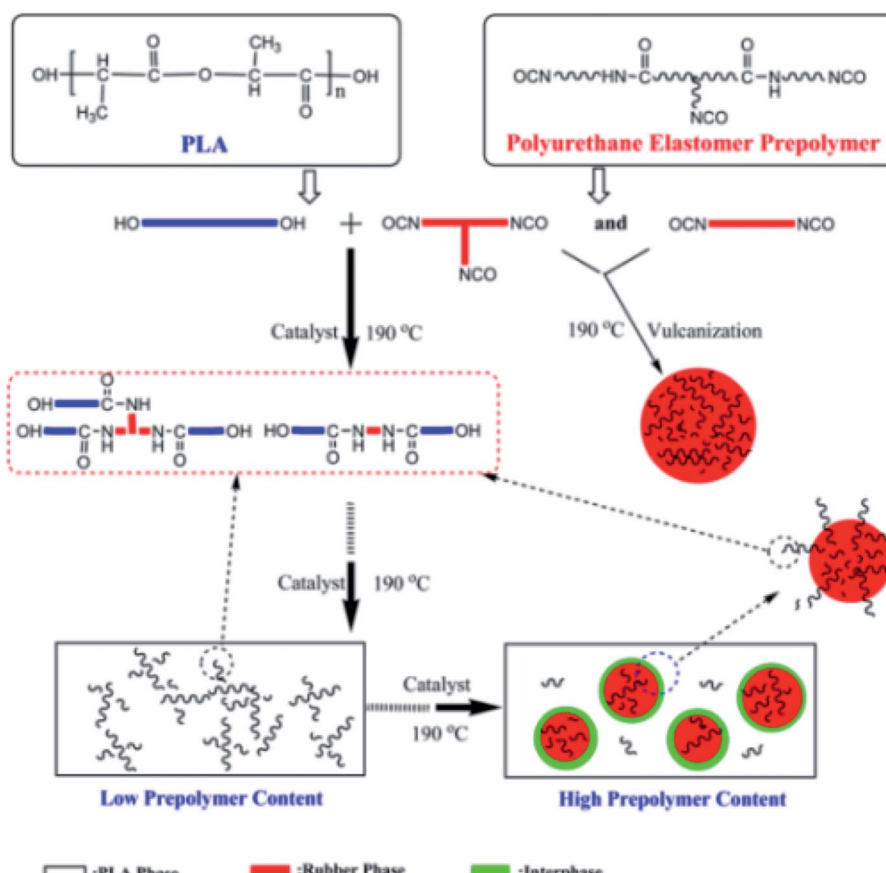


Fig. 9 The chemical routes of PLA reacted with PUEP and the phase morphological model of PLA/PU blends. Ref. 109, copyright 2014. Reproduced with permission from American Chemical Society.

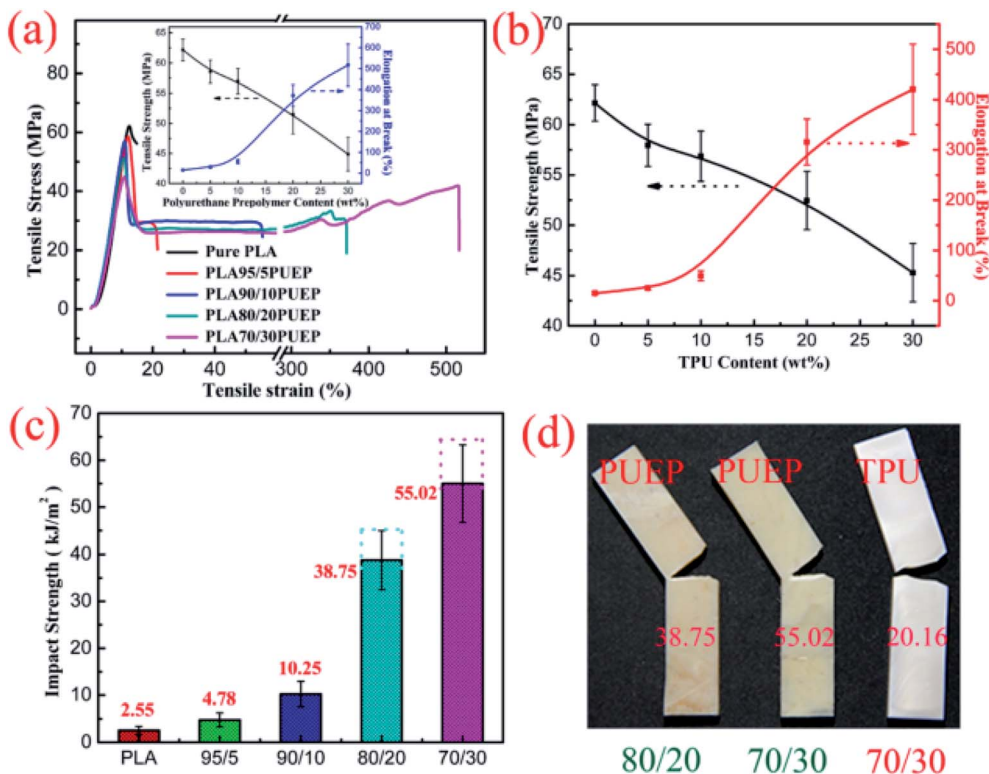


Fig. 10 Tensile properties of (a) dynamically vulcanized PLA/PUEP blends with different PUEP contents and (b) PLA/TPU blends with different TPU contents. (c) Notched Izod impact strength of dynamically vulcanized PLA/PUEP blends with different PUEP contents. (d) Digital picture of PLA/TPU (70/30) and PLA/PUEP (80/20, 70/30) blends after impact measurements. Ref. 109, copyright 2014. Reproduced with permission from American Chemical Society.

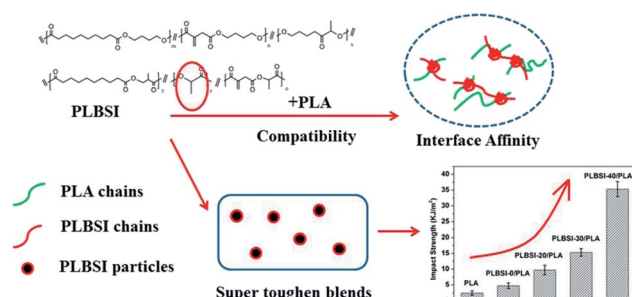


Fig. 11 Reaction routes of PLA and PLBSI, phase structure diagram and mechanical property of PLA/PLBSI blends. Ref. 110, copyright 2016. Reproduced with permission from American Chemical Society.

achieve environmentally friendly PLA blends and eliminates dependence on petroleum resources. As such, this aspect is considered a new research topic on PLA modification. PLA is modified by melt blending with a bio-based and biodegradable elastomer *via* dynamic vulcanization and blending with a polyester elastomer prepolymer. The interfacial compatibilization of PLA/bio-based elastomer blend systems is achieved, and high-performance PLA/bio-based elastomer blends are prepared.

Zhang and Kang *et al.*<sup>110</sup> toughened PLA with a bio-based copolymer (PLBSI) prepared from bio-based monomers, such as lactic acid, butanediol, sebacic acid, and itaconic acid. The

PLBSI chain segment contains lactic acid units and a polyester structure, making it compatible with PLA, as presented in Fig. 11. The impact strength and elongation at break of PLA/PLBSI (60/40) blends increase to 35.7 kJ m<sup>-2</sup> and 324%, respectively, and the tensile strength decreases to about 40 MPa. Zhu *et al.*<sup>111</sup> conducted a similar work on PLA modified using a polyether polyurethane elastomer prepared with biodiol and diacid. The bio-based polyether polyurethane elastomer can improve the crystallization rate and crystallinity and achieve a good toughening effect. Cramail *et al.*<sup>112</sup> also investigated and explained the compatibility and performance of PLA/biocopolyester blends with ultra-high tensile toughness. Copolymers are prepared from the polymerization of sebacic acid, octanediol, and dimeric acid and employed to toughen PLA. Chen and Bian *et al.*<sup>113</sup> prepared new biodegradable polyurethane (PELU) *via* the chain extension reaction between polyethylene glycol-*b*-PLA copolymer and IPDI. PELU is melt blended to toughen PLA, and industrial-grade oligomer of multiple epoxy groups (ADR) is added to improve the interfacial compatibility of PLA/PELU blends. The elongation at break of PLA/PELU/ADR (85/15/0.4) blends is up to 340%, and their tensile strength is 43.8 MPa.

Some related studies have been conducted on bio-based toughened PLA, such as bio-based polyurethane elastomers containing double bonds,<sup>114</sup> biodegradable polyamide elastomer,<sup>115</sup> biodegradable polyether polyurethane,<sup>116</sup> bio-based



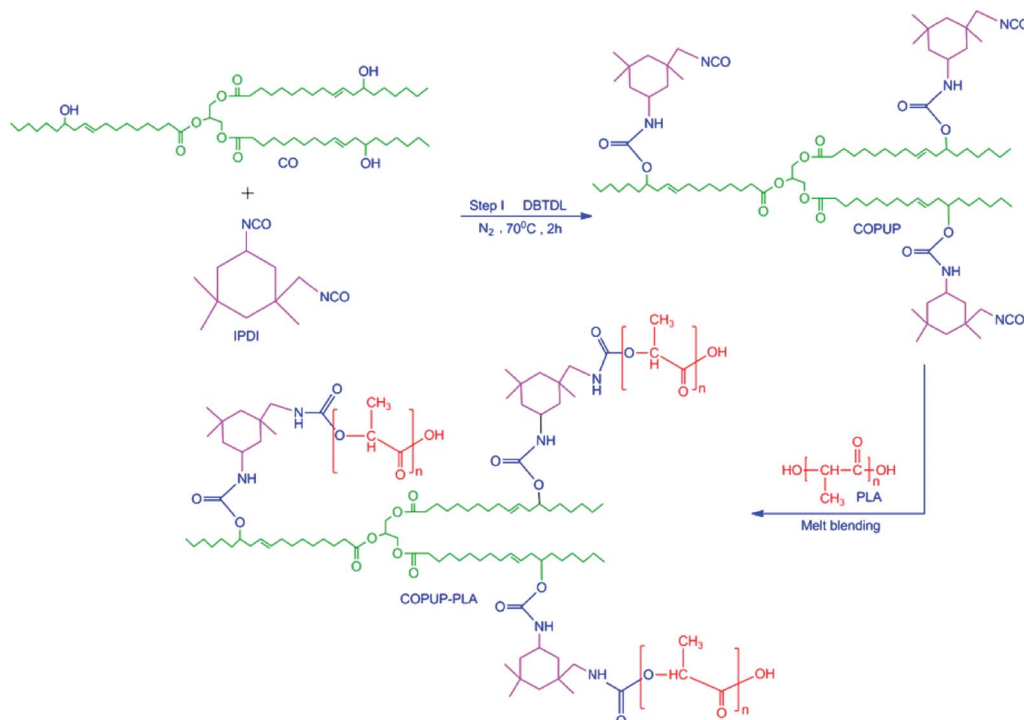


Fig. 12 Synthesis of the COPUP and hydrogen bonding between the molecules of PLA and COPUP. Ref. 117, copyright 2014. Reproduced with permission from Springer.

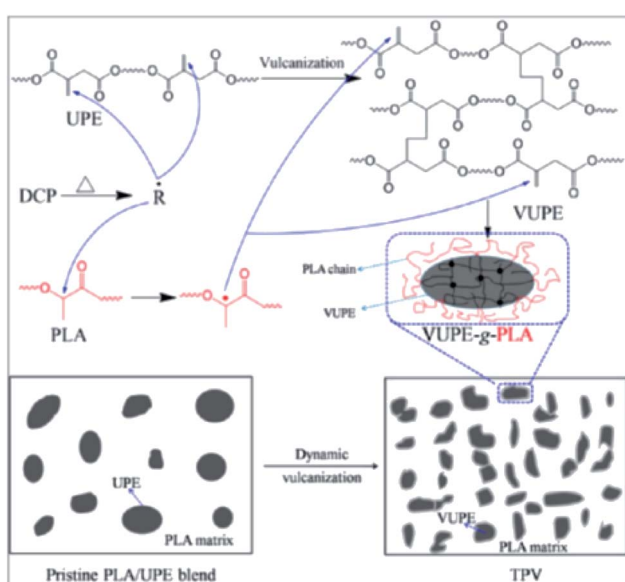


Fig. 13 Proposed interfacial compatibilization of TPV through formation of VUPE-g-PLA during dynamic vulcanization. Ref. 121, copyright 2014. Reproduced with permission from American Chemical Society.

polyurethane prepolymer for castor oil<sup>117</sup> (Fig. 12), and bio-elastomer (BE) prepared from bio-based diol and diacid monomers.<sup>118</sup> These bio-elastomers are used to toughen PLA, thereby considerably improving toughness.

Zeng *et al.*<sup>119</sup> blended bio-based castor oil and PLA with MDI and formed castor oil-based polyurethane elastomer (COP); the COP phase is dispersed in the PLA matrix through dynamic vulcanization. The effects of different kinds of isocyanates (MDI, HDI, and IPDI) on the properties and structures of PLA/COP blends have been further studied,<sup>120</sup> and PLA/castor oil-based polyurethane elastomers with high tensile toughness have been obtained. The impact strength and modulus of PLA/COP blends should be further improved.

Environment-friendly elastomers, such as polyester, polyether, and polyamide elastomers, are synthesized using bio-based monomers. Elastomers with different structures are designed and synthesized by selecting different bio-based monomers and regulating the ratio of monomers to enhance compatibility with PLA. Through simple melt blending, the tensile toughness of PLA/bio-based elastomer blends significantly enhances, but the impact strength is not sufficiently improved. Reactive blending and dynamic vulcanization are introduced in the blending of PLA/bio-based elastomer blends to further improve the impact toughness of PLA/bio-based elastomer blends. With the help of the strong shearing force of the blending equipment, a bio-based elastomer formed in melt blending and uniformly dispersed in a PLA matrix is achieved, thereby improving the comprehensive properties of PLA/bio-based elastomer blends.

Zeng and Wang *et al.*<sup>121</sup> prepared bio-based super-tough PLA thermoplastic vulcanizates (TPV) with PLA and bio-based unsaturated aliphatic polyester elastomer (UPE) through dynamic vulcanization induced by peroxides. The polyester

elastomer (VUPE) formed in blending and the rubber dispersed phase is correlated and produced a continuous structure. PLA/VUPE blends exhibit a quasi-continuous morphology. The internal cavities of VUPE can induce a large amount of the shear yield of the PLA matrix, which plays a good toughening role, as shown in Fig. 13. The impact strength of TPV is up to  $586.6\text{ J m}^{-1}$ .

Zeng *et al.*<sup>122</sup> further investigated different bio-based elastomers, melt blended unsaturated bio-based resin (UBE) with PLLA, and prepared super-tough PLA/UBE blends with an impact strength of  $575.9\text{ J m}^{-1}$  through dynamic vulcanization. A small amount of PDLA is incorporated to the PLA/UBE binary blending system, and the impact strength of PLA/UBE/PDLA blends further increases to  $659.9\text{ J m}^{-1}$ . The improved toughness of the blends is attributed to the formation of SC crystallites. SC crystallites increase the molecular chain entangling and promote PLLA matrix crystallization. Zeng *et al.*<sup>123</sup> investigated the effects of the chemical structure of biodegradable elastomers on the mechanical and thermal properties and revealed that interfacial SC crystallization can be provided by poly(*D*-lactide)-*b*-polyurethane-*b*-poly(*D*-lactide) (DPUD) triblock copolymer in PLA/DPUD blends, whose SC crystallites can enhance the mechanical strength and work as efficient nucleating agents for the crystallization of PLA matrix. In the case of the annealed samples of PLLA/DPUD-15, the impact toughness is up to  $325.9\text{ J m}^{-1}$ , and excellent heat resistance is achieved.

Although bio-based elastomers improve in comparison with traditional petroleum-based elastomers in strength and modulus, bio-based elastomers can be comparable with or better than petroleum-based elastomers in many aspects, such as elongation at break and elasticity. Bio-based elastomers, such as sebacic acid, butanediol, itaconic acid, and vegetable oil, can be synthesized from bio-based monomers. The compatibility of PLA/bio-based elastomers can be manipulated from the perspective of molecular design through the regulation of monomer type and content ratio and the designation of bio-based elastomers with different molecular structures. Toughened PLA modified with a bio-based elastomer has an important research value, thereby guaranteeing the source of bio-based materials and considerably improving the toughness of PLA. Further research and development of bio-based elastomers and the emergence of new biodegradable bio-based elastomer will further expand the application of bio-based and PLA/bio-based elastomer materials.

The blends prepared *via* TPE direct blend PLA toughening have poor interfacial compatibility and weak interfacial adhesion. As a result, effectively toughening PLA is difficult. The strength and modulus of PLA blends are remarkably reduced. The strategy of reactive blending and dynamic vulcanization can effectively improve the interfacial compatibility and dispersion between an elastomer-dispersed phase and a PLA matrix. The compatibility and interface bonding between the elastomer and the PLA matrix have been effectively improved by dynamic vulcanization by adding initiators and cross-linking agents. The super-toughened PLA blends with a relatively high modulus and tensile strength can be obtained through *in situ* compatibilization. Developing new high-strength and high-

modulus elastomers, designing and synthesizing bio-based and biodegradable elastomers, and applying them in toughening PLA are emerging research fields and key research direction of polymer blending.

### 3. Glycidyl ester material-toughened PLA

Glycidyl ester materials are functional monomers/polymers containing epoxy groups, with high reactive epoxy groups in a molecular structure. In mixing with PLA or PLA blends, we should form copolymers,<sup>124,125</sup> which play a role in self-compatibilization or *in situ* compatibilization for different PLA blend systems, which are widely used in PLA blending modification. For example, glycidyl methacrylate (GMA)<sup>126</sup> is a monomer that has an acrylate double bond and an epoxy group. Acrylate double bond has high reactivity and can react with free radicals or copolymerize with many other monomers. Epoxy groups can react with hydroxyl, amino, carboxyl, or anhydride, providing options and design ideas in the field of material modification and introducing functional groups to provide additional functionality to materials. Glycidyl ester materials have a small GMA molecule,<sup>126</sup> low-molecular-weight prepolymer, such as styrene-glycidyl acrylate copolymer (Joncryl-R, ADR series),<sup>127,128</sup> high-molecular-weight copolymers, such as ethylene-butyl acrylate-glycidyl methacrylate (E-MA-GMA),<sup>129,130</sup> poly(ethylene octene) grafted with glycidyl methacrylate (POE-g-GMA),<sup>131,132</sup> ethylene/methacrylate/glycidyl methacrylate terpolymer (EGA),<sup>133</sup> and EGMA.<sup>134</sup> The reactivity of glycidyl ester materials containing epoxy groups is higher than that of maleic anhydride (MAH), which can effectively improve the sensitivity of PLA materials to notch impact strength. Glycidyl ester materials are used to modify PLA and its blends,<sup>135-137</sup> which can effectively promote the uniform dispersion of the dispersed phase in a PLA matrix, increase the interfacial compatibility among blending components, and improve the mechanical properties of the materials. The mechanical properties of high-tough and super-tough PLA/glycidyl ester copolymer blends are presented in Tables 3 and 4, respectively.

#### 3.1. Physical blending of PLA with glycidyl ester elastomer

Glycidyl ester elastomer has good compatibility with PLA. The epoxy groups in glycidyl ester copolymer can react with PLA during melt blending, which can effectively improve their compatibility and significantly improve the flexibility and impact properties of PLA blends.

Su and Han *et al.*<sup>138</sup> used dicumyl peroxide (DCP) as an initiator for preparing ultra-tough PLA by the reactive blending of PLA and EGMA. The interfacial bonding of the blends is enhanced, and EGMA particles become more evenly dispersed. DCP promotes the reaction between PLA and EGMA and improves the interface compatibility of blends. A PLA/EGMA/DCP (95/5/0.1, w/w/w) blend has excellent tensile properties with an elongation at break of 290% and a tensile strength of 67 MPa, but the impact strength increases slightly. The work



Table 3 Mechanical performance results for highly toughened PLA/glycidyl ester materials blends<sup>a</sup>

Comments	Impact strength/(kJ m <sup>-2</sup> )	Tensile strength/(MPa)	Elongation at break/(\%)	Ref.
PLA/EGMA (80/20)	5.54	67	290	138
PLA/E-AE-GMA (80/20) microalloys	331 (69.5)	40.2	252	139
PLA/E-AE-GMA (80/20) nanoalloys	183	40.2	329	
PLA/BA-EA-GMA (80/20)	29.6	~45	>300	140
PLA/PA11/EGMA-g-A5 (55/45/6)	361 (69.7)	55.11	321.6	161
PLA/PA11/EGMA-g-A5 (55/45/9)	365	48.1	287	
PLA/EMA-GMA/EMA-GMA-g-PDLA (85/15/0.625)	35.1	—	—	163

<sup>a</sup> The values in brackets ( ) are the impact strength corresponding to neat PLA.

Table 4 Mechanical performance results for super toughened PLA/glycidyl ester materials blends

Comments	Impact strength/(kJ m <sup>-2</sup> )	Tensile strength/(MPa)	Elongation at break/(\%)	Ref.
PLA/EMA-GMA/DMSA (80/20/0.2)	83.5	~40 MPa	—	141
PLA/EGMA (80-20)	72	40	>200	142
PLA/EGMA (80/20)	94	~40	120	143
PLA/(EBA-GMA/EMAA-Zn) 80/20	>700 J m <sup>-1</sup>	—	—	144
PLA/EBA-GMA (75/25)	736 J m <sup>-1</sup>	~40 MPa	~80	148
PLA/EBA-GMA/EMAA-Zn (80/10/10)	737 J m <sup>-1</sup> (210 °C)	~35	—	149
PLA/EBA-GMA/EMAA-Zn (80/10/10)	777.2 J m <sup>-1</sup> (240 °C)	36.2	229	150
PLA/EBA-GMA/EMAA-Zn (80/15/5)	680 J m <sup>-1</sup>	37.4	23.5	151
PLA/VESO (80/20)	542.3 J m <sup>-1</sup>	~34.4	445	152
PLA/EGA (80/20)	59.8	33.8	232	153
PLA/POE-g-GMA (80/20)	87.3	42.1	—	154
PLA/MPOE (55/45)	54.7	36.3	282	155
PLA/PEBA-/g-GMA (70/30)	68.6	—	—	156
PLA/ABS-/g-GMA (70/30)	540 J m <sup>-1</sup>	—	~70%	157
PLA/MB-g-GMA (75/25)	59.5	38.1	200	158
PLA/NR-GMA (80/20)	73.4	35	130	159
PLA/SEBS/EGMA (70/20/10)	92	—	185	160
PLA/PC/SEBS/EGMA (40/40/15/5)	>60	—	~90	161
PLA/OBC/EMA-GMA (90/7/3)	64.21	55	~30	162
PLA/EMA-GM/PEBA (70/20/10)	500 J m <sup>-1</sup>	~45	72.7	163

provides an effective way to largely improve the flexibility of PLA without sacrificing its stiffness and transparency.

Li *et al.*<sup>139</sup> prepared PLA/ethylene-*co*-acrylic ester-*co*-glycidyl methacrylate (E-AE-GMA) blend micron and nanometer alloys by employing different melt blending techniques and investigated the parameters of the dispersed phase particle on the properties of PLA blends. The dispersed phase size of micron alloy formed during melt blending is 200 nm, and a Y-shaped graft copolymer is formed. The dispersed phase size of a nano-alloy formed by blends ranges from 10 nm to 100 nm, and a comb-like graft copolymer is formed. The toughness of the blends greatly improves. The toughness of the PLA/E-AE-GMA blend micron alloy enhances because the micron dispersed phase as the stress concentration point is more conducive to energy-dissipating stress. Dong *et al.*<sup>140</sup> adopted butyl acrylate (BA), ethylacrylate (EA) and glycidyl methacrylate (GMA) copolymer (BA-EA-GMA) as a toughening component for PLA modification. BA-EA-GMA is dispersed uniformly in the PLA matrix with strong interface adhesion. The impact strength

of PLA/BA-EA-GMA (80/20) blend is increased to 29.6 kJ m<sup>-2</sup>, the elongation at break is more than 300%, and the tensile strength is maintained at approximately 45 MPa.

Zhao and Jiang *et al.*<sup>141</sup> reported an example of super-tough PLA blends. PLA/EMA-GMA (80/20, w/w) blends with ultrahigh toughness and an impact strength of 35.6 kJ m<sup>-2</sup> were fabricated. The notched Izod impact strength of PLA/EMA-GMA (80/20, w/w) blend is further improved to 83.5 kJ m<sup>-2</sup> by adding 0.2 wt% *N,N*-dimethylstearylamine (DMSA) as a catalyst. The reaction between the epoxide group of EMA-GMA and the end groups (−OH, −COOH) of PLA is promoted by DMSA. The reactive compatibilization between PLA and EMA-GMA with DMSA is studied *via* Fourier transform infrared spectroscopy. The dispersion of EMA-GMA in the PLA matrix is promoted at a particle size of 0.91 μm. The morphology evolution of PLA blends was exhibited in Fig. 14.

The reaction degree of PLA and glycidyl ester copolymer is enhanced during blending. The crystallization behavior of a PLA matrix can be improved *via* annealing post-treatment,



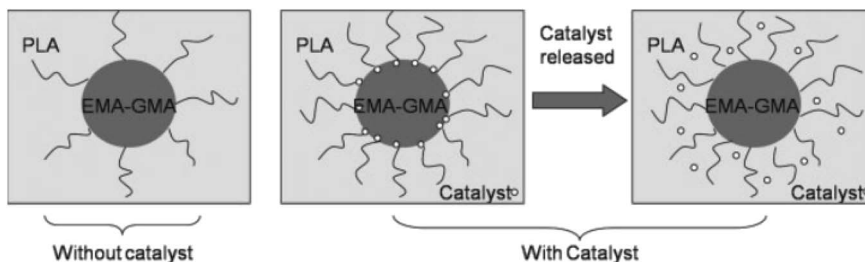


Fig. 14 Proposed morphology evolution of PLA blends with and without catalyst. Ref. 141, copyright 2013. Reproduced with permission from John Wiley and Sons.

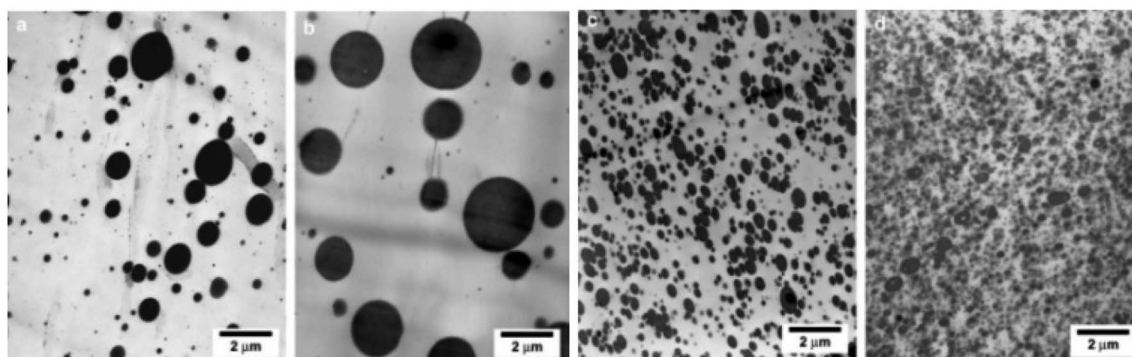


Fig. 15 TEM micrographs of PLA/EGMA blends stained by  $\text{RuO}_4$  vapor (a) (95/5) PLA-L/EGMA prepared with screw rotation speed of 30 rpm, L95-30, (b) (80/20) PLA-L/EGMA prepared with screw rotation speed of 30 rpm, L80-30, (c) (80/20) PLA-L/EGMA prepared with screw rotation speed of 200 rpm, L80-200, and (d) (80/20) PLA-H/EGMA prepared with screw rotation speed of 200 rpm, H80-200. Ref. 142, copyright 2009. Reproduced with permission from Elsevier.

thus further improving the toughness and strength of PLA blends. Oyama *et al.*<sup>142</sup> demonstrated a dramatic improvement in the mechanical characteristics of PLA by its reactive blending with poly(ethylene-glycidyl methacrylate) (EGMA) and examined the influence of annealing treatment technology and crystallinity on the properties of PLA/EGMA blends. Their results indicated that the crystallization of a PLA matrix plays

a significant role in toughening. During reactive blending, PLA-EGMA copolymers are *in situ* formed at the PLA/EGMA blend interface, and the interface compatibility is enhanced with the particle size of the dispersed phase is smaller than 100–300 nm, as shown in Fig. 15. EGMA also promotes the crystallization of PLA. When the blend is annealed at 90 °C for 2.5 h, the crystallinity of PLA/EGMA blends is increased from 6% of pure PLA to 40%. The resulting PLA/EGMA (80/20) blends exhibit high toughness with an impact strength of  $72 \text{ kJ m}^{-2}$  (Fig. 16), elongation at break of more than 200%, and a tensile strength of 40 MPa.

Wang *et al.*<sup>143</sup> found a similar result on PLA/EGMA blends, they fabricated PLA/EGMA blends *via* reactive blending and induced PLA/EGMA blends to crystallize by annealing to obtain super-tough PLA with good heat resistance. The thermal annealing model of PLA/EGMA blend was shown in Fig. 17. After annealing is conducted at 80 °C for 8 h, the crystallinity of the PLA matrix in the blend is approximately 25%, the impact strength of the material is  $94 \text{ kJ m}^{-2}$ , the elongation at break is 120%, and the tensile strength is approximately 40 MPa. The heat resistance of the blend is also improved (Fig. 18).

The interfacial compatibility of polymer blends and the reaction degree of glycidyl ester elastomer influence the toughening effect of PLA/elastomer blends.<sup>144–147</sup> During the melting of PLA blends, the dispersion of glycidyl ester elastomers and the reaction degree of components are mainly

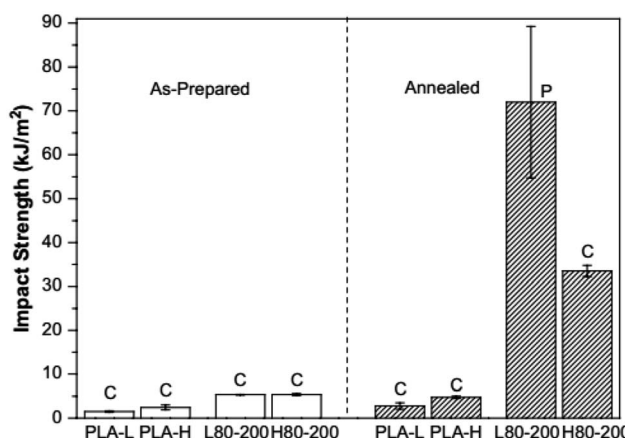


Fig. 16 Notched impact strength of PLAs and PLA/EGMA blends [C: complete break, P: partial break]. Ref. 142, copyright 2009. Reproduced with permission from Elsevier.



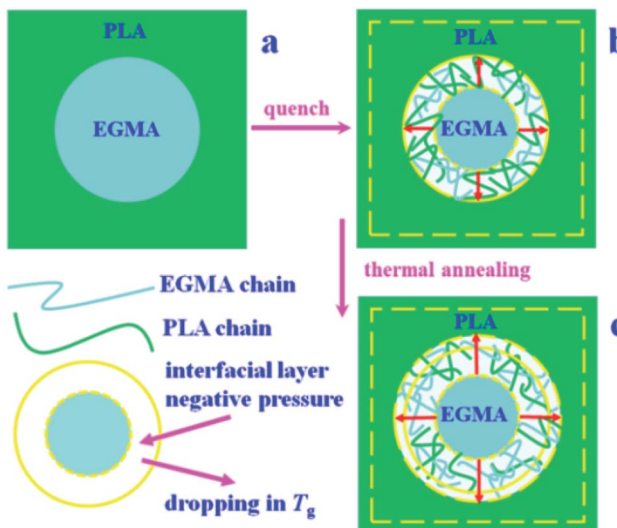


Fig. 17 Schematic illustration of generation of negative pressure in the interfacial layer causing the dropping of glass transition temperature during the quench (from a to b) and thermal annealing (from b to c) processes. Ref. 143, copyright 2018. Reproduced with permission from American Chemical Society.

controlled by diffusion in the molten state. The temperature and reaction time of molten blends have significant influences on the phase structure and mechanical properties of the resulting blends.

Mohanty and Misra *et al.*<sup>148</sup> prepared super-tough PLA/poly(ethylene-*n*-butylene-acrylate-*co*-glycidyl methacrylate) (EBA-GMA) blends *via* reactive blending and examined the toughening effects of EBA-GMA on PLA. The chemical structure of the EBA-GMA reacted with PLA was presented in Fig. 19. The blending temperature greatly influences the impact toughness of the blends. When the processing temperature exceeds 200 °C, the reaction bonding between PLA and EBA-GMA effectively increases, thereby significantly improving the interface compatibility, reducing the dispersed phase particle size, and

increasing the dispersion uniformity. The schematic of interaction between PLA/EBA-GMA blend components and the PLA/EBA-GMA interface structure was proposed in Fig. 20. At the blending temperature of 240 °C and an amount of EBA-GMA that exceeds 20 wt%, the blend has excellent super toughness. The impact strength of a PLA/EBA-GMA (75/25) blend reaches 736 J m<sup>-1</sup>, and the tensile strength and elongation at break are approximately 40 MPa and 80%, respectively.

A series of works has reported the preparation of PLA ternary blends with super toughness.<sup>144,149–152</sup> In previous works, the super toughened PLA ternary blends comprising an EBA-GMA elastomer and the zinc ionomer of ethylene/methacrylic acid (EMAA-Zn) are obtained by simultaneous dynamic vulcanization and interfacial compatibilization during reactive extrusion blending.<sup>149,150</sup> The interaction of microstructures and the interfacial adhesion on the impact performance of PLA ternary blends have been investigated in detail. The reactions during reactive blending process, together with schematic phase morphologies of the PLA/EBA-GMA/EMAA-Zn ternary blends are also shown in Fig. 21. And the phase morphology evolution as a function of EMAA-Zn content in the PLA/EBA-GMA/EMAA-Zn blends is also shown in Fig. 22. The results have shown that zinc ions catalyze the cross-linking of an epoxy-containing elastomer and promote the reactive compatibilization at the interface of PLA and the elastomer. The “salami”-like phase structure is formed in PLA ternary blends characterized by transmission electron microscopy (TEM, Fig. 23). An increase in blending temperature slightly affects the tensile properties of the resulting blends but greatly changes the impact strength. For the blends prepared by extrusion blending at 240 °C, the resulting PLA ternary blends display super toughness with moderate levels of strength and modulus. An increase in processing temperature not only improves the cross-linking degree of the elastomer but also promotes the reactivity and compatibilization of the blend components with decreasing dispersed phase particle size and particle size distribution. The impact strength and elongation at break of PLA/EBA-GMA/EMAA-Zn (80/10/10) blends reach 777.2 J m<sup>-1</sup> and 229.1%, respectively.

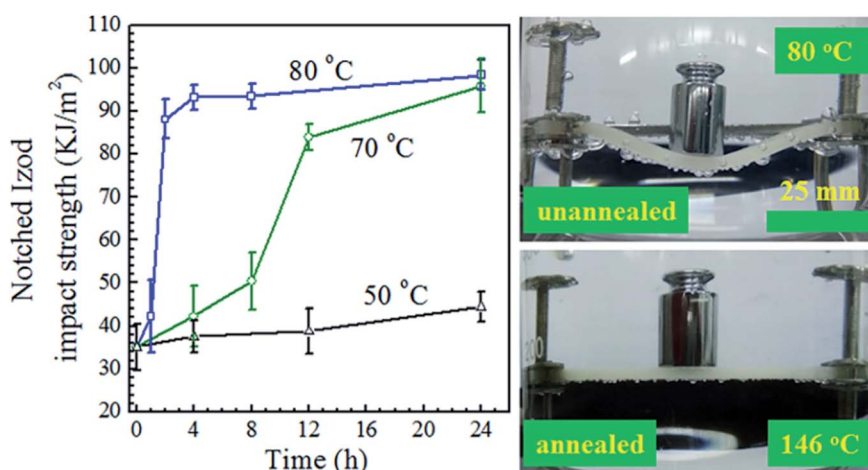


Fig. 18 Changes of notched Izod impact strength as functions of annealing time for PLA/EGMA 80/20 blend annealed at 70 and 80 °C, respectively. Ref. 143, copyright 2018. Reproduced with permission from American Chemical Society.



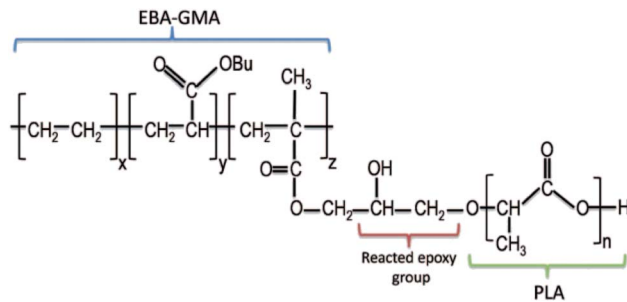


Fig. 19 The chemical structure of the EBA-GMA reacted with PLA. The hydroxyl group of PLA reacted with epoxy group was shown. Ref. 148, copyright 2016. Reproduced with permission from John Wiley and Sons.

Specially, the ternary blend with 15 wt% EBA-GMA and 5 wt% EMAA-Zn exhibits the impact strength of up to  $860 \text{ J m}^{-1}$ . The impact strength of PLA ternary blends can be further increased to  $860 \text{ J m}^{-1}$  by increasing the amount of EBA-GMA. The effects of reactive blending temperature and the ratio of EBA-GMA/EMAA-Zn on the impact toughness of PLA ternary blends have also been examined.<sup>144</sup> A sharp brittle to ductile transition (BDT) of the resulting blends occurs when the blending temperature increases to  $195\text{--}210^\circ\text{C}$ , and the EBA-GMA/EMAA-Zn ratio is equal to or larger than 1. The dispersed phase particle size and particle size distribution decrease when the processing temperature increases. The particle size of the dispersed phase ranges from  $0.8 \mu\text{m}$  to  $1.5 \mu\text{m}$ , and the impact strength of blends exceeded  $700 \text{ J m}^{-1}$ .<sup>144</sup> The effects of ionomer characteristics on the reactions and properties of PLA ternary blends prepared by reactive blending have been further investigated.<sup>151</sup> The results indicate that ionomers derived from a precursor with a high MAA content and a high degree of neutralization (DN) of ionomer tend to yield PLA blends with a superior impact strength. The zinc ion in the zinc ion-containing ionomer can promote the reaction of PLA with EBA-GMA and EBA-GMA cross-linking. Interfacial

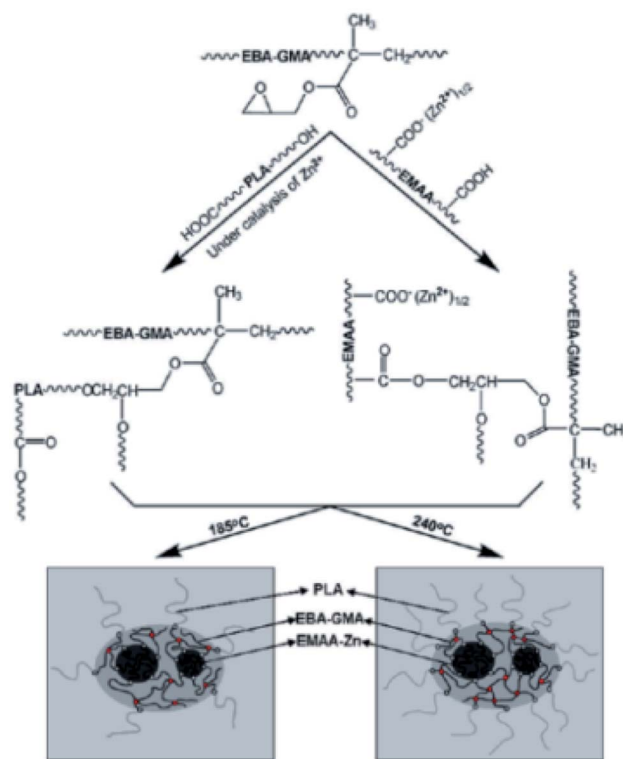


Fig. 21 Proposed reactions during reactive blending process, together with schematic phase morphologies of the PLA/EBA-GMA/EMAA-Zn ternary blends prepared at  $185$  and  $240^\circ\text{C}$ , respectively (More PLA molecules were grafted at interfaces, and higher cross-linking degree inside EBA-GMA domains resulted for the ternary blend prepared at  $240^\circ\text{C}$ ). Ref. 149, copyright 2010. Reproduced with permission from American Chemical Society.

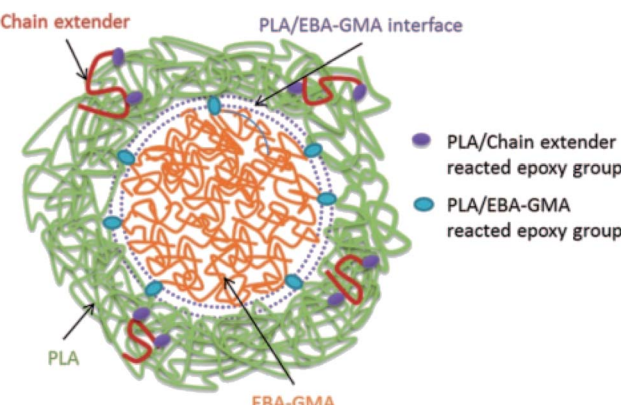


Fig. 20 A schematic of proposed interaction between PLA/EBA-GMA blend components and the PLA/EBA-GMA interface structure. Ref. 148, copyright 2016. Reproduced with permission from John Wiley and Sons.

compatibilization reaction and crosslinking reaction of EBA-GMA with ionomer during melt compounding were shown in Fig. 25. Zhang *et al.*<sup>152</sup> demonstrated the effects of metal ion type on the ionomer-assisted reactive toughening of PLA blends. They also evaluated four commercial ionomers of zinc, magnesium, sodium, and lithium ions based on an EMAA precursor in the toughening of PLA through reactive blending with epoxy-containing elastomer. Notably, the toughening effects of the metal ions of ionomers are in the order of  $\text{Zn} > \text{Mg} > \text{Li} \approx \text{Na}$ . A high blending temperature and a high elastomer/ionomer ratio promote the effective toughening of PLA ternary blends. The effects of blending temperature and ionomer content on impact strength of PLA/EBA-GMA/EMAA-M ternary blends were shown in Fig. 24. Hence, the balance between the interfacial compatibilization and cross-linking of the elastomer are critical to achieve super-tough PLA blends.

To obtain super-tough and sustainable PLA blends, Zeng *et al.*<sup>153</sup> fabricated fully bio-based and bio-based PLA/sebacic acid cured epoxidized soybean oil (VESO) blends by the dynamic vulcanization of PLA with sebacic acid (SA)-cured ESO precursors. A series of SA-cured ESO precursors (SEPs) is prepared with different carboxyl/epoxy equivalent ratios ( $R$ ), which play a critical role in obtaining super-tough PLA blends. ESO precursors with different chemical structures (from dimer



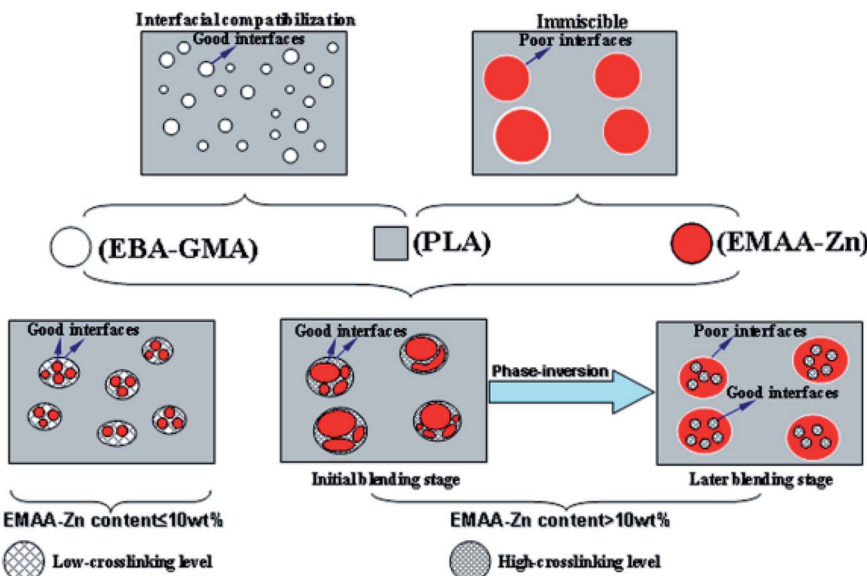


Fig. 22 Proposed morphology evolution as a function of EMAA-Zn content in the PLA/EBA-GMA/EMAA-Zn (80/20-x/x, w/w/w) blends. Ref. 150, copyright 2011. Reproduced with permission from American Chemical Society.

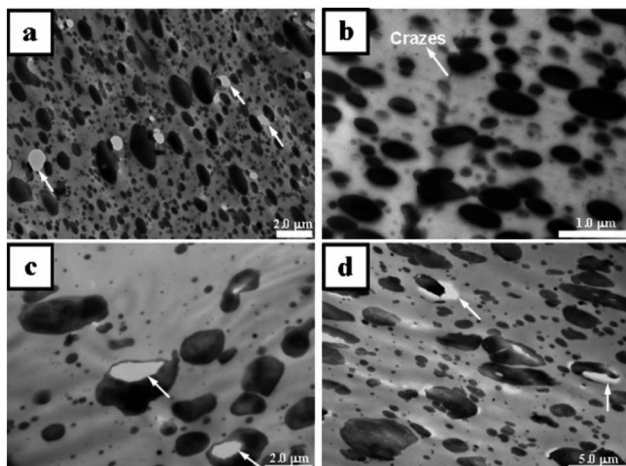


Fig. 23 TEM micrographs of stress-whitening zone: (a) PLA/EBA-GMA (80/20) binary blend, low-magnification (7500); (b) PLA/EBA-GMA (80/20) binary blend, high magnification (30 000) at the localized area; (c) PLA/EBA-GMA/EMAA-Zn (80/15/5) ternary blend; (d) PLA/EBA-GMA/EMAA-Zn (80/5/15) ternary blend. Ref. 150, copyright 2011. Reproduced with permission from American Chemical Society.

to branched and cross-linked: Fig. 26) are constructed by adjusting the ratio of SA to ESO, which can regulate PLA/VESO phase structure, dispersed phase particle size, and toughening mechanism. The results indicate that the dynamic vulcanization of SA with ESO and the reactive interfacial compatibilization simultaneously occur in molten blending, thus achieving the super toughening of PLA. A morphological study on the toughening mechanism has confirmed that the chemical structure of VESO is a key indicator of toughening efficiency. The interfacial compatibilization mechanisms and phase morphologies for the dynamic vulcanization of PLA with SEP

were shown in Fig. 27 and 28. The super toughened blends are available with an optimized *R*-value of 0.3–0.5, which is related to the uniformly dispersed morphology with suitable interfacial adhesion. The elongation at break increases to 629%, and the impact strength of the resulting blends increases to 542.3 J m<sup>-1</sup> compared with those of pure PLA (7% and 34.1 J m<sup>-1</sup>, respectively). For the PLA/VESO blends, at the optimized *R*-value, the fracture energy can be dissipated efficiently through the shear yielding of the PLA matrix induced by internal VESO cavitation to achieve super toughening.

In another approach, Dong *et al.*<sup>154</sup> investigated the effects of reactive compatibilization and crystallization behavior on the mechanical properties of PLA/EGA blends, which are prepared by subjecting PLA to reactive molten blending with an EGA ternary copolymer containing epoxy groups. The reaction between the epoxy group of EGA and the end group of PLA effectively improves the interface compatibility. The crystallization rate and crystallinity of the PLA matrix in blends are promoted by the addition of EGA. The super-tough PLA/EGA blend with the dispersed particle size of EGA is 0.67 μm, which is obtained by the addition of 20 wt% EGA. The impact strength and elongation at break of super-tough PLA/EGA blends increase to 59.8 kJ m<sup>-2</sup> and 232%, respectively.

### 3.2. Glycidyl ester graft copolymer toughened PLA

The toughening modification of a PLA material is difficult to achieve through simple blending modification because most blending systems are incompatible. Glycidyl ester materials containing epoxy groups have high reactivity and can react with the end groups of PLA, which can significantly improve the compatibility of blends. The macromolecular glycidyl ester graft copolymer is employed to toughen the PLA blend system because the graft copolymer has high reactivity, which can



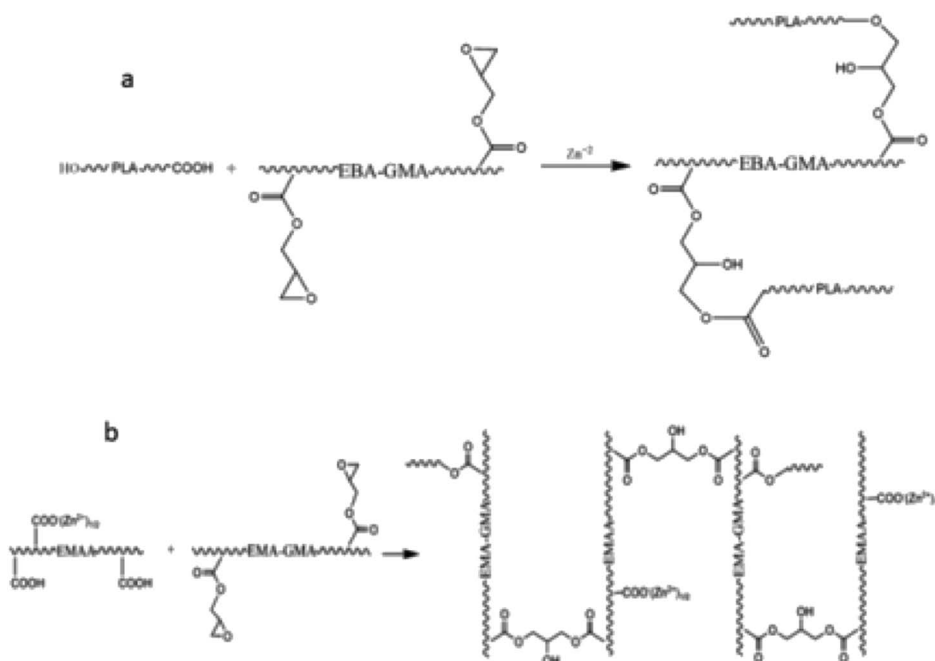


Fig. 24 (a) Interfacial compatibilization reaction catalyzed by  $Zn^{2+}$  in the ionomer (b) schematic crosslinking reaction of EBA-GMA with ionomer during melt compounding. Ref. 151, copyright 2012. Reproduced with permission from Elsevier.

improve the interfacial compatibility of PLA blend components and the strength and modulus of blends.

Zhao and Jiang *et al.*<sup>155</sup> reported the reaction of PLA with POE-g-GMA. The reactive compatibilization between PLA and POE-g-GMA and the relationship between toughness and morphology of PLA/POE-g-GMA blends have been studied. The dispersibility and the critical inter-particle distance of the dispersed domains for the super impact toughness of PLA/POE-g-GMA blend system have been determined. The dispersed phase particle size of POE-g-GMA increases, whereas the critical inter-particle distance of the dispersed domains decreases as the POE-g-GMA content increases. The morphology images were presented in Fig. 29. The impact strength of the PLA/POE-g-GMA blend increases to 87.3  $kJ\ m^{-2}$ , the tensile strength is

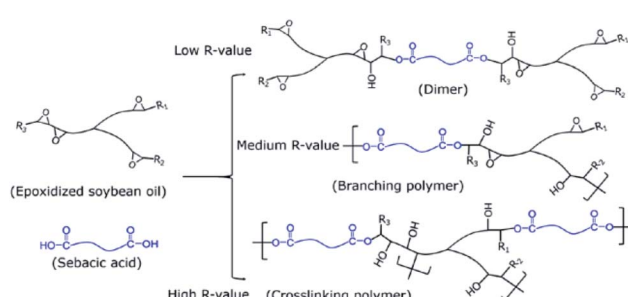


Fig. 26 Dependence of VESO structures during the curing process of ESO and SA by varying carboxyl/epoxy equivalent ratio ( $R$ ). Ref. 153, copyright 2018. Reproduced with permission from American Chemical Society.

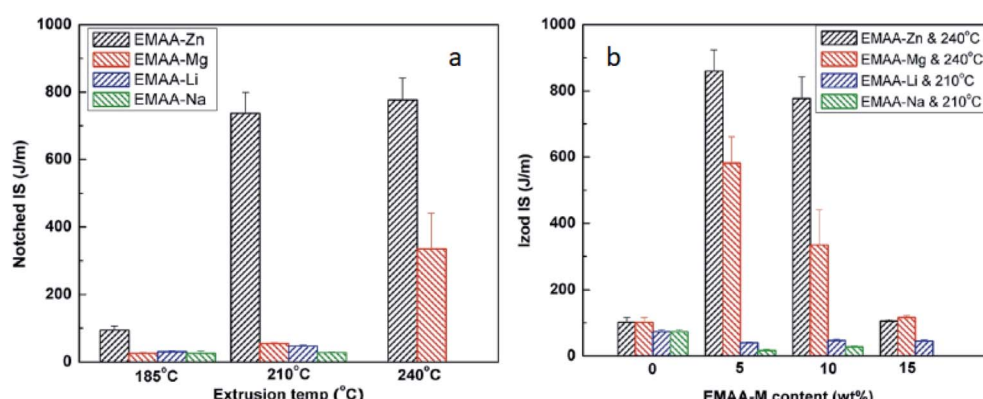


Fig. 25 (a) Effect of blending temperature on impact strength of PLA/EBA-GMA/EMAA-M (80/10/10, w/w) ternary blends (b) effect of ionomer content on impact strength of PLA/EBAGMA/EMAA-M (80/20-x/x, w/w) blends. M =  $Zn^{2+}$ ,  $Mg^{2+}$ ,  $Li^+$ , or  $Na^+$ . Ref. 152, copyright 2013. Reproduced with permission from American Chemical Society.

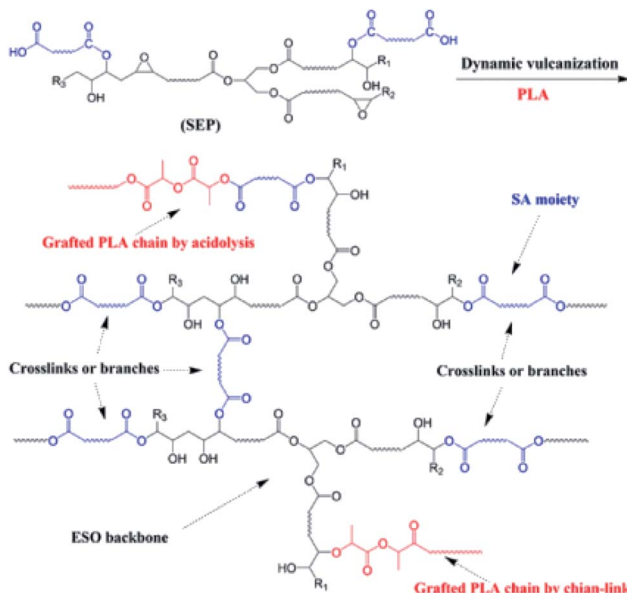


Fig. 27 Interfacial compatibilization mechanisms for the dynamic vulcanization of PLA with SEP. Ref. 153, copyright 2018. Reproduced with permission from American Chemical Society.

42.1 MPa, the particle size of the dispersed phase is 1.3  $\mu\text{m}$ , the distribution index is 1.06, and the interparticle distance ( $L$ ) is 0.35  $\mu\text{m}$ .

Zhao and Jiang *et al.*<sup>156</sup> similarly explored the compatibility and super tough of PLA blends and prepared super tough PLA/polyether-block-amide-graft-glycidyl methacrylate (PEBA-g-GMA) blends *via* reactive blending. The impact strength of PLA/PEBA-g-GMA (70/30) blends increases from 4.4  $\text{kJ m}^{-2}$  of pure PLA to 68.6  $\text{kJ m}^{-2}$ , as shown in Fig. 30. For a decreased cost, starch is incorporated into the PLA/PEBA-g-GMA binary blends to obtain biodegradable PLA/PEBA-g-GMA/starch blends with high notched impact resistance. The influences of thermoplastic starch acetate (TPSA) with different esterification degrees on the mechanical properties are examined. The results show that the impact strength of the blend increases from 11.4  $\text{kJ m}^{-2}$  to 46.9  $\text{kJ m}^{-2}$  as the esterification degree increases from 0 to 0.04 when the added amount of TPSA is 18 wt%.

Wu and Hu *et al.*<sup>157</sup> investigated the compatibility, phase structure, and component interaction of PLA and glycidyl methacrylate grafted poly(ethylene octane) (GMA-g-POE) denoted as (mPOE) blend through FTIR spectroscopy, dynamic mechanical analysis (DMA), scanning electron microscopy (SEM), and wide-angle X-ray diffraction (WAXD). The impact strength and elongation at break of PLA/mPOE (55/45, w/w) blends reach 54.7  $\text{kJ m}^{-2}$  and 282%, respectively, and the tensile strength decreases significantly. Zhang *et al.*<sup>158</sup> used ABS-g-GMA to toughen PLA and achieve the reactive compatibilization between ABS-g-GMA and PLA in the molten blending. Chemical reaction analysis suggests that compatibilization and cross-linking reactions occur simultaneously between the epoxy

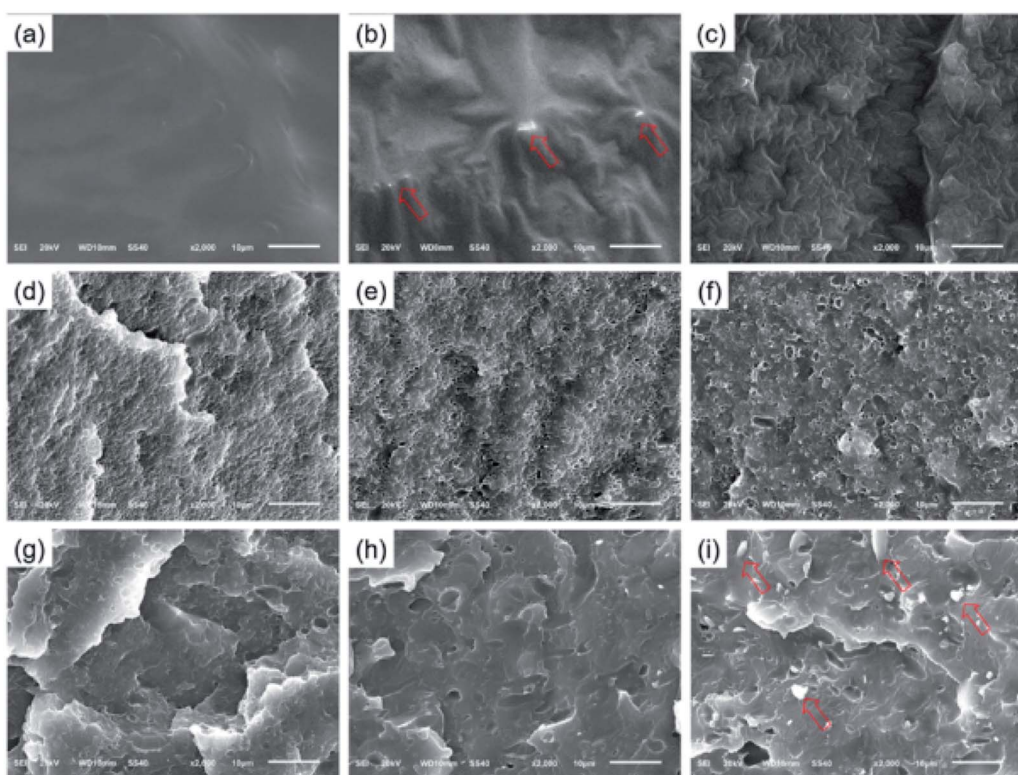


Fig. 28 SEM images for the cryofractured surfaces of neat PLA (a), PLA/ESO (b), PLA/VESO-0.2 (c), PLA/VESO-0.3 (d), PLA/VESO-0.4 (e), PLA/VESO-0.5 (f), PLA/VESO-0.6 (g), PLA/VESO-0.8 (h), and PLA/VESO-1.0 (i). Ref. 153, copyright 2018. Reproduced with permission from American Chemical Society.



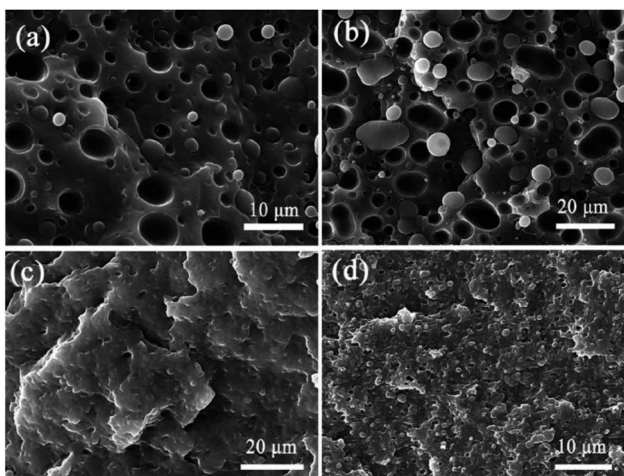


Fig. 29 SEM micrographs of freeze-fractured surfaces of the blends. (a) 10 wt% POE, (b) 20 wt% POE, (c) 10 wt% POE-g-GMA, and (d) 20 wt% POE-g-GMA. Ref. 155, copyright 2012. Reproduced with permission from John Wiley and Sons.

groups of ABS-g-GMA and the end carboxyl or hydroxyl groups of PLA. The impact strength and elongation at break of PLA/ABS-g-GMA (70/30, w/w) with the dispersed phase particle size of 0.41  $\mu\text{m}$  increase to 540  $\text{J m}^{-1}$  and 70%, respectively, as presented in Fig. 31.

Using another approach to prepare super tough PLA, Zhang and Dong *et al.*<sup>159</sup> fabricated glycidyl methacrylate-functionalized methyl methacrylate-butadiene (MB-g-GMA) copolymers *via* emulsion polymerization and blended with PLA. As the MB-g-GMA content increases, the tensile strength of the blends decrease, whereas the elongation at break and impact strength increase significantly. Super tough PLA/MB-g-GMA (72/

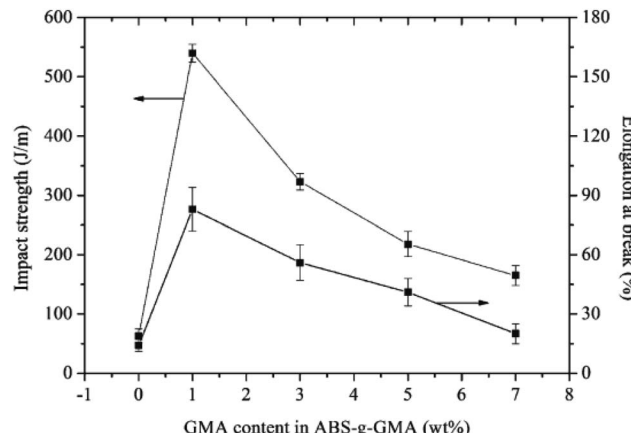


Fig. 31 Mechanical properties of PLA/ABS-g-GMA blends with different GMA contents. Ref. 158, copyright 2011. Reproduced with permission from John Wiley and Sons.

25, w/w) blends are prepared with increased impact strength and elongation of 59.5  $\text{kJ m}^{-2}$  and 200%, respectively, and decreased tensile strength of 38.1 MPa. Investigations on the toughening mechanism have revealed that shear yielding occurs in the PLA matrix as induced by the cavitation of MB-g-GMA particles.

Wu *et al.*<sup>160</sup> toughened PLA by using natural rubber graft-modified glycidyl methacrylate (NR-GMA). The interfacial reactive compatibilization of super tough PLA/NR-GMA TPV is achieved by *in situ* dynamic vulcanization with DCP as a free radical initiator (Fig. 32). Good interfacial bonding and excellent micron and nanometer dispersed phase structure effectively improve the toughness of the blends. The well-dispersed super-tough PLA-based thermoplastic vulcanizate with 20 wt% NR-GMA exhibits greatly improved notched impact strength of

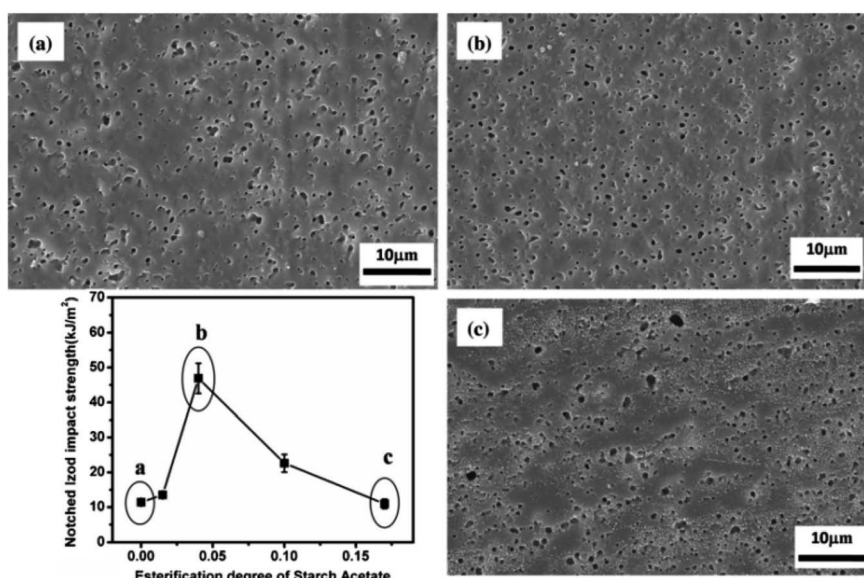


Fig. 30 SEM photographs of PLA/PEBA-g-GMA/TPSA blends (70/12/18, w/w/w) at different esterification degrees of starch acetate: (a) 0; (b) 0.04; and (c) 0.17. Ref. 156, copyright 2015. Reproduced with permission from Elsevier.

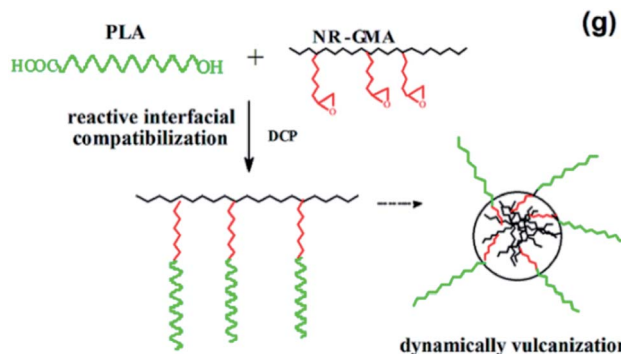


Fig. 32 Schematic diagram of interfacial compatibilization mechanism during dynamic vulcanization of PLA/NR-GMA. Ref. 160, copyright 2017. Reproduced with permission from American Chemical Society.

73.4  $\text{kJ m}^{-2}$  and an elongation yield of 136%, which represent a 26- and 33-fold increase, respectively, compared with pure PLA. This strong interfacial interaction, in combination with a fine microscale and nanoscale dispersed phase structure, is responsible for the high toughness of PLA/NR-GMA TPV. The SEM images taken at cryofracture surface of PLA/NR-GMA TPV were shown in Fig. 33.

### 3.3. PLA blends compatibilized with glycidyl ester materials

Glycidyl ester materials are used as efficient compatibilizers to toughen PLA *via* the reaction of epoxy groups in glycidyl ester materials with hydroxyl, amino, carboxyl, or anhydride. Through the interfacial bonding and improvement of interfacial compatibility, the aggregation and the particle size of the

dispersed phase decrease, thus greatly enhancing the mechanical performance of PLA blends.

To improve the modulus and strength of PLA blends, Li *et al.* blended bio-based PA11 with high modulus and strength to toughen PLA.<sup>161</sup> Ethylene glycidyl methacrylate-*graft*-styrene-*co*-acrylonitrile (EGMA-g-AS) is used to compatibilize the PLA/PA11 blends. The epoxide groups in EGMA-g-AS can react with PA11 and PLLA. Thus, EGMA-g-AS can be manipulated to locate mainly in either PA11 phase or PLLA phase by varying the blending sequence. PLA is premixed with EGMA-g-AS, and blending with PA11 is facilitated to enhance the mechanical properties. The results suggest that the blends with EGMA-g-AS are mainly found in the PA11 phase fracture in a brittle mode with low toughness. By contrast, the blend with a salami structure with EGMA-g-AS predominantly dispersed in the PLLA phase not only significantly improves the tensile ductility but also results in an excellent film impact strength while keeping a relatively high modulus. Zhao *et al.*<sup>162</sup> also reported a similar work. High-performance fully bio-based poly(lactic acid)/polyamide11 (PLA/PA11) blends are prepared by reactive blending with multi-functionalized epoxy as a reactive compatibilizer. The interfacial compatibility of PLA/PA11 blends is greatly enhanced by the reactive multifunctional epoxy compatibilizer. The fine average particle size and narrow distribution of PA11 dispersed phase can be obtained in the presence of compatibilizer. The compatibilized PLA/PA11 blend exhibits a significantly improved tensile strength, elongation at break, and notch impact strength of 77.57 MPa, 454.41%, and 9.59  $\text{kJ m}^{-2}$ , respectively, in comparison with those of pure PLA (58.26 MPa, 13.64%, and 2.97  $\text{kJ m}^{-2}$ , respectively). The enhancement and toughening are attributed to the excellent interfacial adhesion and the resultant morphologies with

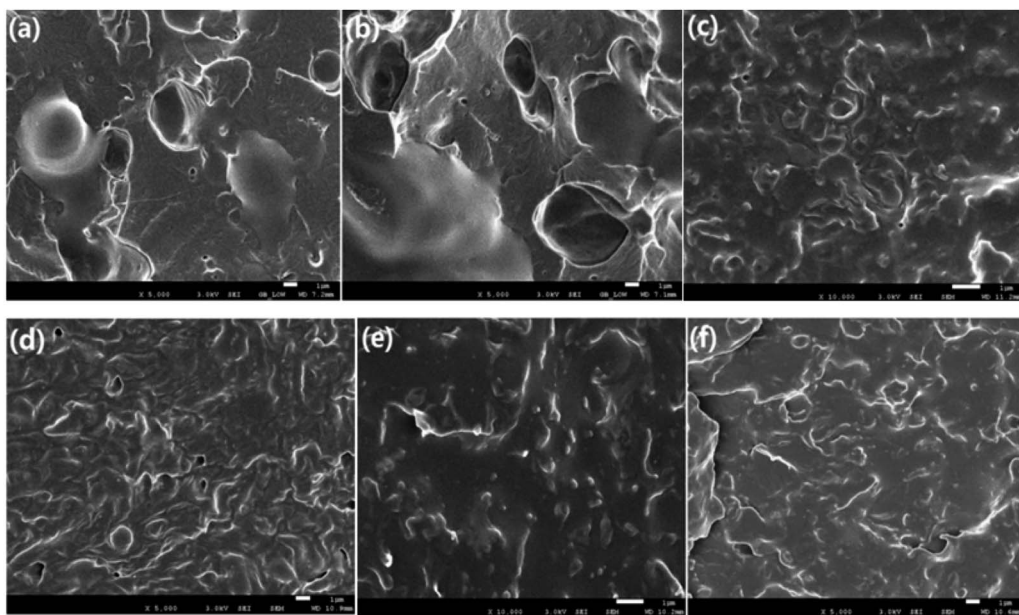


Fig. 33 SEM images taken at cryofracture surface of (a) PLA/20 wt% NR, (b) PLA/30 wt% NR, (c) PLA/20 wt% NR-GMA vulcanizate, and (e) PLA/30 wt% NR-GMA vulcanizate. SEM images impact-fracture surface of (d) PLA/20 wt% NR-GMA and (f) PLA/30 wt% NR-GMA. Ref. 160, copyright 2017. Reproduced with permission from American Chemical Society.



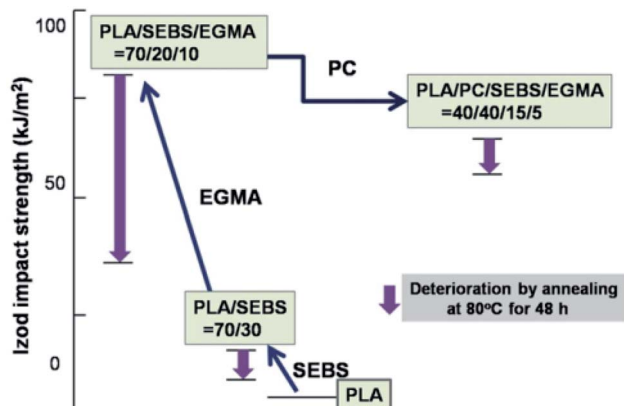


Fig. 34 Summarized stream for the development of super-tough 4 component alloy. Ref. 164, copyright 2010. Reproduced with permission from Elsevier.

transition from typical sea-island morphology to a strip form. Our work provides an effective method to greatly improve the mechanical properties with high strength and toughness, which are important for the wide application of PLA polymeric materials.

Bai and Fu *et al.*<sup>163</sup> reported a unique and facile strategy to prepare PLA blends with high toughness. PLA/EMA-GMA blends with PDLA with good properties are prepared by melt compounding. The stereocomplex (SC) crystallites are formed between poly(L-lactide) (PLLA) and poly(D-lactide), which are selectively distributed at the interface of PLLA blends, and SC exhibits a great potential for application to substantially enhance the crystallization rate of PLLA-based materials as an eco-friendly nucleating agent. The results demonstrate the

dispersion and distribution of SC crystallites within the PLLA matrix by using elastomeric E-MA-GMA as a carrier for the incorporation of PDLA. SC simultaneously improves the nucleation efficiency of PLA matrix and interface bonding. Therefore, the impact toughness of PLA/EMA-GMA (85/15) blends are effectively increased to  $35.1 \text{ kJ m}^{-2}$ .

Nishitsuji *et al.*<sup>164</sup> used hydrogenated SEBS to toughen PLA by the addition of EGMA as a compatibilizer to improve the compatibility of PLA/SEBS blends, suggesting an obvious toughening effect. The impact strength for the development of super-tough component alloy was shown in Fig. 34. The impact strength and elongation at break of PLA/SEBS/EGMA (70/20/10) blends significantly increase to  $92 \text{ kJ m}^{-2}$  and 185%, respectively, but the tensile strength and stiffness decrease sharply. Therefore, PC is incorporated into a PLA/SEBS/EGMA blend system to balance the toughness, heat resistant, and stiffness of PLA blends. The tensile modulus of PLA/PC/SEBS/EGMA (40/40/15/5) is the same as that of pure PLA, and the heat resistance is increased. The impact strength exceeds  $60 \text{ kJ m}^{-2}$ , and the elongation at break reaches approximately 90%.

Fu *et al.*<sup>165</sup> investigated the compatibility and crystallization behavior of super tough PLA. Polyolefin block copolymer elastomer is blended to toughen PLA by adding EMA-GMA as a compatibilizer to improve the compatibility of blend components. When 3 wt% EMA-GMA is added, the dispersed phase size of EMA-GMA decreases from  $0.96 \mu\text{m}$  to  $0.38 \mu\text{m}$ , and several nanoparticles with a size range of 50–100 nm are formed. Then, the particle size of the dispersed phase is increased by  $0.76 \mu\text{m}$  after annealing at  $90^\circ\text{C}$  for 5 h. High crystallinity, large size of elastomer-phase droplets, and thickening interfacial layer resulted from quiescent annealing, indicating a more thermodynamically favorable compatibility

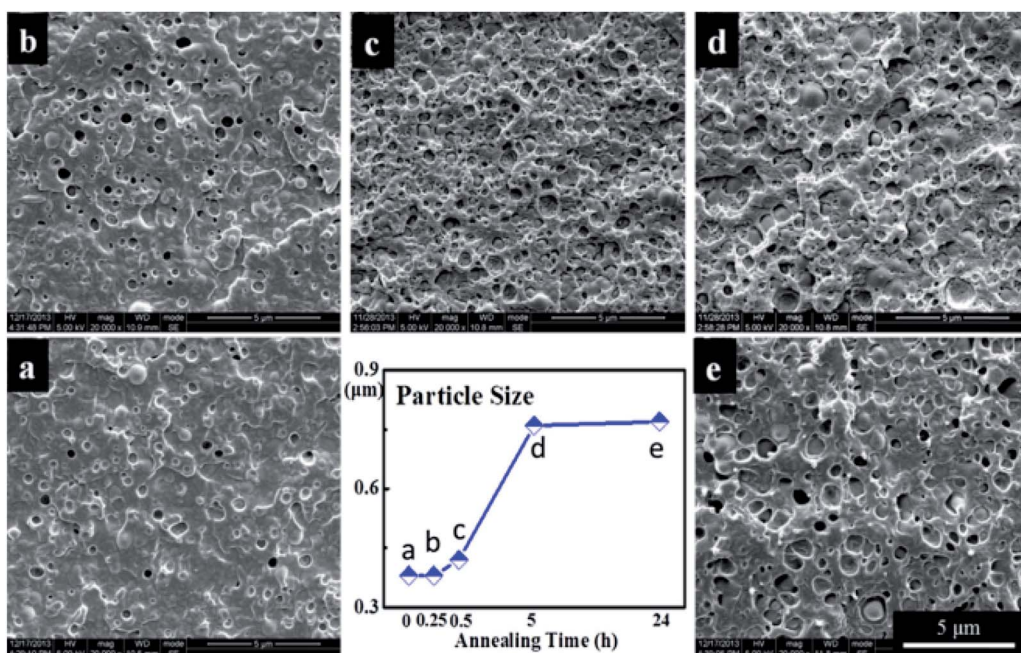


Fig. 35 SEM micrographs of PLA/OBC/EMA-GMA 90/7/3 blends with various annealing time: (a) 0 h, (b) 0.25 h, (c) 0.5 h, (d) 5 h, (e) 24 h and the number average particle size as a function of annealing time. Ref. 165, copyright 2014. Reproduced with permission from Elsevier.



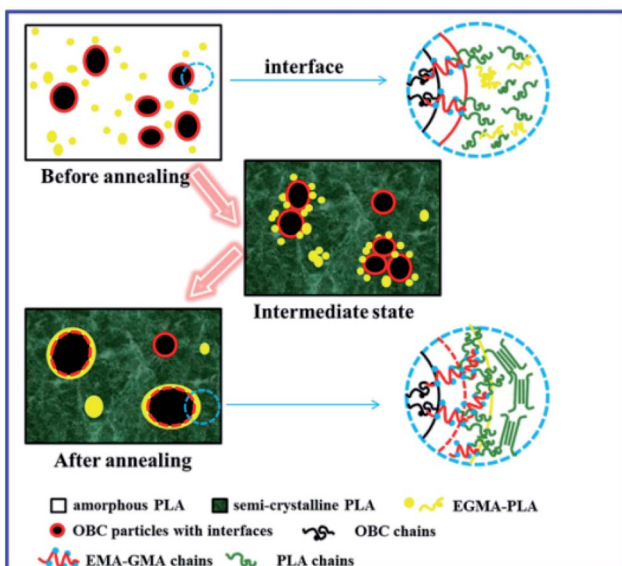


Fig. 36 Schematic diagram of micro-morphology evolution of PLA/OBC/EMA-GMA blends during annealing. Ref. 165, copyright 2014. Reproduced with permission from Elsevier.

and morphology. The phase morphology of PLA/OBC/EMA-GMA blends with various annealing time was shown in Fig. 35. The ternary blend of PLA/OBC/EMA-GMA (90/7/3) experiences a quiescent thermal annealing at 90 °C for 5 h. The impact strength of 64.2 kJ m<sup>-2</sup> is increased by 25 times compared with that of pure PLA, and a tensile strength of about 55 MPa can preserve as 87% of pure PLA. The schematic diagram of micro-morphology evolution of PLA/OBC/EMA-GMA blends during annealing was proposed in Fig. 36.

Wu *et al.*<sup>166</sup> prepared super-tough PLA/PBAT blends *via* reactive blending by using the active epoxy group of EMA-GMA

as a reactive compatibilizer, which effectively improves the compatibility of blend components. The unique dispersed phase with a core-shell structure is formed in the blend system, and the phase morphology is transferred from a sea-island structure to a continuous structure. The strong interfacial bonding between the matrix and dispersed phase and the high shear yield of PLA matrix significantly improve the toughness of blends. The evolution of phase morphology of PLA/PBAT/EMA-GMA blends was presented in Fig. 37. The impact strength and elongation at break of PLA/PBAT/EMA-GMA (75/10/15) blends reach 61.9 kJ m<sup>-2</sup> and 278%, respectively, whereas the tensile strength decreases to 37 MPa.

Zhao *et al.*<sup>167</sup> reported fully biodegradable PLA/PBAT blends with high toughness. Different ratios of PLA/PBAT blends are prepared by melt blending in the presence of a multifunctional epoxy oligomer as a reactive compatibilizer. The reaction mechanism of the blends was proposed in Fig. 38. During reactive blending, a compatibilizer can react with PLA and PBAT chains to increase melt elasticity, viscosity, and compatibility, as indicated by rheological curve and Har plot analyses. Adding a compatibilizer improves the tensile and impact toughness at all ratios of PLA/PBAT blends. The elongation at break and the notched impact strength of blends reach 579.9% and 29.6 kJ m<sup>-2</sup>, which are 75.3 and 12.3 times of that of pure PLA, respectively. The shear yield deformation of the impact fractured surface and the fuzzy phase interface of a cryofractured surface shows that high toughness can be attributed to the reaction of the epoxy group of a reactive compatibilizer with the terminal carboxyl and hydroxyl groups of PLA and PBAT to form many branched copolymers. And the toughening mechanism of PLA/PBAT blends was shown in Fig. 39.

To improve the toughness of PLA, Misra and Mohanty *et al.*<sup>168</sup> fabricated multiphase blends of PLA, EMA-GMA terpolymer, and a series of renewable poly(ether-*b*-amide)

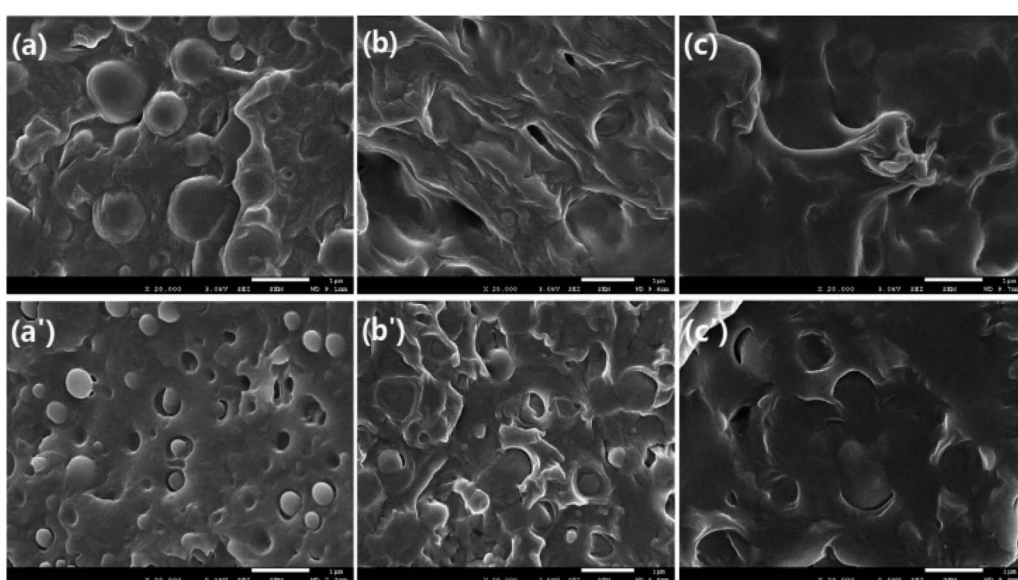


Fig. 37 SEM images of PLA/PBAT (90/10) (a and a') and PLA/PBAT/EMA-GMA (82/10/8) (b and b') and PLA/PBAT/EMA-GMA (75/10/15) (c and c') blends at impact fracture and cryofracture surfaces. Ref. 166, copyright 2017. Reproduced with permission from Elsevier.



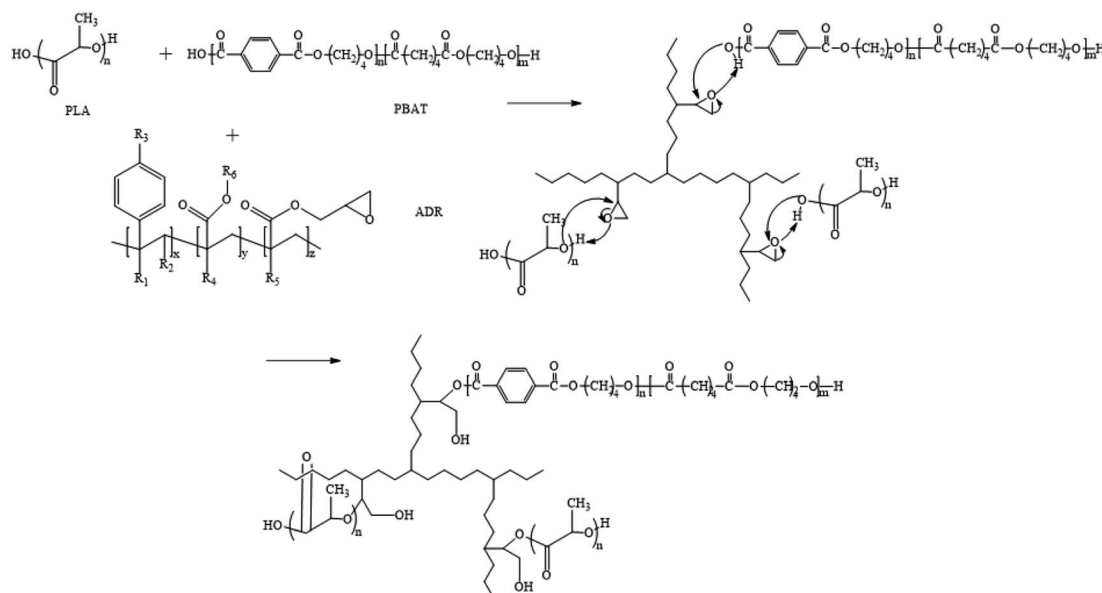


Fig. 38 Predicted mechanism of the reaction between polyester (PLA or PBAT) and multifunctional epoxy oligomer. Ref. 167, copyright 2019. Reproduced with permission from Elsevier.

elastomeric copolymer (PEBA) through reactive melt blending. The correlation between the morphological characteristics and their significant effects on the improved toughness of multiphase blends is investigated and elaborated. A unique “multiple stacked structure” with the partial encapsulation of EMA-GMA and PEBA minor phases is observed in PLA/EMA-GMA/PEBA (70/20/10), revealing the importance of particular blend composition in enhancing toughness. The synergistic effect of good interfacial adhesion and interfacial cavitation followed by the massive shear yielding of the matrix is attributed to the enormous toughening effect observed in these multiphase blends. Detail structure of the PLA/EMA-GMA/PEBA (70/20/10) blend with the SEM and AFM phase images, and the schematic structure were presented in Fig. 40 and 41. Super tough PLA/EMA-GMA/PEBA (70/20/10) blends with an impact strength of  $500 \text{ J m}^{-1}$ , elongation at break of 72.7%, and tensile strength of approximately 45 MPa are achieved.

Glycidyl ester materials can be used as effective reactive compatibilizers and high-efficient toughening components.

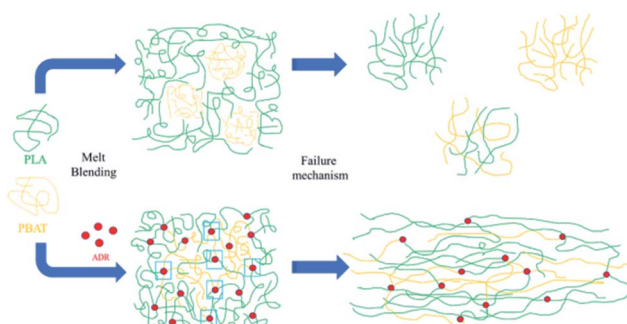


Fig. 39 Toughening mechanism of PLA/PBAT blends. Ref. 167, copyright 2019. Reproduced with permission from Elsevier.

During melt blending, chemical reactions with blend components occur at the interface, and block or graft copolymers can be generated *in situ* to reduce interfacial tension and form a stable phase structure.<sup>169,170</sup> A copolymer forms during reactive compatibilization at the interface of polymer blends, while the kinetic barrier of the interfacial diffusion of the copolymer phase decreases. The efficiency of compatibilization improves. The compatibilization of PLA blend systems with a glycidyl ester material is an effective method to improve the interface compatibility of blend components and the mechanical properties of materials. It is an important research direction for developing new types of highly reactive compatibilized systems

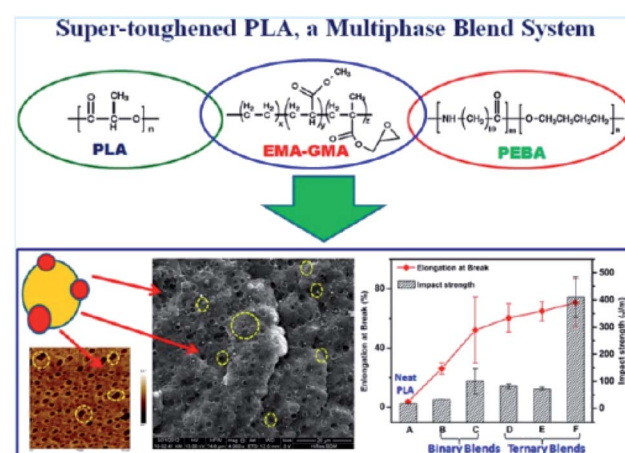


Fig. 40 The relationship of interface adhesion, morphology with mechanical properties of PLA/EMA-GMA/PEBA blends. Ref. 168, copyright 2014. Reproduced with permission from American Chemical Society.



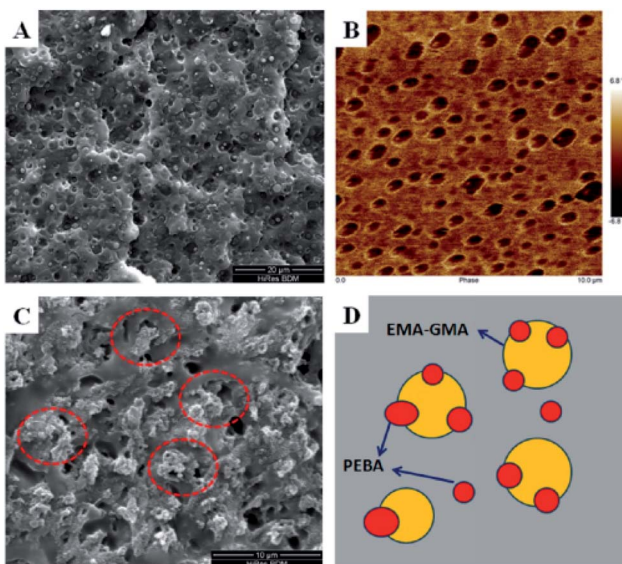


Fig. 41 Detail structure of the PLA/EMA-GMA/PEBA (70/20/10) blend with the SEM and AFM phase images: (A) SEM images of cryofractured surface (4000 $\times$ ), (B) AFM image, (C) SEM images of cryofractured surface after etched (10 000 $\times$ ), and (D) the schematic structure. Ref. 168, copyright 2014. Reproduced with permission from American Chemical Society.

and studying the structure and properties of PLA-based reactive multiphase blend systems.

#### 4. High-performance PLA/traditional petroleum-based plastic blends

Traditional petroleum-based polymer materials have been widely used in daily and industrial fields. Traditional petroleum-based polymer materials have been used to modify PLA for improving its mechanical properties, reducing the cost of PLA materials, and contributing to the application promotion of PLA materials, which are essential for the research and application of biodegradable materials. The molecular structures of traditional petroleum-based polymer materials are different from that of PLA. Preparing high-performance PLA blends is difficult because of poor miscibility and compatibility. The interfacial compatibility between components needs to be improved effectively by adding block/graft copolymers and reactive compatibilizers. In this manner, the mechanical properties of PLA/petroleum-based polymer blends can be improved, and the application field of PLA materials can be broadened. Table 5 shows the properties of highly and super tough PLA-based blends.

Table 5 Mechanical performance results for highly and super toughened PLA/traditional petroleum-based polymer blends<sup>a</sup>

Comments	Impact strength/(kJ m <sup>-2</sup> )	Tensile strength/(MPa)	Elongation at break/(\%)	Ref.
PLA/LLDPE/PLLA- <i>b</i> -PE (80/20/5)	760J m <sup>-1</sup>	24.3	31	172
PLA/LLDPE/ <i>d,L</i> -PLA- <i>b</i> -PE (80/20/5)	730J m <sup>-1</sup>	23	26	
PLA//LLDPE/PLLA- <i>b</i> -PEP (80/20/5)	710J m <sup>-1</sup>	23	19	
PLA/LLDPE/ <i>d,L</i> -PLA- <i>b</i> -PEP (80/20/5)	660J m <sup>-1</sup>	22.6	27	
PLLA/LLDPE/PLLA- <i>b</i> -PE(5-30) (80/20/5)	510J m <sup>-1</sup>	—	—	171
PLLA/LLDPE/PLLA- <i>b</i> -PE(30-30) (80/20/5)	660J m <sup>-1</sup>	—	—	
PLA/EVA (80/20)	64	45	340	173
PLA/EVA (70/30)	83	37	400	
PLA/EVA/DCP (40/60/1)	—	20	300	174
PLA/EVA/AD (40/60/1)	—	21	200	175
PLA/EVA50/starch (50/23/23)	~13	~20	>100	177
PLA/EVA (0.65/0.35 v/v)	53.73	35	164	176
PLA/ACR3 (80/20)	77.1	31.8	93.9	178
PLA/ACR (80/20)	77.2	36.9	79.3	179
PLA/ACR (75/25)	98.0	33.0	85.1	
PLA/BPM (85/15)	—	48.4	134.7	180
PLA/MBS (85/15)	44.7	42.7	360	181
PLA/MBS (80/20)	83.1	38.1	334	
PLA/MBS (75/25)	97.2	33.9	300	
PLA/PEGDA (85/15)	50	490	140	182
PLA/PPA (75/25)	106.5	14.4	410	183
PLA/MAPEG/L101 (79.75/20/0.25)	60	—	241	184
PLA/MAPEG/L101	77.5	—	279	
PLA/L101/AcetylPEG (80/1/20)	101.6	—	155	185
PLA/PDLA-PEPG-PDLA (65/35)	—	—	424	186
PLA/PEG-PPG (90/10)	100 (65)	30	286	187
PLA/PETG/MDA (80/20/3)	—	~50	~90	188
PLA/PC/ADR/BPM (70/30/0.3/5)	50	57	—	189
PLA/ABS/RC (50/50/3)	—	64.8	196.2	190
Biaxially oriented PLA film (BOPLA)	—	180	80	191
PLA/PBA (95/15)	—	41.02	174.52	192
PLA/PBA (89/11)	—	40.82	~173.98	

<sup>a</sup> The values in brackets ( ) are the impact strength corresponding to neat PLA.



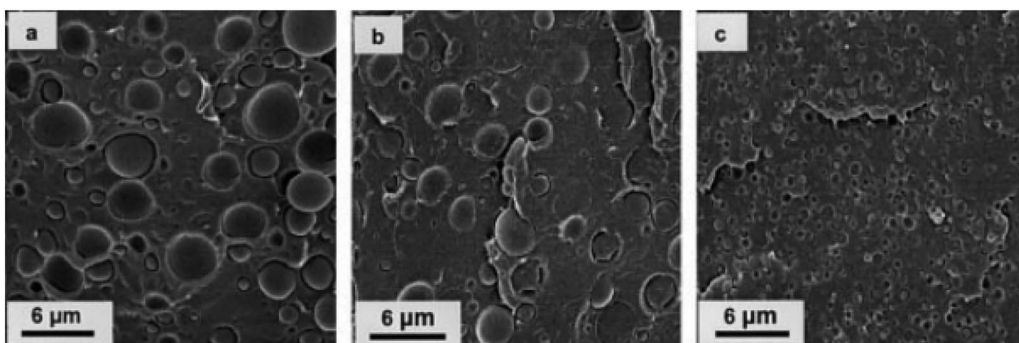


Fig. 42 Representative SEM images of cryofractured surfaces of (a) 80 : 20 PLA/LLDPE; (b) 80 : 20 : 5 PLA/LLDPE/PLLA-PE(5-30); (c) 80 : 20 : 5 PLA/LLDPE/PLLA-PE(30-30). Ref. 171, copyright 2003. Reproduced with permission from John Wiley and Sons.

#### 4.1. Super tough PLA/polyolefin blends

Hillmyer *et al.*<sup>171,172</sup> analyzed the influence of PE types with various values of modulus and toughness on the structure and mechanical properties of PLA/PE blends to achieve super tough PLA/PE blends. They prepared a series of PLA/PE with different modulus blends by melt blending with different PLA-polyolefin block copolymers (PLLA-PE) as compatibilizers. They suggested that all the compatibilizers of PLA-polyolefin block copolymers effectively improve the interfacial adhesion between PLA and PE. In addition, the use of linear low density polyethylene (LLDPE) with a modulus of 8 MPa and elongation at break of 960% is conducive to the preparation of super tough blends. The PLA/LLDPE/PLLA-PE blends containing 80 wt% PLA, 20 wt% LLDPE, and 5 wt% PLLA-*b*-PE exhibit super toughness with impact strength and elongation of break reaching 760 J m<sup>-1</sup> and 31%, respectively, but the tensile strength is greatly reduced to 24.3 MPa. The phase morphologies evolution of the blends was presented in Fig. 42. And the research works

suggested that subtle differences in the degree of adhesion between the matrix and dispersed phase can have a significant influence on the resultant toughening in these blends.

Ma *et al.*<sup>173</sup> studied super tough effects by investigating the effect of ethylene-*co*-vinyl acetate (EVA) containing a high vinyl acetate content on compatibility in PLA/EVA blends. The dispersibility of EVA in PLA matrix tends to improve as a result of the inclusion of EVA with a high vinyl acetate content of 50–60%. With the inclusion of EVA with an amount exceeding 20 wt%, PLA/EVA blends exhibit super toughness with impact strength and elongation at break reaching 64 kJ m<sup>-2</sup> and 340%, respectively. Moreover, as the amount of EVA increases, the toughness of PLA/EVA blends can be further enhanced, but the tensile strength and modulus decrease. When PLA/EVA blends are subjected to force, the PLA matrix generates shear yield without crazing. The phase morphology of stretched PLA/EVA blends was presented in Fig. 43. Therefore, internal cavities and matrix yield are the main toughening mechanisms. Ma<sup>174</sup> and Chen<sup>175</sup> utilized dicumyl peroxide (DCP) and 2,5-dimethyl-2,5-di(*tert*-butylperoxy) hexane (AD) as free radical initiators to prepare high-toughness PLA/EVA bio-based TPV. They indicated that EVA is cross-linked during melt blending, and the reactivity of EVA with free radicals is higher than that of PLA. The phase morphologies of PLA/EVA blends evolve from a typical sea-island structure to a co-continuous-like morphology, and the phase inversion is mainly due to the increased viscosity of the EVA phase caused by dynamic cross-linking. Maiti *et al.*<sup>176</sup> obtained similar results when they prepared high-toughness PLA/EVA blends and investigated the effect of EVA volume fraction on the phase structure and properties of PLA/EVA blends. The EVA droplets of dispersed phase become elongated from spherical-shaped EVA particles. The size increases to 1.91 μm, the critical value of ligament thickness ranges from 0.54 mm to 0.27 mm, and volume fraction varies from 0.06 to 0.35 at high EVA contents. Subsequently, the impact strength and elongation at break of PLA/EVA blends reach 53.73 kJ m<sup>-2</sup> and 164%, respectively, but the tensile strength decreases to 35 MPa. The fibrillation of EVA, crazing, and the shear yield of PLA are the main mechanisms to achieve the super toughness of PLA/EVA blends. Ma *et al.*<sup>177</sup> fabricated PLA/EVA/thermoplastic starch (TPS) blends with high toughness *via* the synergistic effect of

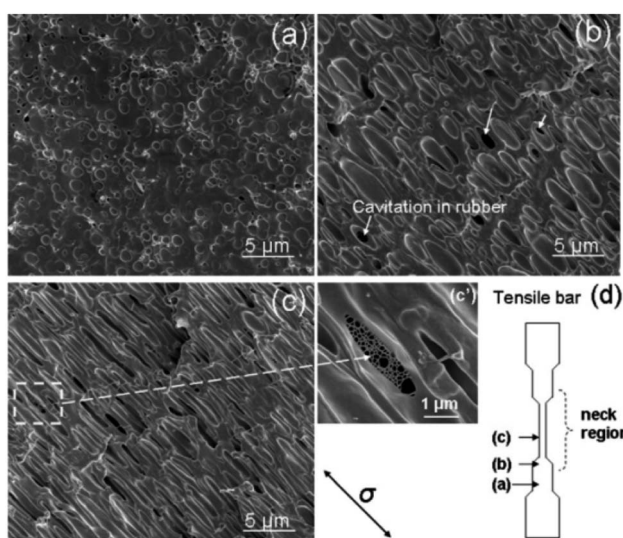


Fig. 43 Morphology of stretched PLA/EVA50 (80/20) blends taken from different zones of a tensile bar after necking as schematically indicated in (d). Ref. 173, copyright 2012. Reproduced with permission from Elsevier.

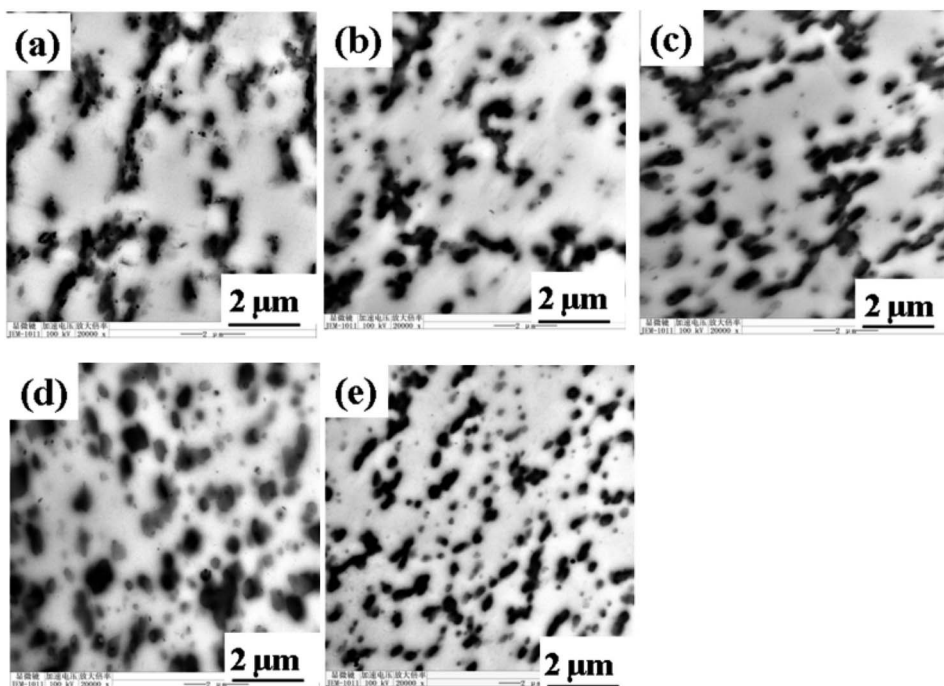


Fig. 44 TEM photographs for PLA/ACR blends: (a) PLA/ACR1, (b) PLA/ACR2, (c) PLA/ACR3, (d) PLA/ACR4, and (e) PLA/ACR5. Ref. 178, copyright 2015. Reproduced with permission from John Wiley and Sons.

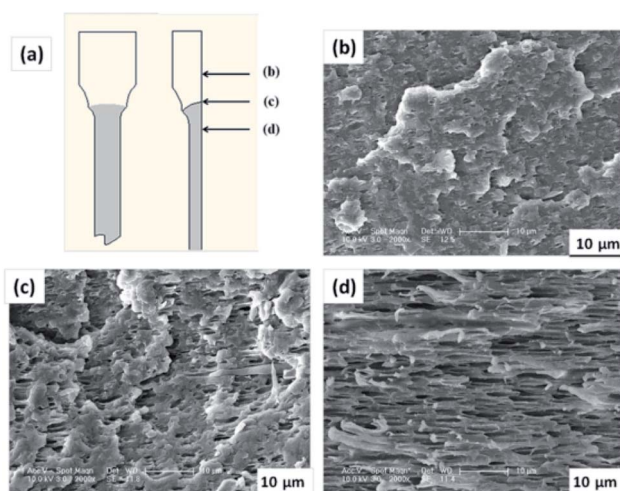


Fig. 45 (a) The internal locations of the tensile sample of PLA/ACR3 for SEM analysis, (b) morphology in location (b), (c) morphology in location (c), and (d) morphology in location (d). Ref. 178, copyright 2015. Reproduced with permission from John Wiley and Sons.

plasticization and compatibilization by using the reactive compatibilization method. They utilized glycerol to plasticize starch and improve the processability and dispersibility of starch and maleic anhydride (MA) as a reactive compatibilizer to enhance interfacial compatibility. The synergistic effect results in a significant reduction in starch particle size and an increase in interfacial adhesion. Starch plasticized with glycerol is uniformly distributed in ternary blends with a dimension of 0.5–2 μm. Furthermore, EVA-coated starch or a starch-in-EVA

type of morphology is observed in the reactively compatibilized PLA/EVA/TPS blends in which the co-continuous phase involves an increase in MA content.

#### 4.2. PLA/impact modifier blends

Zhang and Dong *et al.*<sup>178</sup> prepared methyl methacrylate-ethyl acrylate core-shell copolymer (ACR) *via* seed emulsion polymerization and used it as an impact modifier for melt blending to toughen PLA. The core-shell ratio has an important effect on the properties of PLA-based materials. The effect of the core-shell ratio of ACR with a core-shell weight ratio ranging from 85.5/14.5 to 71.9/28.1 on toughening PLA has been investigated. The particle size and particle size distribution of ACR can be controlled *via* seed emulsion polymerization. The agglomeration of ACR particles can be overcome through a synthesis process. When the ACR core-shell ratio is 79.2/20.8, the PLA/ACR (80/20) blend has partial compatibility, and the impact strength and elongation at break reach 77.1 kJ m<sup>-2</sup> and 93.9%, respectively. However, the tensile strength is relatively low, which is only 31.8 MPa. TEM (Fig. 44) and SEM (Fig. 45) results suggest that the PLA/ACR (80/20) blend has partial compatibility, and ACR is dispersed uniformly in the PLA matrix. Plastic deformation and cavitation are the major mechanisms of toughening PLA/ACR blends.

From an industrial point of view, Zhang and Dong *et al.*<sup>179</sup> employed industrial-grade ACR (industrial grade KM-365) containing a PBA core and a PMMA shell to toughen PLA and investigated the isothermal crystalline behavior, rheological behavior, and compatibility of PLA/ACR blends. The isothermal crystalline behavior reveals that the incorporation of ACR

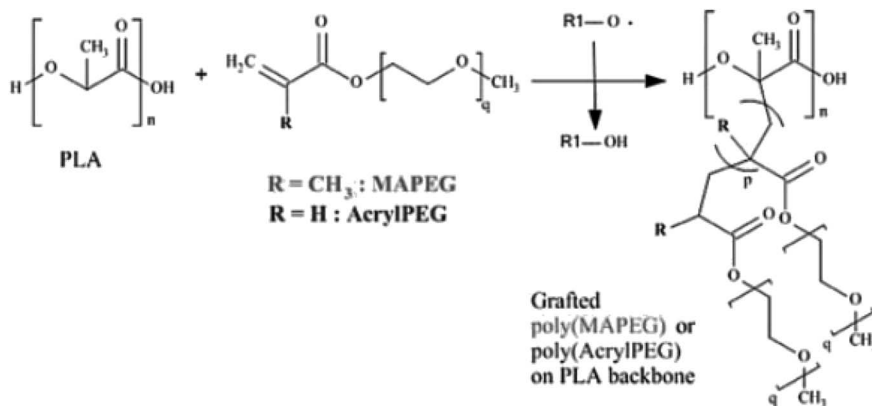


Fig. 46 *In situ* chemical reactions taking place during the reactive extrusion of the ternary reactive blends PLA/MAPEG/L101 and PLA/AcrylPEG/L101. Ref. 184, copyright 2013. Reproduced with permission from John Wiley and Sons.

significantly prevents the crystallization of PLA. The dispersibility of ACR in the PLA matrix and the compatibility and mechanical properties of PLA/ACR blends can be improved by adding ACR. The inclusion of 20 wt% ACR leads to an improvement in the impact strength of PLA from  $2.3 \text{ kJ m}^{-2}$  to  $77.2 \text{ kJ m}^{-2}$ , and the elongation at break of PLA increases from 5.7% to 79.3%. The impact strength and elongation at break of PLA/ACR blends further improve to  $98.0 \text{ kJ m}^{-2}$  and 85.1%, respectively, by the inclusion of 25 wt% ACR. The tensile strength and Young's modulus of PLA/ACR remarkably decrease.

Ge *et al.*<sup>180</sup> conducted similar works on PLA/acrylic impact modifier (BPM) blends and investigated the thermal properties, melting behaviors, and interfacial compatibility of PLA/BPM blends fabricated *via* the melt blending method by using a laboratory twin-screw extruder. Mechanical test results show that the flexibility of PLA/BPM blends is relatively higher than that of pure PLA. However, the notched Izod impact strength improves only when the BPM content is higher than 15 wt%. Dong *et al.*<sup>181</sup> used methyl methacrylate–butadiene–styrene (MBS) copolymer as an effective impact modifier to toughen PLA and enhance the impact strength. They studied the mechanical properties, crystallization behaviors, and phase structures and compatibility of PLA/MBS blends containing 5–25 wt% MBS. DSC, DMA and SEM micrographs indicate that MBS can act as an effective heterogeneous nucleation agent for PLA and significantly improve the crystallinity degree of PLA. Meanwhile, PLA and MBS are compatible. As the MBS content increases to 25 wt%, the tensile strength of the blends decrease to 33.9 MPa. However, the elongation at break and impact strength increased significantly to 300% and  $97.2 \text{ kJ m}^{-2}$ , respectively. Therefore, shear yielding occurs in the PLA matrix as induced by the cavitation of MBS particles.

#### 4.3. PLA/polyols plastics blends

Wang *et al.*<sup>182</sup> prepared super tough biodegradable PLA blends *via* the reactive blending of PLA with a poly(ethylene glycol) diacrylate (PEGDA) monomer. During blending, the acrylic group of PEGDA can be polymerized *via* a free radical reaction,

and cross-linked PEGDA (CPEGDA) is *in situ* formed. The *in situ* polymerization of PEGDA leads to a phase-separated morphology with CPEGDA as the dispersed particle phase dominates. As the amount of CPEGDA increases, the viscosity and elasticity of the blend increase. Moreover, the impact strength and elongation at break of PLA/CPEGDA blends reach  $50 \text{ kJ m}^{-2}$  and 140%, respectively, whereas tensile strength decreases to 49 MPa. The significant improvement in toughness can be attributed to the fine dispersion state of CPEGDA particles in the PLA matrix with a mass-average particle diameter of  $0.35 \mu\text{m}$  and a size polydispersity of 1.5. The toughening mechanisms of PLA/CPEGDA blends can be ascribed to the joint contributions of crazing and shear yielding during deformation based on the analysis of stress-whitening and fracture surface and the measurement of matrix ligament thickness.

Dong *et al.*<sup>183</sup> investigated the thermal, mechanical, and rheological properties of the PLA/poly(1,2-propylene glycol adipate) (PPA) blends fabricated *via* melt blending in a Thermo-Haake mixer. The morphological results of PLA/PPA blends show that PPA is compatible with PLA. Mechanical results indicate that the brittle–ductile transition of the blends is obtained when the PPA content varies from 15% to 20%. The impact strength changes significantly from  $4.7 \text{ kJ m}^{-2}$  for pure PLA to  $106.5 \text{ kJ m}^{-2}$  for PLA/PPA (75/25) blend. Furthermore, the elongation at break increases from 5.7% of pure PLA to 410% for the PLA/PPA (75/25) blend. As the flexibility of the PLA/PPA blends increases, tensile strength, yield stress, and modulus decrease.

Hassouna and Dubois *et al.*<sup>184</sup> tuned the toughness of PLA by melt mixing PEG methyl ether methacrylate (MAPEG) and PEG methyl ether acrylate (AcrylPEG) with PLA in the presence of 2,5-dimethyl-2,5-di(*tert*-butyl peroxy) hexane (L101) as a free radical initiator. Two unsaturated functional reactive PWG plasticizers of MAPEG and AcrylPEG can be successfully homo-oligomerized and grafted onto PLA chains *via* a reactive extrusion process. Fig. 46 shows the *in situ* chemical reactions routes during the reactive extrusion of the ternary reactive blends. The results reveal that the grafting efficiency of AcrylPEG is much higher than that of MAPEG. The functional end-group of the plasticizer

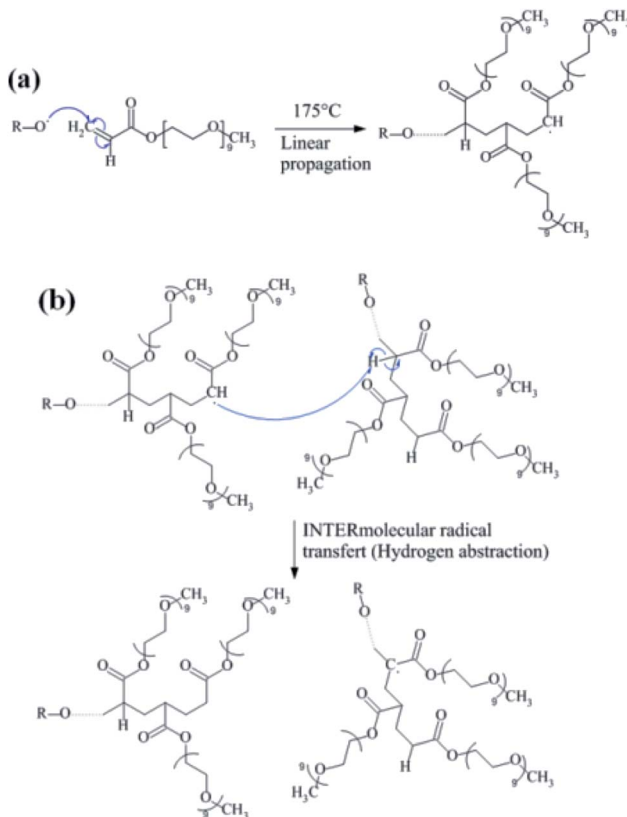


Fig. 47 Free-radical initiation and linear propagation (a); intermolecular free radical hydrogen abstraction and radical transfer (b). Ref. 185, copyright 2015. Reproduced with permission from John Wiley and Sons.

significantly affects the grafting efficiency mainly because of the difference in the reactivity between methacrylic and acrylic functional groups. The elongation at break and impact strength of blends significantly increase compared with that of pure PLA. For PLA/AcrylPEG binary blends, the inclusion of 20 wt% AcrylPEG into PLA improved the elongation at break and impact strength of pure PLA from 4% and  $2.8 \text{ kJ m}^{-2}$  to 230% and  $86.0 \text{ kJ m}^{-2}$ , respectively. Furthermore, PLA/AcrylPEG/2,5-dimethyl-2,5-di(*tert*-butylperoxy) hexane (L101) (79.75/20/0.25) ternary blends exhibit elongation at break and impact strength of 254%, and  $101.6 \text{ kJ m}^{-2}$ , respectively.

Hassouna and Dubois *et al.*<sup>185</sup> further investigated PLA/AcrylPEG blend systems and compared the performance of poly(lactide)-based blends fabricated *via* reactive and physical blending for designing high-performance PLA-based materials. The reactive routes are shown in Fig. 47. The PLA-based blends prepared by reactive blending demonstrate substantially improved impact strength and tensile toughness.

Coughlin *et al.*<sup>186</sup> and Pluta *et al.*<sup>187</sup> found that the mechanical properties of PLA blends can be improved significantly by reactive blending with multiblock copolymers, such as PDLA-poly(ethyleneglycol-random-propylene glycol) midblock (PEPG)-PDLA triblock copolymers and poly(ethylene glycol) (PEG)-*b*-poly(propylene glycol) (PPG)-*b*-PEG multiblock copolymers. For PLA/PDLA-PEPG-PDLA triblock copolymer blends,<sup>186</sup>

PEPG in PDLA-PEPG-PDLA triblock copolymer copolymerizes with ethylene glycol and propylene glycol. The chain segment of PEPG is miscible with PLA. The end block of PDLA in a triblock copolymer can form stereocomplex crystals with the PLLA matrix. Additionally, the PDLA60-EB10k-PDLA60 triblock copolymer is synthesized by replacing PEPG with a poly(ethylene butylene) copolymer (EB). The difference in the chemical nature of the midblock remarkably influences the stereocomplex crystallization between the PDLA end blocks, the PLLA matrix polymer, and the morphological characteristics of PLA-based blends. The results suggest that the miscible mid-block results in a soft continuous amorphous phase. Therefore, highly toughened PLA/PDLA-PEPG-PDLA (65/35) triblock copolymer blends are obtained with elongation at break of 424%. Pluta *et al.*<sup>187</sup> prepared PLA toughened with PEG-*b*-PPG-*b*-PEG multiblock copolymer blends by melt blending PLA with a set of PEG-*b*-PPG-*b*-PEG block copolymers with varying ratios of hydrophilic PEG and hydrophobic PPG blocks. The molar mass of PEG and PPG and the PEG content in PEG-*b*-PPG-*b*-PEG block copolymers strongly affect the miscibility of PLA blends. Under optimum conditions, the elongation at break and tensile impact strength of pure PLA increase from 8% and  $65 \text{ kJ m}^{-2}$  to 300% and  $100 \text{ kJ m}^{-2}$ , respectively.

Yang *et al.*<sup>188</sup> utilized highly flexible poly(ethylene terephthalate glycol) (PETG) to toughen PLA and methylene diphenyl diisocyanate (MDI) to function as a reactive compatibilizer of PLA/PETG blends. During reactive blending, a cross-linking reaction occurs between PLA chains and MDI. Interfacial compatibilization also occurs between PLA and PETG through the reaction of free isocyanate groups on the cross-linked PLA chains with the terminal hydroxyl groups of PETG chains. An elongation at break of 90% is obtained for the reactive compatibilized PLA/PETG/MDI (80/20/3) blends. The improvement is accompanied by a high tensile strength of 50 MPa, which is equivalent to that for pure PLA.

#### 4.4. Super tough and high strength engineering plastics PLA/engineering plastics blends

To simultaneously improve the toughness and heat resistance of PLA, Deng and Wang *et al.*<sup>189</sup> incorporated polycarbonate (PC) into PLA to prepare high-PLA-content ( $\geq 66$  wt%) PLA/PC blends *via* *in situ* reactive compatibilization. They enhanced interfacial compatibility of PLA/PC blends by using an industrial copolymer of styrene and glycidyl methacrylate (coded as ADR) as a reactive compatibilizer and utilized a core-shell impact modifier (BPM) to further improve the impact strength of PLA/PC blends. In their experiment, PLA/PC blends are annealed in a vacuum oven at  $120^\circ\text{C}$  for 6 h to promote PLA phase crystallinity and improve the heat distortion temperature (HDT) of PLA/PC blends. TEM images show that the sea-island structure of the PLA/PC/ADR/BPM (70/30/0.3/5) blends transforms into a lamella-like morphology because of the enhanced interfacial bonding between PLA and PC. For the annealed PLA/PC/ADR/BPM (70/30/0.3/5) blends, the impact strength reaches approximately  $60 \text{ kJ m}^{-2}$ , and the HDT of pure PLA increases from  $61^\circ\text{C}$  to  $136^\circ\text{C}$  under the load of 1.82 MPa. The significant



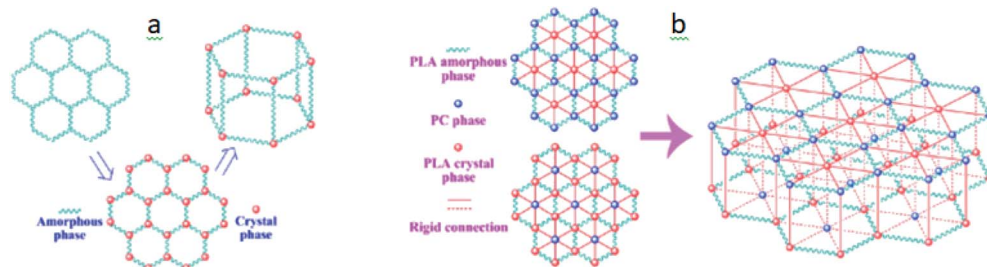


Fig. 48 (a) Representative ideal model of the change of PLA structure after annealing. (b) Representative ideal three-dimensional model for the inner structure of the annealed PLA/PC/ADR0.3/BPM5 blend. Ref. 189, copyright 2015. Reproduced with permission from American Chemical Society.

improvement of impact strength for the annealed PLA/PC blends is attributed to the coexistence of shear-yielding and crazing. PC, as a polymer with high  $T_g$  and HDT, is considered a rigid unit. Hence, a rigid three-dimensional network structure or framework, which can play an excellent role in distortion resistance, can be simultaneously formed in these blends after annealing because of the presence of rigid PC particles and PLA crystals. A model corresponding to the network formed in PLA/PC/ADR0.3/BPM5 blends is proposed (Fig. 48).

Li *et al.*<sup>190</sup> prepared a reactive comb (RC) polymer, which is composed of one poly(methyl methacrylate) (PMMA) backbone, two PMMA side chains, and a few epoxy groups distributed randomly along the PMMA backbone and utilized this polymer as a reactive compatibilizer for immiscible poly(L-lactic acid)/acrylonitrile–butadiene–styrene (PLLA/ABS) blends. The analysis of morphological structures and rheological behaviors reveals that the PLLA-grafted RC polymers *in situ* formed at the interface of PLA and ABS drastically improve the interfacial adhesion between the two phases. For the compatibilized PLLA/ABS blends, double  $T_g$  depression results indicate that the free volume of both PLLA and ABS phases is enlarged. The analysis of energy to break and ductility suggests that all compatibilized blends show significantly increased ductility and toughness compared with those of pure PLLA and pure ABS. This finding indicates the drastic synergistic effects of PLLA and ABS compatibilized by the RC polymer. The SEM images of tensile fracture surfaces show that the morphological fracture surface of PLLA/ABS/RC blends comprises homogeneously and densely distributed and oriented fibrillars, which are parallel to the stress direction. The formation of a fibrillar structure exhibits a typical plastic deformation, and high energy dissipates, resulting in a significantly improved ductility. The high performance of PLA/ABS/RC (50/50/3) blends is achieved with a tensile strength of 64.8 MPa, which is comparable with that of pure PLA at 64.4 MPa. The modulus of these blends is higher than that of ABS. Moreover, the energy at break of the compatibilized blends exceeds 80 MJ m<sup>-3</sup>, and the elongation at break is as high as 196.2%.

Considering the processing technique to improve the performance of PLA materials, Tashiro, Chirachanchai *et al.*<sup>191</sup> used biaxial-stretching (BO) to regulate the microstructure and properties of PLA films and investigated the influences of the stretching rate and draw ratio of biaxial stretching parameters

on the microstructure and properties of PLA films. They also systematically analyzed the development of microstructures, especially in the crystalline phase, the regular chain packing in the crystal lattice, and the evolution of a higher-order structure. Their results reveal that super-tough and high-strength biaxially oriented PLA (BOPLA) with a tensile strength of 180 MPa and elongation at break of 80% is successfully fabricated when the stretching rate and the draw ratio exceed 75 mm s<sup>-1</sup> and 5 × 5, respectively, thus forming approximately 10 nm  $\delta$ -crystallites with isotropic orientation. The microstructural change in BOPLA films under varied biaxial stretching rates is shown in Fig. 49. The crystallinity of BOPLA is increased by approximately 30%. A good linear relationship between the mechanical properties and the inverted crystallite size of the BOPLA films prepared under different conditions is successfully established. The well-dispersed higher-order structure consisting of many but small  $\delta$ -crystallites induced by biaxial stretching remarkably enhances BOPLA.

Wu *et al.*<sup>192</sup> utilized polybutyl acrylate (PBA) prepared *via* free radical polymerization to toughen PLA by melt blending. Their

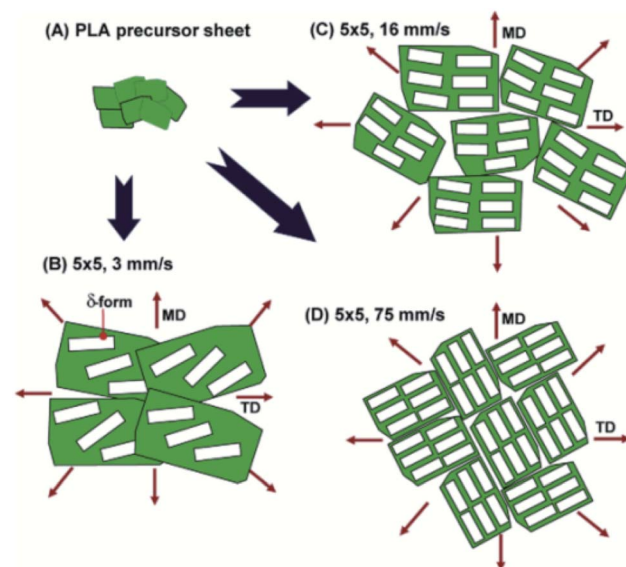


Fig. 49 Illustration for microstructure change of BOPLA films under varied biaxial-stretching rates. Ref. 191, copyright 2015. Reproduced with permission from Elsevier.



results indicate that PBA can promote PLA crystallization with less than 15 wt% PBA. The tensile toughness and elongation at break of PLA/PBA (85/15) blends greatly increase to 47.02 MJ m<sup>-3</sup> and 174.52%, respectively, whereas the tensile strength decreases to 41 MPa.

High-performance PLA/traditional petroleum-based polymer blends can be obtained through compatibilizer addition, reactive blending, and processing. The application fields of PLA materials in industrial and 3C fields are broadened by improving mechanical properties and greatly reducing the costs of PLA-based blends, especially by blending engineering materials with PLA to prepare PLA multiphase blends with high toughness, high modulus, and high strength. However, the addition of traditional petroleum-based polymer materials affects the biodegradability of PLA materials. The environmental impact and assessment of PLA-based material application should be further studied.

## 5. PLA/rubber blend system

### 5.1. Direct blending of rubber and PLA

PLA and NR are two major renewable resources of polymer materials. However, resulting blends do not meet engineering needs largely because of the lack of interfacial adhesion between a continuous PLA phase and dispersed NR droplets.

To maximize the excellent performance of rubber with reversible deformation, high elasticity, excellent mechanical properties, and heat resistance, researchers toughened PLA, thereby increasing the elasticity and impact resistance and effectively improving the low-temperature brittleness of PLA materials.<sup>193-197</sup> Rubber-toughened PLA blends are prepared by melt blending through which rubber is dispersed as a stress concentration point in a PLA matrix to form a blend system with a sea-island phase structure. A rubber component is co-vulcanized through dynamic vulcanization. The vulcanization cross-linking during the mixing process can facilitate the formation of a co-continuous phase structure of a rubber

elastomer and a PLA matrix material, leading to a significant improvement in the mechanical properties of PLA blends. The use of highly tough and highly elastic rubber is an effective strategy to toughen PLA. The mechanical performance results for highly and super toughened PLA/rubber blends are summarized in Table 6.

Ning and Fu *et al.*<sup>198</sup> employed ultrafine full-vulcanized powdered ethyl acrylate rubber (EA-UFPFR) with a particle size of only 30 nm as a toughening agent. They found that EA-UFPFR can be uniformly dispersed in a PLA matrix. Morphological analysis reveals the excellent compatibility of PLA/EA-UFPFR blends. With the addition of 1 wt% EA-UFPFR, the elongation at break of PLA/EA-UFPFR blends increases significantly to 219.93%, and the tensile strength and modulus are comparable with those of pure PLA.

NR is a bio-based material with excellent elasticity and ductility; it is considered an ideal candidate for toughening PLA. Generally, rubber-toughened PLA can notably improve the toughness of brittle materials, but this improvement is accompanied with a great loss in mechanical strength and modulus. Considering PLA and NR complementary properties, Dan *et al.*<sup>199</sup> fabricated high-toughness PLA/NR blends with a slight loss in tensile stress by melt blending with pre-hot sheared NR. Structural characterization reveals that the generation of carbonyl groups in NR chains after hot shearing enhances the interfacial adhesion between PLA and NR. The results of SEM and rheological behavior analyses suggest that the compatibility of the blends is enhanced with the pre-hot shearing of NR for a prolonged time, and NR is uniformly dispersed in the PLA matrix. The mechanical analysis results also demonstrate that the elongation at break and tensile toughness of PLA/NR blends are significantly improved from 16.3% and 8.8 MJ m<sup>-3</sup> of pure PLA to 196.2% and 77.5 MJ m<sup>-3</sup>, respectively, with as low as 3% pre-hot sheared NR for 10 min.

Lopez-Manchado and Bitinis *et al.*<sup>200-202</sup> also reported the preparation and characterization of PLA/NR blend systems. Rubber content and melt blending parameters, such as

Table 6 Mechanical performance results for highly and super toughened PLA/rubber blends<sup>a</sup>

Comments	Impact strength/(kJ m <sup>-2</sup> )	Tensile strength/(MPa)	Elongation at break/(\%)	Ref.
PLA/NR-GMA (80/20)	73.4	35	130	160
PLA/SEBS/EGMA (70/20/10)	92	—	185	164
PLA/PC/SEBS/EGMA (40/40/15/5)	>60	—	~90	
PLA/OBC/EMA-GMA (90/7/3)	64.21	55	~30	165
PLA/UFPFR (99/1)	2.2	66.26	219.93	198
PLA/NR (95/5)	3.5(2.1)	76.9(84.5)	196.2(16.3)	199
PLA/NR (90/10)	—	40	200	200
PLA/NR/C15A (90/10/1)	—	45	275	202
PLA/NR/C30B (90/10/1)	—	38.2	118	201
PLA/NR (65/35)	58.3	—	—	205
PLA/NR/DCP (80/20/1.5)	58.3	23	~200	206
PLA/NR (60/40)	42.5	~22	>100	207
PLA/ENR (60/40)	47	~28	~150	208
PLA/NBR/DCP (90/9.955/0.045)	~18	~48	>300	249

<sup>a</sup> The values in brackets ( ) are the impact strength corresponding to neat PLA.



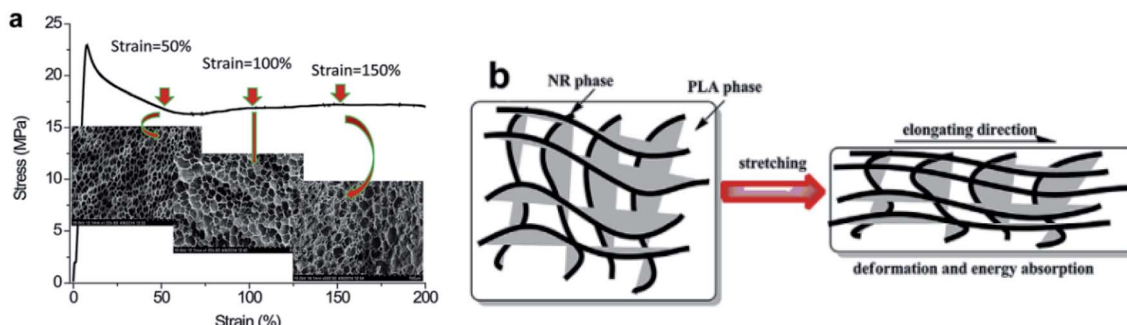


Fig. 50 (a) The NR phase in elongated D65/35; (b) illustration of the deformation of crosslinked NR phase with net-like structure during stretching. Ref. 206, copyright 2014. Reproduced with permission from Elsevier.

processing windows, temperature, time, and rotor rate, are optimized to obtain high-toughness PLA/NR blends. The incorporation of NR not only increases the crystallization rate but also enhances the crystallization of PLA. For PLA/NR (90/10) blends, the dispersed phase of NR is evenly distributed in the PLA matrix with a dispersed phase particle size of only 1.1–2.0  $\mu\text{m}$ . Furthermore, the elongation at break of the blend increases to approximately 200%, and the tensile strength reduces to 40 MPa.<sup>200</sup> To further improve the mechanical properties of PLA/NR blends, the team<sup>201</sup> incorporated several montmorillonites (MMTs) into PLA/NR blends to prepare a novel toughened PLA/NR bio-nanocomposite with tunable properties by melt blending. The results indicate that organoclays are preferentially located at the interface and act as compatibilizers between PLA and NR phases. As a result, the tensile toughness of PLA/NR/MMT blends remarkably improves. Another study<sup>202</sup> has investigated the micromechanical deformation mechanisms of PLA/NR/organoclay bio-nanocomposites through small and wide-angle X-ray scattering under tensile conditions. With the addition of an organoclay, the formation of cavities between PLA and NR is prevented because the organoclay is mainly located at the interface of the PLA/NR blends. The results show the synergistic effects of the mechanical reinforcement mechanism of the PLA matrix obtained with the addition of NR and an appropriate amount of nanofillers.

## 5.2. Dynamic vulcanization of PLA/rubber blend system

The PLA/rubber blend is prepared through dynamic vulcanization in the melt blending process. The blends are subjected to a strong shearing force in special plastic processing equipment, such as an internal mixer and an extruder, which dynamically vulcanizes and uniformly disperses the rubber component in the PLA matrix.<sup>203,204</sup> The formation of a stable cross-linked structure is promoted by a micron-sized rubber. A PLA-rubber copolymer is formed during dynamic vulcanization to improve the compatibility of the blend components and the mechanical properties of the PLA/rubber blends.

To improve the interfacial adhesion between the continuous PLA phase and dispersed NR droplets, Chen *et al.*<sup>205,206</sup> designed super toughened bio-based PLA/NR blends by using DCP as a cross-linking agent and adopting dynamic vulcanization

techniques. SEM and dissolution/swell experiment data show that a continuous cross-linked NR phase is formed. Peroxide initiates reactive compatibilization at the interface between PLA and NR, leading to the cross-linking of the NR phase with a specific continuous “net-like” structure. In addition, the PLA-NR graft copolymer is formed during blending, which effectively increases the interfacial compatibility of PLA and NR. Therefore, a sharp brittle–ductile transition occurs in the blend with 35 wt% NR, obtaining impact strength and elongation at break of 58.3  $\text{kJ m}^{-2}$  and approximately 200%, respectively; however, the tensile strength is reduced to approximately 23 MPa only. The reduction in tensile strength is mainly attributed to the rubbery nature of NR and the reduction in the rigid PLA phase, as shown in Fig. 50. These results can provide evidence of a continuous “net-like” NR located in the PLA matrix with good interfacial adhesion and enhanced mechanical properties for various functional applications.

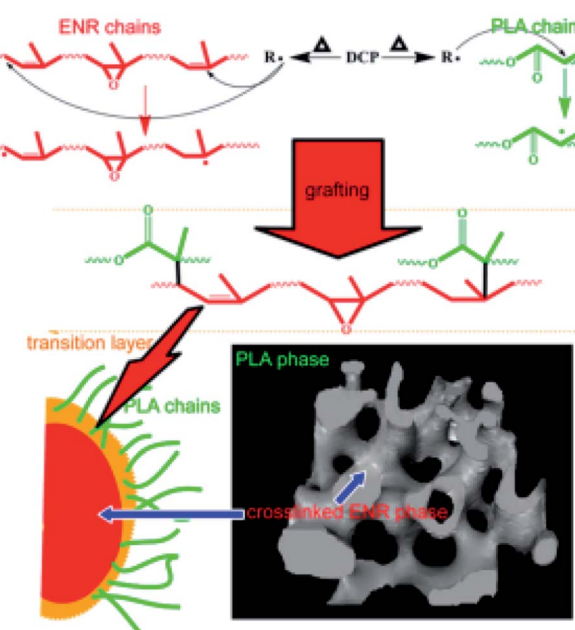


Fig. 51 Scheme of possible *in situ* compatibilization and the transition layer at the interface between PLA and ENR phases. Ref. 208, copyright 2015. Reproduced with permission from American Chemical Society.



Xu and Chen *et al.*<sup>207</sup> fabricated PLA/NR blends through dynamic vulcanization by using DCP, S, and phenolic resin as curing agents. The cross-linked NR phase is found to be a continuous structure in all the prepared PLA/NR blends. Based on the results of FT-IR and SEM for studying the interfacial compatibility, the cross-linking reaction of NR with DCP as a curing agent is carried out to form a continuous phase distribution in the PLA matrix. Meanwhile, a small amount of PLA with a cross-linking or branching structure is also produced, which improves the interfacial compatibility of the blended components. The PLA/NR blends (60/40 w/w) fabricated by DCP-induced dynamic vulcanization exhibit optimum comprehensive properties, with a strength of  $42.5 \text{ kJ m}^{-2}$ , which is approximately 16 times that of pure PLA, elongation at break of 100%, and tensile strength of 22 MPa. Chen *et al.*<sup>208</sup> further fabricated a PLA/epoxy NR bio-based thermoplastic elastomer through dynamic vulcanization by using DCP as an initiator. The scheme of possible *in situ* compatibilization and the transition layer at the interface between PLA and ENR phases was illustrated in Fig. 51. The morphological characteristics of brittleness-toughness transformation are formed with "sea-sea" bicontinuous morphology. The impact strength and elongation at break of the blend reach  $47 \text{ kJ m}^{-2}$  and 150%, respectively, and the tensile strength decreases to 28 MPa.

Wu *et al.*<sup>160</sup> utilized NR-GMA to toughen PLA for preparing a super tough TPV through dynamic vulcanization. The chemical reaction between NR-GMA and PLA matrix *via* bulk-free radical polymerization dramatically improves the interfacial adhesion and compatibility between the PLA matrix and the rubber phase. FT-IR spectra show that an interfacial chemical reaction occurs between the epoxy group of NR-GMA and the terminal carboxyl or hydroxyl group of the PLA matrix during dynamic vulcanization. The size of the dispersed phase with micron or even nanometer can effectively improve the toughness of PLA/NR-GMA TPVs. The impact strength and elongation at break of PLA/NR-GMA blends significantly increase to  $73.4 \text{ kJ m}^{-2}$  and 130%, respectively, representing 26 and 33 fold increases, respectively, compared with those of pure PLA; the tensile strength decreases to 35 MPa. The fine microscale and nanoscale rubber phase structure and strong interfacial adhesion play key roles in achieving the high toughness of PLA/NR-GMA TPVs.

Nishitsuji *et al.*<sup>164</sup> utilized hydrogenated SEBS-toughened PLA and improved the compatibility of blends by adding EGMA and balanced the heat resistance and stiffness of the blends by adding PC. They successfully fabricated highly tough PLA/SEBS/EGMA and PLA/PC/SEBS/EGMA. Duan<sup>209</sup> used DCP as an initiator to prepare PLLA/NBR TPVs by dynamic vulcanization. During the blending process, DCP promoted the formation of the cross-linked structure of NBR rubber and triggered the branching reaction of PLA, leading to the increase in the entanglement of the PLA molecular chain. Therefore, the interfacial compatibility and adhesion of PLLA/NBRTPVs and the toughness of the resulting blends are greatly improved.

The toughening modification of PLA by utilizing the elasticity and flexibility of rubber is an effective strategy to improve the toughness of PLA. The cavity of the rubber phase causes the

local relaxation of the triaxial stress around the dispersed phase, resulting in the shear yield of the matrix and a large amount of energy dissipation<sup>165,210-213</sup> during the stress process. This process is the mechanism of the rubber toughening of PLA. The size of the dispersed phase is closely related to the toughness of the PLA material. Within a certain range, the cavitation resistance decreases as the rubber size increases, and this condition is favorable to the shear yielding in the PLA matrix. With the combination of a compatibilizer, reactive compatibilization, and dynamic vulcanization, the interfacial bonding and interfacial compatibility between PLA and rubber phase can be increased; thus, the mechanical properties of PLA/rubber blend can be improved. Although rubber can effectively improve the toughness of PLA, it greatly reduces the strength and modulus of PLA. This occurrence in rubber-toughened PLA should be further investigated.

## 6. Biodegradable polymer-material-toughened and modified PLA

Considering the fact that the use of petroleum-based plastics to toughen PLA would partially sacrifice the sustainability, the flexible petroleum-based synthesis polymers or biobased polymers, such as PBAT, PBS, PCL, PHAs *et al.*<sup>214-217</sup> have recently been employed to toughen PLA. The wide application of biodegradable materials provides a good approach to reduce plastic pollution caused by non-biodegradable materials. Fully biodegradable polymer blends have attracted more and more attention due to their environmentally benign. Therefore, fully biodegradable polymer blends has become a very active and important research field of materials science. Generally, the high performances with good tensile toughness and impact toughness of fully biodegradable PLA blends could be obtained *via* enhancing interfacial action and refining phase morphology. And some important achievements of fully PLA-based biodegradable polymer blends with high toughening efficiency and even super toughness have been obtained. The mechanical performance results for highly and super toughened PLA/bio-based and biodegradable polymer blends are summarized in Table 7.

### 6.1. Super tough PLA/PBS blends

PBS has good biodegradability and impact toughness, excellent processability, good elongation at break, and good heat resistance. The temperature of PBS materials ranges from 30 °C to 100 °C. PLA/PBS blends can maintain good biodegradability and biocompatibility and complement one another in terms of performance. However, the interfacial compatibility of PLA and PBS is poor; hence, it must be enhanced to obtain high-performance fully biodegradable PLA/PBS blends. The high toughness of materials can be achieved by adding an efficient compatibilizer, especially in combination with reactive blending to improve the interfacial compatibility between PLA and PBS.

DCP, as a free radical initiator, has been utilized extensively to compatibilize PLA/PBS blends. Zhang *et al.*<sup>218</sup> fabricated



Table 7 Mechanical performance results for highly and super toughened PLA/bio-based and biodegradable polymer blends<sup>a</sup>

Comments	Impact strength/(kJ m <sup>-2</sup> )	Tensile strength/(MPa)	Elongation at break/(%)	Ref.
PLA/PBAT/EMA-GMA (75/10/15)	61.9	~37	278	166
PLA/PBAT/ADR (60/40/0.75)	29.62	40.88	579.91	167
PLA/PBS/DCP/PBS- <i>g</i> -CNC (70/30/0.2/2.0)	726 J m <sup>-1</sup>	43.3	298	218
PLA/PBS/DCP (80/20/0.1)	30	49.3	249	219
PLA/PBS/DCP (80/20/3)	—	80(89)	205	220
PLA/PBS/LTI (90/10/0.3)	50-70	~55	~220%	221
PLA/PBS (80/20)	—	32.6	242	222
PLA/PBS/CBC (80/20/1)	—	40	340	
PLA/PBS/CBC/PBO (80/20/1/1)	—	40.6	309	
PLA/PBS/PBO (80/20/2)	—	41.3	398	
PLA/PBS/PBO (80/20/4)	—	43.7	402	
PLA/PBS/PLA- <i>g</i> -MA (80/20/4)	—	38.3	390	
PLA/PBS (90/10)	—	~63	~100	223
PLA/PBSL (90/10)	—	~58	~180	
PLA/PBAT (80/20)	4.5	~47	200	227
PLA/PBAT/BOZ/PA (80/20/1/1)	—	45.3	515.7	231
PLA/PBAT/BOZ/PA (70/30/1/1)	—	39.8	567.8	
PLA/PBAT/ADR (43 705) (80/20/1)	—	~40	~450	232
PLA/PBAT/HDE (80/20/1)	—	~40	~450	
PLA/PBAT/ADR (80/20/0.5)	—	47	135	233
PLA/PBAT/TBT (70/30/0.5)	9	45	298	234
PLA/PBAT/DCP (80/20/0.5)	110 J m <sup>-1</sup>	45	~230	235
PLA/PBAT/ESA (85/15/0.3)	~30	~46	>150	236
PLA/PCL/0.3TMC-130 (85/15/0.3)	~25	—	—	241
PLA/PCL (80/20)	31	—	—	242
PLA/PCL/LTI (80/20/0.5)	17.3	47.3	268	243
PLA/dPHB (80/20)	—	~30	538	245
PLA/PHBV (80/20)	11	42	230	246
PLA/p(3HB- <i>co</i> -4HB)/DCP (70/30/0.1)	—	28.2	317	247
PLA/p(3HB- <i>co</i> -4HB)/DCP/TAIC (70/30/0.1/0.1)	—	29.3	310	
PLA/PBSA/ADR (60/40/0.6)	38.4	—	179%	248
PLA/PBSA/TPP (90/10/2)	16.4(6.8)	86.2(78.8)	36.8	249
PLA/PBSA/TPP/C20A (90/10/2/2)	11.8	88.7	31	250
PLA/PBSA/SiO <sub>2</sub> (70/30/10)	116 J m <sup>-1</sup> (28)	42.7	261	251
PLA/MGST/ESO (80/10/10)	42(18)	43	140	257
PLA/TKGM (60/40)	14(18)	36.5	234.8	258
PLA/P(CL- <i>co</i> -LA)/SiO <sub>2</sub> (90/10/5)	27.3	47	42	259
PLA/P(CL- <i>co</i> -LA) (90/10)	11.4	48	~20	
PLA/P(CL- <i>co</i> -LA)/SiO <sub>2</sub> (90/10/10)	39.7(2.7)	42	18	260
PLA/PCO- <i>g</i> -PLA (80/20)	—	~40	~125	261
PLA/SGC/MDI (40/10/2)	48.6	—	236%	262
PLA/PCNL	—	~60	>250	263
PLA/PBAC (70/30)	10.1	44	196.1	269

a PLA/PBS blend by using DCP as an initiator to achieve blends with high impact toughness. Biodegradable PBS-*g*-CNC is added to further increase the impact strength and modulus of the PLA/PBS/DCP blends. The addition of DCP and PBS-*g*-CNC simultaneously promotes the dispersion of PBS (Fig. 52) and the crystallization of PLA. The dispersibility of PBS-*g*-CNC in PLA and PBS is improved. The cross-linking effect initiated by DCP in the blend increases the thermal stability of the PLA/PBS blends. The PLA/PBS/DCP/PBS-*g*-CNC blend maintains high modulus and strength and exhibits excellent toughness. The impact strength and elongation at break of PLA/PBS/DCP/PBS-*g*-CNC (70/30/0.2/2.0) blends are up to 726 J m<sup>-1</sup> and 298%, respectively. The tensile strength remains at a moderate level of 43.3 MPa.

Zhang and Ma *et al.*<sup>219</sup> investigated the effects of DCP as an initiator on the morphological characteristics, rheological behaviors, and thermal and mechanical properties of PLA/PBS blends. They showed that DCP induces the *in situ* compatibilization of the blended components, promotes the uniform dispersion of PBS, and improves the interfacial adhesion properties of the blends. The SEM images of the impact fracture surface of PLA blends were shown in Fig. 53. With the addition of a small amount of DCP, the impact strength and elongation at break of the PLA/PBS/DCP (80/20/0.1) blends are significantly improved to 30 kJ m<sup>-2</sup> and 249%, respectively, and the tensile strength is 49.4 MPa. Liu *et al.*<sup>220</sup> also successfully obtained high-toughness PLA/PBS blends *via* reactive blending by adding DCP as a free radical initiator. The *in situ* formation of a PLA-



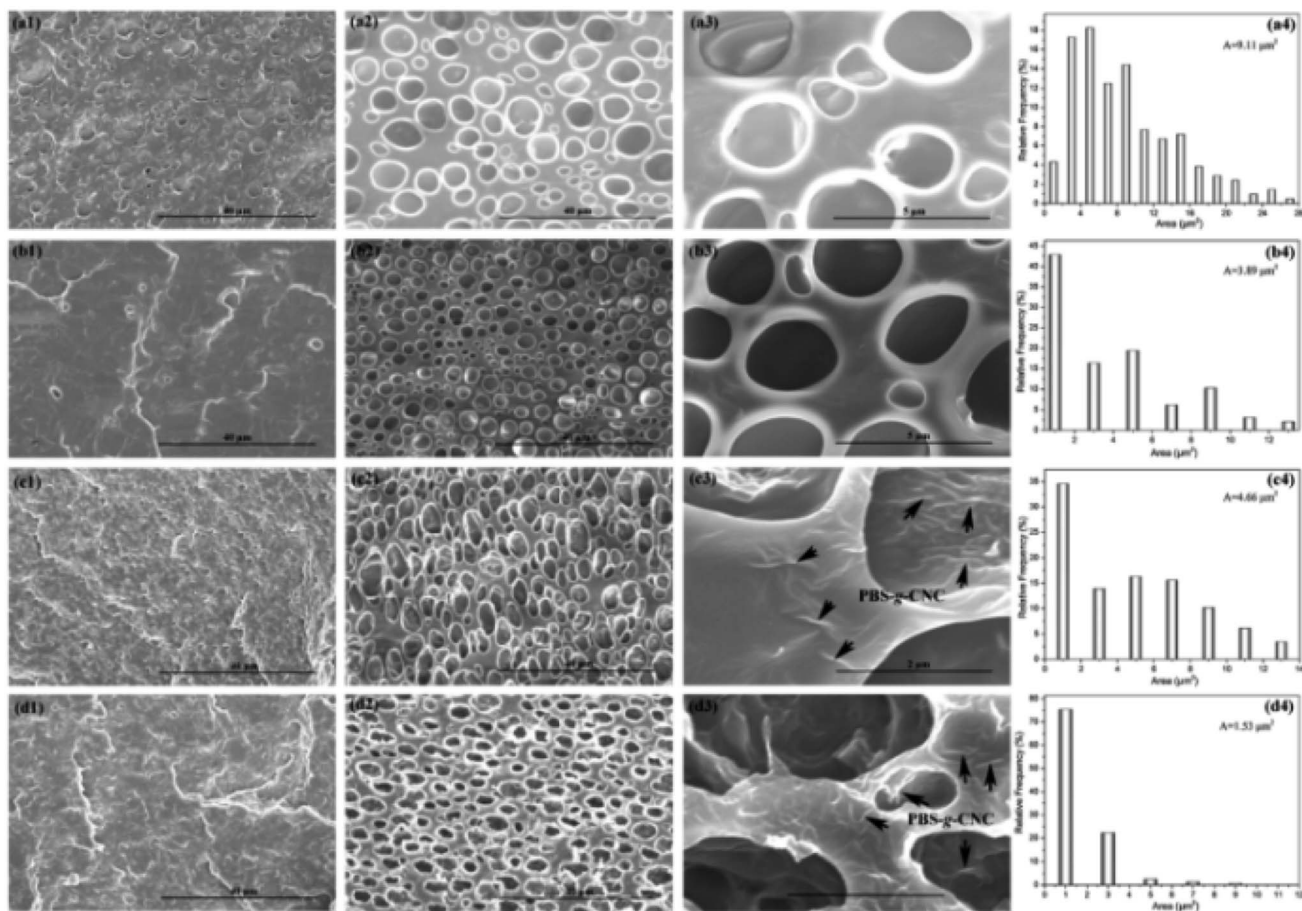


Fig. 52 SEM images of cryogenically fractured surface of composites with PBS/PLA/DCP/(PBS-g-CNC) ratio of (a1) (30/70/0/0), (b1) (30/70/0.2/0), (c1) (30/70/0/2) and (d1) (30/70/0.2/2). (a2)–(d2) present the dispersed-phase morphology of PBS and CNC after etching the PLA matrix of (a1)–(d1), which produce the quantitative analyses in terms of the distribution of PBS phase size as shown in (a4)–(d4), respectively. The higher resolution version of (a2)–(d2) are exhibited in (a3)–(d3). The average area (A) is marked in the right up corner of (a4), (b4), (c4) and (d4). Ref. 218, copyright 2016. Reproduced with permission from Elsevier.

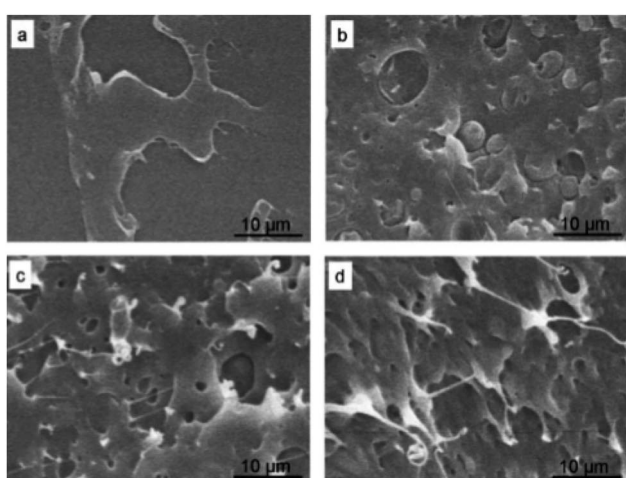


Fig. 53 SEM micrographs of the impact fracture surface of (a) PLLA and PLLA/PBS/DCP blends, (b) 80/20/0, (c) 80/20/0.05, and (d) 80/20/0.1. Ref. 219, copyright 2008. Reproduced with permission from John Wiley and Sons.

PBS copolymer effectively enhances the compatibility of the blended components; thus, high strength and tensile toughness of PLA/PBS blends are obtained.

Highly reactive lysine triisocyanate (LTI) is used as an efficient reactive compatibilizer for PLA/PBS blends. For instance, Iida *et al.*<sup>221</sup> utilized LTI as a reactive compatibilizer to fabricate super tough PLA/PBS blends through extrusion. The isocyanate groups of LTI react with the terminal carboxyl or hydroxyl groups of PLA and PBS during melt extrusion, improving the interfacial compatibility of the blends. PBS is uniformly dispersed in the PLA matrix with spherical particles of approximately 1 μm. The impact strength and elongation at break of the PLA/PBS/LTI (90/10/0.5) blends are increased to approximately 50–70 kJ m<sup>-2</sup> and 220%, respectively.

Dubois *et al.*<sup>222</sup> investigated the effect of 1,1'-carbonylbiscaprolactam, 2,2'-(1,3-phenylene)-bis-(2-oxazoline), PLA-g-MA, and PBS-g-MA as compatibilizer on the compatibility of PLA and PBS components. A series of high-toughness PLA/PBS blends has also been prepared through reactive blending. Shibata *et al.*<sup>223,224</sup> toughened PLA by melt blending with PBS and poly(butylene succinate-co-L-lactate). The tensile toughness of

the resulting blends is greatly improved, and a high tensile strength is maintained.

## 6.2. Super tough PLA/PBAT blends

PBAT is a thermoplastic elastomer polymer with a hard segment and a soft segment. It has a long aliphatic soft chain and a rigid side group composed of an aromatic ring. It has the properties of PBA and PBT, which are also biodegradable polyesters. The PBAT chain segment is softer and more ductile than PLA, which is inherently brittle.<sup>225,226</sup> The addition of PBAT to PLA can improve the toughness and elongation at break of PLA.<sup>227</sup> The properties of the blends are highly dependent on their morphological characteristics when PBAT and PLA are simply physically blended because of the difference in the molecular segments between components.<sup>228</sup> Furthermore, when the PBAT content is between 20% and 50%, PLA is almost incompatible with PBAT. Defects in crystallinity and compatibility lead to the poor mechanical properties of blends.<sup>229</sup> Interfacial structure and compatibility should be enhanced to improve the performances of PLA/PBAT blends and the dispersibility of PBAT in the PLA matrix.

Zhang *et al.*<sup>230</sup> prepared high-toughness PLA/PBAT blends through physical blending with a twin-screw extruder. Morphological results indicate that PBAT as a dispersed phase is uniformly distributed in the PLA matrix with a particle size of approximately 300 nm, which improves the tensile toughness of PLA, but the PLA strength and modulus decrease, and the impact strength is not considerably improved. Wu *et al.*<sup>166</sup> prepared super tough PLA/PBAT/EMA-GMA multicomponent blends through reactive blending. The inclusion of highly reactive EMA-GMA promotes the *in situ* reactive compatibilization of the blended components. The morphological characteristics of the blend also change from a sea-island structure to a continuous structure. As shown in Fig. 54. The impact strength and elongation at break of PLA/PBAT/EMA-GMA blends are as high as 61.9 kJ m<sup>-2</sup> and 278%, respectively, and the tensile strength decreases to 37 MPa. Zhao *et al.*<sup>167</sup> prepared high toughness fully biodegradable PLA/PBAT blends with high

toughness by melt blending in the presence of a multifunctional epoxy oligomer as a reactive compatibilizer.

Ma and Chen *et al.*<sup>231</sup> examined PLA/PBAT blends by melt blending with 2,2'-(1,3-phenylene)bis(2-oxazoline) and using PA as compatibilizers. The interface bonding and compatibility of the blends are significantly improved with the addition of a small amount of the compatibilizer. The elongation at break increases to as high as 515.7%, but the tensile strength reduces to 45.3 MPa. They<sup>232</sup> also used multifunctionally active epoxy oligomers (ADR) and hexanediol glycidyl ether as chain extenders and a reactive compatibilizer, respectively, to toughen PLA/PBAT blends. The results show that the compatibility and tensile toughness of the PLA/PBAT blend are effectively improved. Maazouz *et al.*<sup>233</sup> added ADR as a reactive compatibilizer to PLA/PBAT blends, and the compatibility and tensile toughness of the PLA/PBAT blends are significantly improved.

Wang *et al.*<sup>234</sup> studied the melt extrusion characteristics of PLA/PBAT blends by using tetrabutyl titanate (TBT) as a catalyst. The results show that the addition of TBT promotes transesterification reaction, resulting in the improvement of the compatibility, mechanical properties, strength, and resilience of the PLA/PBAT blends. Ma *et al.*<sup>235</sup> incorporated DCP as a free radical initiator into PLA/PBAT blends to achieve *in situ* reactive compatibilization. Ren *et al.*<sup>236</sup> found that the interfacial compatibility and bonding in PLA/PBAT blends can be enhanced through the inclusion of epoxy-functional styrene acrylic (ESA) copolymer as an efficient compatibilizer. As a reactive processing agent, ESA elicits a certain chain extension effect, which enhances melt strength and elasticity and results in the excellent toughness of the blend. The impact strength of PLA/PBAT/ESA (85/15/0.3) blend increases to 30 kJ m<sup>-2</sup>, the elongation at break is more than 150%, and the tensile strength is approximately 46 MPa.

## 6.3. Super tough PLA/PCL blends

PCL is an excellent material with comprehensive and excellent mechanical properties, biodegradability, and biocompatibility.<sup>237</sup> It can be compatible with a variety of conventional

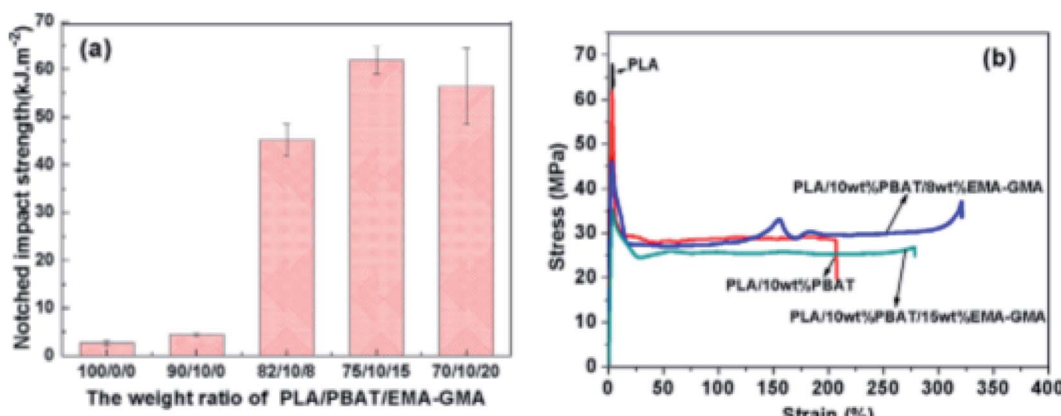


Fig. 54 (a) Notched impact strengths and (b) stress-strain curves of PLA, PLA/PBAT and PLA/PBAT/EMA-GMA blends. Ref. 166, copyright 2017. Reproduced with permission from Elsevier.



polymers. In addition, PCL has a good shape memory and can be used for the toughening modification of PLA.<sup>238</sup> PLA/PCL blends exhibit good toughness balance and special properties; hence, they have great potential for application in medical, packaging, and dairy fields.<sup>239,240</sup>

Bai and Fu *et al.*<sup>241</sup> investigated the influence of the crystallinity of a PLA matrix on PLA/PCL blends prepared by melt blending. They controlled the crystallinity of the PLA matrix by adding different amounts of TMC-328 nucleating agent and by annealing and systematically studied the relationship between the crystallinity of PLA and the impact strength of PLA/PCL blends. They found that the crystallinity of the matrix is in a good linear relationship with the impact strength of the PLA/PCL blends. When the crystallinity of PLA is increased to approximately 50%, the impact strength of the PLA/PCL blends is approximately  $25 \text{ kJ m}^{-2}$ . The particle size of PCL dispersed phase is controlled through the adjustment of the processing technology to further improve the compatibility.<sup>242</sup> When the high-crystallinity PLA and the dispersed phase PCL particle size of  $0.39 \mu\text{m}$ , the impact strength of the blend is further increased to  $31 \text{ kJ m}^{-2}$ .

Iida *et al.*<sup>243</sup> studied the reactive compatibilizing efficiency of different isocyanates and industrial-grade epiclon 725 for PLA/PCL blends. The comparison data show that LTI has the most obvious compatibilization effect. The tensile strength of the PLA/PCL/LTI (80/20/0.5) blends can be maintained at 47.3 MPa, and the impact strength and elongation at break increase to  $17.3 \text{ kJ m}^{-2}$  and 268%, respectively. Zhao *et al.*<sup>244</sup> used a PCL-based polyurethane elastomer to toughen PLA through an *in situ* reaction of PCL polyol with isocyanate in a melt blending process. The interfacial compatibility is markedly improved by the reaction of the terminal hydroxyl groups of PLA and the N=C=O groups of IPDI, as confirmed by FTIR spectroscopy. The elongation at break and impact strength of the blends prepared by reactive blending are as high as 242.4% and  $14.5 \text{ kJ m}^{-2}$ , respectively. The blends exhibit an excellent tensile strength of 52.7 MPa and a tensile modulus of 1496.46 MPa. Excellent interfacial adhesion enables the dispersed polyurethane elastomeric particles to act as effective stress concentration areas. The shearing yielding of PLA matrix triggered by internal cavitation is the main mechanical toughening mechanism.

To maintain the strength and modulus and improve the heat resistance of PLA, Fu *et al.*<sup>242</sup> utilized TMC-328 to improve the crystallinity of the PLA matrix and adjusted the processing technology to regulate the particle size of the dispersed phase. PLLA matrix crystallinity is controlled by adding a highly effective nucleating agent, and PCL particle size is tailored under varying processing conditions while maintaining constant interfacial adhesion. The results suggest that the crystallinity of the PLA matrix increases, and the impact toughness of the PLA/PCL blends significantly enhances. The combined effects of matrix crystallization and impact modifier particle size in toughening are systematically characterized. The results indicate that a suitable particle size of  $0.3\text{--}0.5 \mu\text{m}$  is the precondition for a highly crystalline matrix to work effectively in the toughening and for the range of particle size to be effective

in the trigger shear yielding mechanism of the matrix. By contrast, relatively large particles ( $0.7\text{--}1.1 \mu\text{m}$ ) can effectively toughen an amorphous matrix by initiating the multiple crazing of the matrix. The present work can provide a general guideline for the fabrication of flexible polymer-toughened PLLA blends with good heat resistance.

#### 6.4. Super tough PLA/PHB blends

Hakkarainen *et al.*<sup>245</sup> prepared high-toughness PLA/PHB blends by using a two-step extrusion process. A PLA-g-dPHB copolymer is formed *via* the reaction of PLA with PHB oligomer (dPHB), which is produced through the thermal degradation of PHB during melt processing. Thus, the segmental mobility and crystallization of PLA are improved with the formation of PLA-g-dPHB copolymer; the toughness and processability of PLA/PHB blends also increase. Although the tensile strength of the PLA/dPHB blends decreases to 30 MPa, the elongation at break increases to 538%. Ma *et al.*<sup>246</sup> fabricated PLA/PHBV blends by melt blending. The results reveal that the PLA/PHBV blends exhibit excellent compatibility when the content of  $\beta$ -hydroxyvalerate is high (more than 40 mol% in a PHBV structure).

Han and Dong *et al.*<sup>247</sup> prepared PLA/poly(3-hydroxybutyrate-*co*-4-hydroxybutyrate) [P(3HB-*co*-4HB)] blends through reactive blending by using DCP as an initiator to form a graft copolymer. The PLA/P(3HB-*co*-4HB) blends exhibit excellent tensile toughness with enhanced compatibility between PLA and P(3HB-*co*-4HB) components. A similar toughening effect is also achieved by adding triallyl isocyanate (TAIC) as a cross-linking agent to the blend system. However, with the combination of DCP with TAIC, the elongation at break decreases because the cross-linking network limits the mobility of polymer chains to deform under a tensile load. The fracture surface morphology in the SEM images (Fig. 55) shows that the toughening mechanism involves the plastic deformation of a PLA matrix and a debonding process.

#### 6.5. Super tough PLA/poly[(butylene succinate)-*co*-adipate] (PBSA) blends

Ray *et al.*<sup>248</sup> prepared super tough PLA/PBSA blends by adding multifunctionally active epoxy oligomers (ADR) to achieve *in situ* reactive compatibilization of PLA and PBSA. During blending, ADR acts as a chain extension, and the reactive compatibilizer improves the melt strength and thermal stability of the blends. The crystallization nucleation ability of PLA is promoted. A nonlinear copolymer forms during blending and induces a good compatibilizing effect on PLA and PBSA components. When the amount of PBSA exceeds 30 wt%, the interfacial morphologies of PLA/PBSA blends undergo a transition from a sea-island structure to a co-continuous phase. After the addition of 0.6 wt% ADR PLA/PBSA (60/40) blend, the particle size of the dispersed phase is greatly reduced from  $2.69 \mu\text{m}$  to  $0.7 \mu\text{m}$ , the impact strength of the blend increases to  $38.4 \text{ kJ m}^{-2}$ , and the elongation at break is improved to 179%. Ray *et al.*<sup>249</sup> obtained a high toughness of PLA/PBSA blends through *in situ* reactive blending by using triphenyl phosphite (TPP) as a reactive compatibilizer. The interfacial compatibility of the blends is enhanced, and the particle



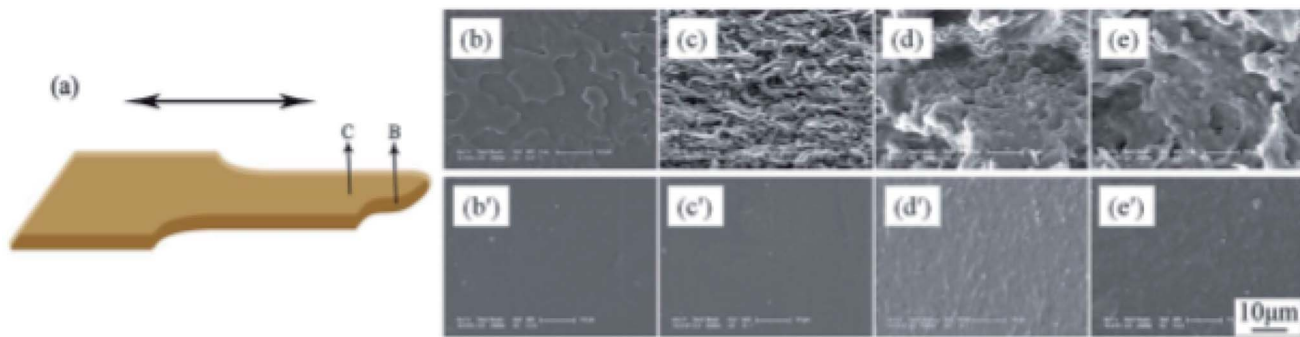


Fig. 55 (a) A schematic diagram of the measurement locations (B), fractured surface, and (C), surface parallel tensile direction near the broken points and the SEM of the PLA/P(3HB-co-4HB) blends in tensile strength tests, (b and b') PLA, (c and c') XPLA, (d and d') P(3HB-co-4HB) and (e and e') XP(3HB-co-4HB) in tensile strength tests. (b-e), fractured surface, (b'-e'), surface parallel tensile direction near the broken points. Ref. 247, copyright 2014. Reproduced with permission from Royal Society of Chemistry.

size of the dispersed phase is reduced. Microfibrillation between the dispersed phase of PBSA and PLA matrix is formed, effectively ensuring the strength and toughness of PLA/PBSA blends. The tensile strength of PLA/PBSA/TPP blends increases to 86.2 MPa compared with that of pure PLA at 78.8 MPa, and the impact strength and elongation at break increase to  $16.4 \text{ kJ m}^{-2}$  and 36.8%, respectively. The improvement in the impact strength and elongation at break is attributed to the yielding deformation in the matrix, as initiated by the debonding between PLA/PBSA phases. The intraphase chain extension and interphase compatibilization of blends was illustrated in Fig. 56. On the basis of a previous work, another research group<sup>250</sup> further studied the effect of clay-montmorillonite clay (C20A) on blends. The toughness of C20A-based compatibilized blends is greater than that of the pure PLA because of the lesser crystallinity of the PLA component and the enhanced chain extensions/coupling in the C20A-based samples. In addition to the improved barrier

properties and thermal stability, the toughness of C20A-based compatibilized blends is greater than that of pure PLA.

Zhang *et al.*<sup>251</sup> investigated the mechanical properties, rheological and thermal behavior, and phase morphology of PLLA/PBSA/SiO<sub>2</sub> composites by using two types of SiO<sub>2</sub> (hydrophilic or hydrophobic). The results reveal that hydrophobic SiO<sub>2</sub> is more uniformly dispersed in the blends than hydrophilic SiO<sub>2</sub> and mainly located in the PLLA matrix, which is desirable for the optimum reinforcement of the PLLA/PBSA blend. The notched impact strength, tensile strength, and elongation at break of PLLA/PBSA/hydrophobic SiO<sub>2</sub> (70/30/10) composites are greatly improved from  $28 \text{ J m}^{-1}$ , 69.3 MPa, and 4% of pure PLA to  $116 \text{ J m}^{-1}$ , 42.7 MPa, and 261%, respectively.

## 6.6. Other fully biodegradable super tough PLA blends

Starch is a low-cost, biodegradable, and biocompatible polysaccharide obtained from renewable resources. It can be utilized as a filler or thermoplastic polymer to modify PLA. The utilization of starch in modifying PLA is of great interest in a wide range of applications, especially food packaging.<sup>252-256</sup> Zhu *et al.*<sup>257</sup> fabricated high-performance PLA/starch blends by using ESO as a reactive compatibilizer through reactive extrusion. Starch granules are grafted with MA during extrusion to improve the reactivity of starch with ESO and dispersibility in the PLA matrix. The impact strength of PLA/MGST/ESO (80/10/10) blends increase from  $18 \text{ kJ m}^{-2}$  for pure PLA to  $42 \text{ kJ m}^{-2}$ , elongation at break is as high as 140%, and tensile strength is maintained at 43 MPa.

Luo *et al.*<sup>258</sup> synthesized a new biodegradable thermoplastic konjac glucomannan (TKGM) through the graft copolymerization of vinyl acetate and methyl acrylate onto konjac glucomannan (KGM). In addition, TKGM is utilized to toughen PLA by melt blending. The addition of TKGM facilitates an increase in the elongation at break of the PLA blend. The elongation at break of the PLA/TKGM (60/40) blend is 234.8%, the impact strength is slightly increased, and the tensile strength is reduced to 36.5 MPa.

Raquez *et al.*<sup>259</sup> prepared rubbery random aliphatic P(CL-*co*-LA) copolymers with different molar ratios of caprolactone (CL) and LA monomers. P(CL-*co*-LA) copolymers are used as

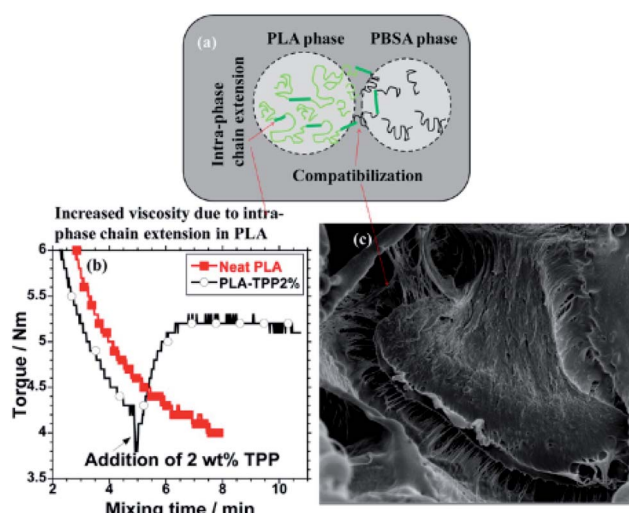


Fig. 56 (a) "Cartoon" model depicting intraphase chain extension and interphase compatibilization, (b) torque/time graph for the neat PLA and PLA-TPP2% samples showing intraphase chain extension, and (c) high magnification of SEM images of compatibilized blends. Ref. 249, copyright 2013. Reproduced with permission from American Chemical Society.

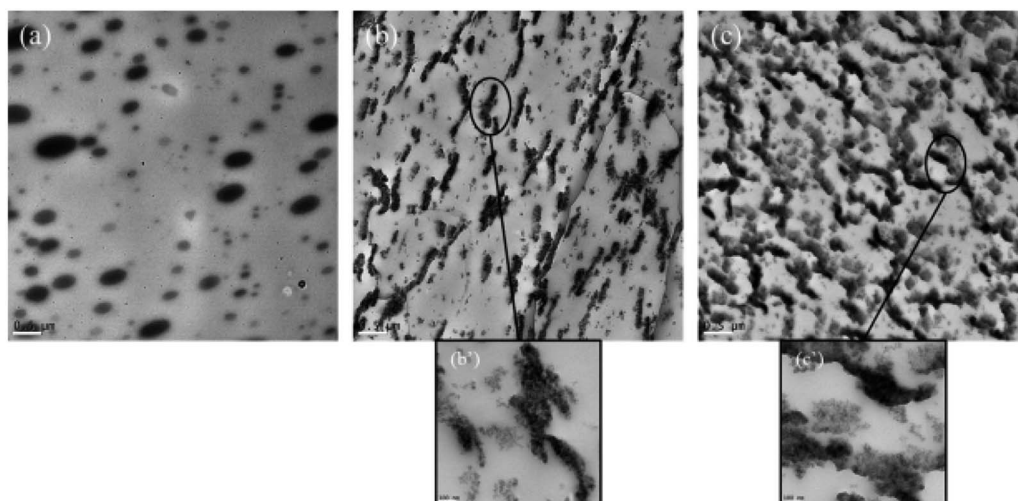


Fig. 57 TEM images of room-temperature notched surfaces of PLA-based materials containing 10 wt% of P(CL-co-LA) copolyester without silica nanoparticles (a), with 5 wt% (b and b') and 10 wt% of silica nanoparticles (c and c'). Scale bar: 0.5  $\mu$ m (a–c) and 100 nm (b' and c'). Ref. 260, copyright 2013. Reproduced with permission from Elsevier.

biodegradable impact modifiers to tailor phase morphology with P(CL-co-LA) as random copolymers. SEM, TEM, and AFM reveal that the dependence between the improvement of toughness and the morphological characteristics of the resulting blends is established in terms of domain shape, average size, and related size distribution of the dispersed rubbery microdomains within a PLA matrix. The results indicate that the dispersion of P(CL-co-LA) copolymer containing 28 mol% LA comonomer is increased by four times, which is approximately 11.4  $\text{kJ m}^{-2}$  for the resulting PLA blend. This occurrence can be attributed to the presence of ribbon-like rubbery microdomains. The same team<sup>260</sup> also tailored the interfacial compatibility and morphological characteristics of PLA/P(CL-co-LA) blends through the inclusion of  $\text{SiO}_2$  nanoparticles and altered the morphological characteristics of the blends to a continuous one, as TEM images shown in Fig. 57. The high toughness of PLA/P(CL-co-LA) blends is achieved with an impact strength of 39.2  $\text{kJ m}^{-2}$ .

Chen *et al.*<sup>261</sup> synthesized graft PLLA with a hydroxyl end group through the ring opening polymerization of L-LA. Branched

poly(castor oil) (PCO) polymers are synthesized by reacting castor oils with HDI and then grafting into PCO to produce renewable and biodegradable branched PCO-g-PLLA copolymers. Thus, the tensile toughness of PLA is improved by melt blending PLLA with PCO-g-PLLA, an efficient modifier and compatibilizer. A strong interfacial interaction, the homogeneous dispersion of the copolymer in the PLLA matrix, and the cross-linking structure of PCO and PLLA play important roles in the enhancement of toughness. The elongation at break of 130% of PLLA/PCO-g-PLLA (80/20) blends is 30 times higher than that of pure PLLA (4%). The tensile strength of the blend is maintained at 40 MPa. Zhang and Ito *et al.*<sup>262</sup> prepared highly toughened PLA with a novel sliding graft copolymer through *in situ* reactive compatibilization, cross-linking, and chain extension. A “sliding graft copolymer” (SGC) is fabricated with PCL as side chains connected to the cyclodextrin rings of polyrotaxane (PR). SGC is used to toughen PLA, and MDI, as a reactive compatibilizer, is added to improve the interfacial compatibility. SGC is *in situ* cross-linked and therefore transformed from a crystallized plastic into a totally amorphous elastomer during reactive blending. FTIR, GPC, SEM, and TEM reveal

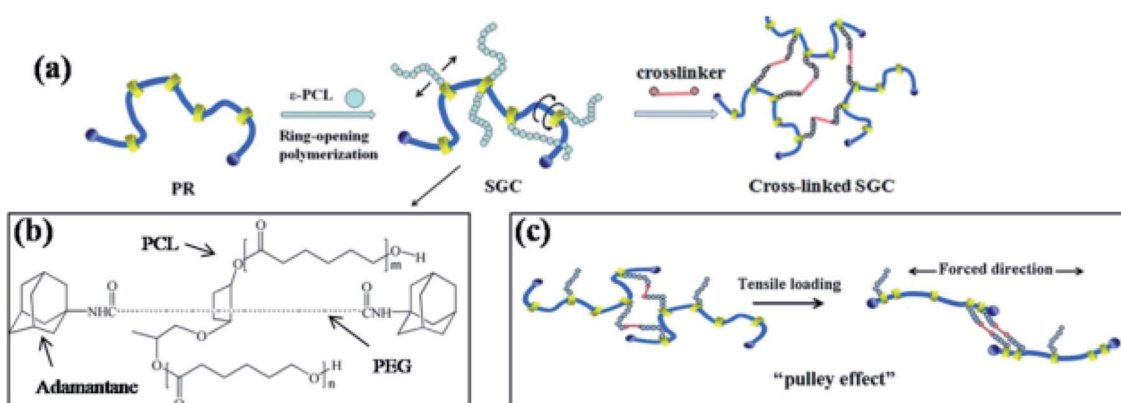


Fig. 58 (a) Schematic illustration of the preparation of a sliding graft copolymer (SGC), (b) structure schematic of SGC, (c) pulley effect. Ref. 262, copyright 2014. Reproduced with permission from Elsevier.

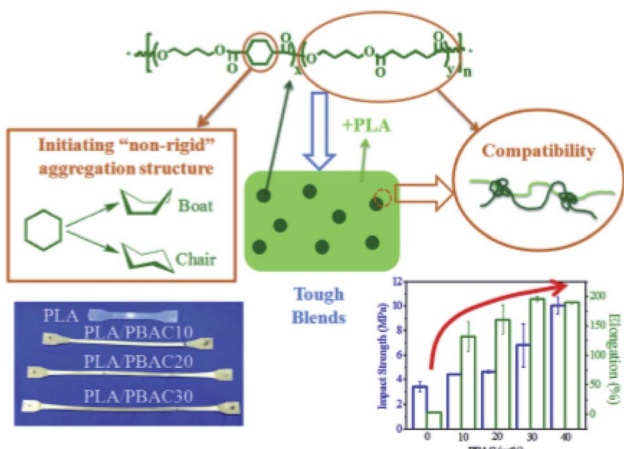


Fig. 59 The two key factors to achieve high toughness of PLA with non-planar ring contained polyester. Ref. 269, copyright 2016. Reproduced with permission from Elsevier.

that a PLA-*co*-SGC copolymer is formed at the interface to greatly improve the compatibility between PLA and SGC, and the chain extension of PLA also occurs. Moreover, the formation of the SGC elastomer containing the sliding cross-linking point exhibits a pulley effect, as illustrated in Fig. 58, which effectively improves the toughness of the blend. The impact strength and elongation at break of the PLA/SGC/MDI blends significantly increase to 48.6 kJ m<sup>-2</sup> and 236%, respectively.

Hillmyer *et al.*<sup>263</sup> prepared poly(1,5-cyclooctadiene-*co*-5-norbornene-2-methanol-*graft*-D,L-lactide) [PCNL] through ring opening metathesis polymerization and ring opening transesterification polymerization. PCNL is used to toughen PLA by melt blending. A good toughening effect is obtained without a major loss of strength or rigidity of PLA/PCNL blends. The PLA/PCNL blend tensile strength of 65 MPa is comparable with that of pure PLA, and the elongation at break is significantly improved to 250%.

According to previous studies,<sup>264–268</sup> the materials containing nonplanar ring structures possess good rigidity and toughness. Nonplanar ring structures can be used as effective toughening agents. Na and Zhu *et al.*<sup>269</sup> synthesized a poly(butylene adipate-*co*-1,4-cyclohexanedicarboxylate) (PBAC) containing a nonplanar ring structure and utilized it as a toughening agent for the melt-toughening modification of PLA. The structural model of high tough PLA with non-planar ring contained polyester was shown in Fig. 59. With the addition of 40 wt% PBAC, the elongation at break and the notched impact strength increase from 3.8% and 3.5 kJ m<sup>-2</sup> of pure PLA to 196.1% and approximately 10 kJ m<sup>-2</sup>, respectively.

## 7. Strategies for the formation of super tough PLA via controlling phase structure parameters

### 7.1. Particle size of flexible or elastic polymers in PLA matrix

For PLA-based blends toughened with flexible or elastic polymers, the parameters of the blend components influence the

final properties of PLA bio-based blends:<sup>71,107,182</sup> (1) the type and amount of flexible or elastic polymers; (2) particle shape, particle size, particle size distribution, and interparticle distance of the dispersed phase; (3) and the interfacial adhesion and phase structure of PLA-based blends. The type and amount of flexible or elastic polymers are discussed above, and the influence of interfacial adhesion on the properties of PLA-based blends is presented. The interfacial adhesion and phase morphology parameters of blends can be achieved by applying a compatibilization strategy and adjusting processing techniques.<sup>149,171</sup> The particle size parameters of the dispersed phase are the most studied structure parameters in flexible polymer-toughened PLA systems, and they are essential for the determination of the impact toughness of PLA blends.

The interfacial bonding and parameters of the particle size of the dispersed phase are mutually influenced and correlated with the compatibility of PLA-based blends. With the enhanced interfacial compatibility, the improvement of the interfacial adhesion of blend components and the reduction of the particle size of dispersed phase result in a remarkable increase in impact strength. For example, for PLA/PE blend systems,<sup>171</sup> the average particle size of the LDPE dispersed phase decreases from 6.4  $\mu\text{m}$  for pure PLA/PE binary blends to 0.9  $\mu\text{m}$  for compatibilized PLA/PE blends with the addition of 5 wt% PLLA-PE block copolymer as a compatibilizer. The impact strength of compatibilized PLA/PE blends increase from 34 J m<sup>-1</sup> for PLA/PE binary blends to 460 J m<sup>-1</sup>. The reduction in the particle size is the goal for PLA-based blends. However, the optimum particle size of the dispersed phase is necessary for super tough PLA.<sup>125</sup> In fact, extremely large particle size leads to the reduction in the sufficient area between the dispersed phase and a PLA matrix, which likely induce premature crack propagation due to the coalescence of crazes.<sup>242</sup> By contrast, an extremely small particle size cannot be used as a stress concentration point, so it is inefficient in initiating cavitation and terminating the growth of crazes.

Wu<sup>42,60</sup> indicated that entanglement density ( $V_e$ ) is considered one of the main factors governing the deformation mechanism. For brittle polymers in general super toughening is predicted to occur at an optimum  $V_e$  of 0.1 mmol cm<sup>-3</sup>, as massive crazing and yielding go the matrix occurs at this level of  $V_e$ .<sup>60</sup> Depending on the composition,  $V_e$  of PLA is predicted to be in the range of 0.12–0.14 mmol cm<sup>-3</sup>.<sup>64,65</sup> Using Wu's proposed relationship between optimum flexible or elastic polymer particle size ( $d_0$ ) and  $V_e$ , as follows eqn (5):

$$\log d_0 = 1.19 - 1.41 \nu_e \quad (5)$$

Therefore, the optimum particle size is determined by matrix chain parameters. The optimum particle size varies among different flexible or elastic polymers because of the different matrix chain parameters.  $d_0$  for PLA can be calculated to be in the range of 0.16–0.31  $\mu\text{m}$ . Theoretical investigations indicate that this range can be used as a reference value of particle size in future PLA work to achieve a successful super toughening effect.

After correlating toughening efficiency with particle size and matrix chain parameters, Wu<sup>60</sup> concluded that optimum



particle size decreases as  $V_e$  of flexible- or elastic-polymer-toughened brittle polymers ( $V_e < 0.15 \text{ mmol cm}^{-3}$  and  $C_\infty > 7.5$ ) increases. In the case of an amorphous brittle PLA matrix ( $V_e = 0.1 \text{ mmol cm}^{-3}$ ), Bai *et al.*<sup>242</sup> estimated the optimum particle size to be *ca.* 0.75  $\mu\text{m}$ , which is in agreement with the experimental results in various studies, showing that the optimum particle size for the high toughening efficiency of amorphous PLA-based blends is 0.7–1.1  $\mu\text{m}$ .<sup>107,108,125,242</sup> Notably, the optimum particle size for a highly crystalline PLA matrix is small at 0.3–0.5  $\mu\text{m}$ .<sup>242</sup>

The difference in the optimum particle size between amorphous and highly crystalline PLA matrixes is attributed to the different dominating toughening mechanisms. Generally, large particles are efficient in initiating multiple crazes, which dominate in an amorphous PLA matrix. By contrast, relatively small particles are effective in triggering the matrix shear yielding, which dominate in a highly crystalline PLA matrix.

Several works have reported the effect of particle size on the properties of PLA blends. The optimum particle size in PLA/EMA-GMA/DMSA,<sup>141</sup> PLA/LLDPE/PLA-*co*-PE,<sup>171,172</sup> PLA/PBS/LTI,<sup>221</sup> and PLA/TPU blends<sup>89</sup> is approximately 0.9  $\mu\text{m}$ . Similar findings have been obtained in other works; that is, optimum particle size ranges from 0.7  $\mu\text{m}$  to 0.9  $\mu\text{m}$  in PLA/CPU,<sup>107,108</sup> PLA/PBSA/ADR,<sup>248</sup> PLA/EBA-GMA,<sup>148</sup> and PLA/EMA-GMA/EMAA-Zn blends.<sup>149–152</sup> For example, the impact strength reaches 777.2  $\text{J m}^{-1}$  when the optimum particle size is 0.82  $\mu\text{m}$ . In other studies, a large particle size of more than 1  $\mu\text{m}$  is also obtained. When the particle size is 1.91  $\mu\text{m}$ , the impact strength of super tough PLA/LLDPE/PLA-*co*-PE blends reaches 510  $\text{J m}^{-1}$ .<sup>171</sup> Small particle size is also revealed in some studies, especially for highly crystalline PLA matrix. When the optimum particle size is 0.67  $\mu\text{m}$ ,<sup>154</sup> the impact strength of PLA/EGA blends is up to 59.8  $\text{kJ m}^{-2}$  as the crystallinity of the PLA matrix increases from 2.7% for pure PLA to 29.0%. Highly tough PLA/PCL blends containing a highly crystalline PLA matrix with an optimum particle size of 0.39  $\mu\text{m}$  are also obtained. These results demonstrate that a suitable particle size can lead to a dramatic enhancement in the performance of PLA-based blends.

Differences in optimum particle size are mainly attributed to the complexities of polymer chain movements and polymer blending systems. In addition to  $V_e$  and crystallinity of a PLA matrix, the optimum particle size strongly depends on material characteristics, such as viscosity and viscosity ratio, modulus of flexible or elastic polymers, and interfacial tensions of polymer blends; mechanical parameters, such as blending temperature and shear rate; and morphological characteristics of the dispersed particles.

## 7.2. Interparticle distance of PLA-based blends

Another factor to consider for efficient flexible or elastic polymer toughening is interparticle distance ( $L$ ). This factor plays an important role in controlling the toughness of PLA-based blends. According to toughening theories,<sup>14</sup> interparticle distance is directly related to particle size and flexible or elastic polymer content. It must be below the critical value of polymer blends to obtain high-toughness PLA-based blends, which

dispersed particles of flexible or elastic polymers can effectively initiate plastic deformation in the surrounding matrix. The critical value is affected by many intrinsic properties, such as the modulus of flexible or elastic polymers, modulus ratio, blend component fraction, and dispersed phase. Hillmyer *et al.*<sup>171</sup> revealed that the impact strength of PLA/LLDPE/PLA-*co*-PE blends increases as the interparticle distance decreases for LLDPE-toughened PLA systems, and the critical interparticle distance of PLA blends is approximately 1.0  $\mu\text{m}$ . Hillmyer *et al.*<sup>171</sup> further investigated the influence of a block copolymer microstructure on the toughness of compatibilized PLA/LLDPE blends. The results also indicate that the impact strength of PLA/LLDPE/PLA-*co*-PE blends sharply increases to 760  $\text{J m}^{-1}$  as the interparticle distance decreases to 0.4  $\mu\text{m}$ . In addition, the super tough PLA blends are obtained through *in situ* reactive blending with a PEG-based diacrylate monomer. The impact strength increases to 50  $\text{kJ m}^{-2}$  when the interparticle distance is 0.27  $\mu\text{m}$ .<sup>182</sup> The same findings are also observed in PLA/PU blends with an interparticle distance of 0.91  $\mu\text{m}$ .<sup>99</sup> In general, a high or super tough PLA blend can be obtained if the interparticle distance is less than 1.0  $\mu\text{m}$ .

In another work, the interparticle distance of PLA/POE-g-GMA blends is reduced with the increase in rubber content and particle size. The critical value of interparticle distance for the effective toughening of the blend is found to be 0.5  $\mu\text{m}$ .<sup>155</sup>

The amount of flexible or elastic polymers and compatibilization can tailor the size and distribution of dispersed phases; thus, the interparticle distance below the critical value of interparticle distance. The relation of interparticle distance with the amount of dispersed phase and particle size should be studied further.

## 7.3. Phase morphologies of PLA-based blends

The improvement in the final properties is determined by the intrinsic properties of blend components and significantly depends on the morphological characteristics of blends. Therefore, the factor to consider for super tough PLA blends is phase morphology. This factor significantly affects the final performance of PLA blends. Sea-island morphology, laminar, fibrillar, co-continuous morphology, quasi co-continuous structure, and network-like structure are typical morphologies in polymer blends. The blend component ratio and its corresponding viscoelastic properties, interfacial tension, and process conditions, such as blend methods, processing technology, blending temperature, and time, are considered important factors in the evolution of the morphologies of polymer blends. Sea-island morphology with a flexible or elastic polymer dispersed in a PLA matrix is normally observed. However, with this morphology, highly tough PLA is difficult to obtain. The formation of a co-continuous phase structure, a quasi co-continuous structure, and a network-like structure is a highly efficient way to prepare super tough PLA.<sup>97,121,205,206,208</sup> For PLA/EBA-GMA/EMAA-Zn blends,<sup>144,149</sup> salami-like phase morphologies are formed, leading to the improvement in impact strength, exceeding 700  $\text{J m}^{-1}$ .

The morphological transition of a dispersed TPU phase from a sea-island structure to a unique network-like structure is



observed in super tough PLA/TPU/PDLA blend systems.<sup>96,97</sup> Unique network-like morphologies are also observed in super tough PLA/PU/SiO<sub>2</sub> blends with an impact strength of 59.42 kJ m<sup>-2</sup>. Some related studies on continuous phase morphology have also been conducted. The quasi-*co*-continuous morphologies induced by CNTs are selectively localized in the TPU phase. Consequently, super tough PLA/TPU/CNTs blends are fabricated successfully.<sup>100</sup> Quasi-*co*-continuous morphologies are also obtained in fully bio-based and super tough PLA-based thermoplastic vulcanizates fabricated *via* peroxide-induced dynamic vulcanization and interfacial compatibilization.<sup>121</sup> Furthermore, specific *co*-continuous phase morphologies are found in super tough PLA/PBAT/EMA-GMA blends,<sup>166</sup> dynamically vulcanized PLA/NR blends,<sup>205</sup> and highly tough poly(lactide)/ethylene-*co*-vinyl acetate thermoplastic vulcanizates.<sup>175</sup>

Therefore, PLA-based multicomponent blends containing reactive copolymers are being developed to tune phase morphology and obtain PLA-based blends with moderate stiffness and sufficient toughness. Hence, techniques such as *in situ* reactive compatibilization and dynamic vulcanization are effective in achieving the desired phase morphology. These processes increase interfacial strength by promoting chemical reactions between blending components, establishing a strong bridge for the transmission of stresses, and obtaining the desired particle parameters of the dispersed phase and phase morphologies of PLA-based blends. The improved properties of PLA blends demonstrate their high potential for use in environmentally friendly materials.

## 8. Conclusion and future perspectives

PLA is a bio-based biodegradable and biocompatible plastic that shows great potential for various applications because of its excellent mechanical properties, such as high modulus and high strength. However, the application fields of PLA are limited because of its inherent brittleness, low elongation at break, and sensitivity to notches with low impact strength. Thus, PLA should be toughened and modified. Conventional toughening systems generally include plasticizers, inorganic/organic rigid particles, thermoplastic elastomers, and biodegradable plastics. Among them, plasticizers belong to a small-molecule toughening system, and they easily migrate. The interface compatibility between rigid particles and a PLA matrix is poor, and an excellent toughening modification effect is difficult to obtain. Thermoplastic elastomers and degradable plastics cannot obtain excellent toughening modification effects because of PLA's excellent mechanical properties, such as high modulus, high strength, and degradability.

However, the sustainability of materials is decreased by blending with petroleum-based polymers. As such, elastic fossil-based polymers are not ideal toughening components for PLA. Even though this area has remarkably improved, further studies should be conducted.

(1) The designation, synthesis, and application of high-performance bio-based materials, especially biodegradable

elastomers, in toughening PLA are new research topics. The design and development of environmentally friendly compatibilizers with high reactivity through a combination of reactive compatibilization methods can effectively regulate the phase structure and morphological characteristics of PLA. Thus, high-performance PLA-based blends can be achieved.

(2) Nanoparticles may be used to enhance PLA blend systems, especially with the selective dispersion effect, and manipulate the compatibility and phase structure of blends. The synergistic strengthening and toughening effects of nanoparticles on PLA blends will be realized, and these aspects have important research and industrial values.

(3) Crystallinity influences the properties of PLA-based blends. The improvement in the crystallinity of a PLA matrix in PLA-based blends is promoted by using nanoparticles, annealing techniques, and PDLA to form SC crystallites. Various parameters, including crystallization morphology, crystallite dimension, and crystallinity, and the crystallization mechanism of super tough PLA-based blends should be considered in future research.

(4) Many studies have been carried out to toughen PLA. Research on PLA-based blends with excellent heat resistance and high toughness should be conducted in the future.

(5) Common natural polymer materials, such as starch, cellulose, chitosan, and so on, should be further strengthened for modifying PLA materials. The development of low-cost and high-performance PLA/natural polymer materials plays an important role in the application and promotion of bio-based and biodegradable materials.

(6) Many works have been carried out on the structure and properties of PLA blends, but few studies have focused on evaluating the biodegradability of PLA blends and the whole life cycle of PLA products. Strengthening the evaluation of the biodegradability of PLA materials can effectively promote the development and application of biodegradable materials and is essential for promoting the development of industrial chains in the field of biodegradable materials.

## Abbreviations

PLA	Poly(lactic acid) or poly(lactide)
PET	Poly(ethylene terephthalate)
PS	Polystyrene
PE	Polyethylene
ABS	Acrylonitrile–butadiene–styrene copolymer
PU	Polyurethanes
EGMA	Poly(ethylene- <i>co</i> -glycidyl methacrylate)
PCL	Polycaprolactone
PA11	Polyamide 11
PBAT	Poly(butylene adipate- <i>co</i> -terephthalate)
PBS	Poly(butylene succinate)
EBA-GMA	Poly(ethylene- <i>n</i> -butylene-acrylate- <i>co</i> -glycidyl methacrylate)
AP	Amylopectin
PMMA	Poly(methyl methacrylate)
TPE	Thermoplastic elastomer



TPU	Polyurethane thermoplastic elastomer	MB-g-GMA	Glycidyl methacrylate-functionalized methyl methacrylate-butadiene copolymers
TPO-PLA	Thermoplastic polyolefin elastomer- <i>graft</i> -polylactide	NR-GMA	Natural rubber graft-modified glycidyl methacrylate
TPO-MAH	Grafting polylactide onto maleic anhydride-functionalized TPO	EGMA-g-AS	Ethylene glycidyl methacrylate- <i>graft</i> -styrene- <i>co</i> -acrylonitrile
EVA	Ethylene-vinyl acetate	PA11	Polyamide11
EAE	Ethylene acrylic elastomer	LLDPE	Linear lowdensity polyethylene
PEBA	Poly(ethylene oxide- <i>b</i> -amide-12)	ACR	Methyl methacrylate-ethyl acrylate core-shell copolymer
PDLA	Poly( <i>D</i> -lactide)	BPM	Acrylic impact modifier
SC	Stereocomplex crystallites	MBS	Methyl methacrylate-butadiene-styrene
CNT	Carbon nanotube	PEGDA	Poly(ethylene glycol)diacrylate
SiO <sub>2</sub>	Hydrophilic silica	PPA	Poly(1,2-propylene glycol adipate)
TiO <sub>2</sub>	Titanium dioxide	MAPEG	PEG methyl ether methacrylate
PUP	Polyurethane prepolymer	AcrylPEG	PEG methyl ether acrylate
MDI	4,4'-Methylenedi- <i>p</i> -phenyl diisocyanate	L101	2,5-dimethyl-2,5-di( <i>tert</i> -butylperoxy)hexane
PBA	Poly-1,4-butylene glycol adipate dio	EB	Poly(ethylene butylene) copolymer
PDI	1,4 phenylene diisocyanate	PEPG	Poly(ethyleneglycol-random-propylene glycol) midblock
PUS	Polyurethane elastomer	PEG	Poly(ethylene glycol)
PPG	Polyester polyol	PPG	Poly(propylene glycol)
TDI	Toluene-2,4-diisocyanate	PETG	Poly(ethylene terephthalate glycol)
PEG	Polyethylene glycol	BPM	Core-shell impact modifier
PUEP	Polyurethane elastomer prepolymer terminated with an isocyanate group	PBA	Polybutyl acrylate
PLBSI	Bio-based copolymer prepared from bio-based monomers, such as lactic acid, butanediol, sebacic acid, and itaconic acid	EA-UFPR	Ultrafine full-vulcanized powdered ethyl acrylate rubber
PELU	Biodegradable polyurethane <i>via</i> the chain extension reaction between polyethylene glycol- <i>b</i> -PLA copolymer and IPDI	MMTs	Montmorillonites
ADR	Industrial-grade oligomer of multiple epoxy groups	LTI	Lysine triisocyanate
BE	Bioelastomer	TBT	Tetrabutyl titanate
UPE	Bio-based unsaturated aliphatic polyester elastomer	P(3HB- <i>co</i> -4HB)	Poly(3-hydroxybutyrate- <i>co</i> -4-hydroxybutyrate)
VUPE	Polyester elastomer	TPP	Triphenyl phosphite
UBE	Unsaturated bio-based resin		
DPUD	Poly( <i>D</i> -lactide)- <i>b</i> -polyurethane- <i>b</i> -poly( <i>D</i> -lactide)		
GMA	Glycidyl methacrylate		
EMA-GMA	Ethylene-methyl acrylate-glycidyl methacrylate random terpolymer		
EGA	Ethylene/methacrylate/glycidyl methacrylate terpolymer		
MAH	Maleic anhydride		
POE- <i>g</i> -GMA	Poly(ethylene octene) grafted with glycidyl methacrylate		
DCP	Dicumyl peroxide		
E-AE-GMA	Ethylene- <i>co</i> -acrylic ester- <i>co</i> -glycidyl methacrylate		
BA-EA-	Butyl acrylate (BA), ethylacrylate (EA) and glycidyl methacrylate (GMA) copolymer		
GMA	Poly(ethylene-glycidyl methacrylate)		
EGMA	Zinc ionomer of ethylene/methacrylic acid		
EMAA-Zn	Sebacic acid cured epoxidized soybean oil		
VESO	Epoxidized soybean oil		
ESO	Sebacic acid		
SA	Sebacic acid cured epoxidized soybean oil precursors		
SEPs	Thermoplastic starch acetate		
TPSA	Polyether- <i>block</i> -amide- <i>graft</i> -glycidyl methacrylate		
PEBA- <i>g</i> -GMA			

## Conflicts of interest

There are no conflicts to declare.

## Acknowledgements

The work is funded by National Natural Science Foundation of China (51273060), and Key Project of Science and Technology Research Plan of Hubei Provincial Education Department, the Open Fund of Hubei Provincial Key Laboratory of Green Materials for Light Industry.

## References

- 1 P. R. Christensen, A. M. Scheuermann, K. E. Loeffler, *et al.* Closed-loop recycling of plastics enabled by dynamic covalent diketoenamine bonds, *Nat. Chem.*, 2019, **11**(5), 442–448.
- 2 S. Haritz and P. D. Andrew, Plastics recycling with a difference, *Science*, 2018, **360**(6387), 380–381.
- 3 R. Chandra and R. Rustgi, Biodegradable polymers, *Prog. Polym. Sci.*, 1998, **23**(7), 1273–1335.



4 L. Yu, K. Dean and L. Li, Polymer blends and composites from renewable resources, *Prog. Polym. Sci.*, 2006, **31**(6), 576–602.

5 Y. Q. Zhu, C. Romain and C. K. Williams, Sustainable polymers from renewable resources, *Nature*, 2016, **540**(7633), 354–362.

6 Z. Liu, D. Hu, L. Huang, *et al.* Simultaneous improvement in toughness, strength and biocompatibility of poly(lactic acid) with polyhedral oligomeric silsesquioxane, *Chem. Eng. J.*, 2018, **346**, 649–661.

7 R. G. Sinclair, The case for polylactic acid as a commodity packaging plastic, *J. Macromol. Sci., Part A: Pure Appl. Chem.*, 1996, **33**(5), 585–597.

8 A. Garlotta, literature review of poly(lactic acid), *J. Polym. Environ.*, 2001, **9**(2), 63–84.

9 L. T. Sin, A. R. Rahmat and W. A. W. A. Rahman, *Polylactic Acid*, William Andrew, 2012, ch. 4, vol. 47, pp. 1530–1542.

10 P. Saini, M. Arora and M. N. V. R. Kumar, Poly(lactic acid) blends in biomedical applications, *Adv. Drug Delivery Rev.*, 2016, **107**(15), 47–59.

11 A. Södergård and M. Stolt, Properties of lactic acid based polymers and their correlation with composition, *Prog. Polym. Sci.*, 2002, **27**(6), 1123–1163.

12 B. Gupta, N. Revagade and J. Hilborn, Poly(lactic acid) fiber: an overview, *Prog. Polym. Sci.*, 2007, **32**(4), 455–482.

13 S. Saeidlou, M. A. Huneault, H. Li, *et al.* Poly(lactic acid) crystallization, *Prog. Polym. Sci.*, 2012, **37**(12), 1657–1677.

14 L. T. Lim, R. Auras and M. Rubino, Processing technologies for poly(lactic acid), *Prog. Polym. Sci.*, 2008, **33**(8), 820–852.

15 M. Kaseem, Properties and medical applications of polylactic acid: A review, *eXPRESS Polym. Lett.*, 2015, **9**(5), 435–455.

16 K. Anderson, K. Schreck and M. Hillmyer, Toughening polylactide, *Polym. Rev.*, 2008, **48**(10), 85–108.

17 R. M. Rasal, A. V. Janorkar and D. E. Hirt, Poly(lactic acid) modifications, *Prog. Polym. Sci.*, 2010, **35**(3), 338–356.

18 Y. Yang, L. Zhang, Z. Xiong, *et al.* Research progress in the heat resistance, toughening and filling modification of PLA, *Sci. China: Chem.*, 2016, **59**(11), 1355–1368.

19 V. H. Sangeetha, H. Deka, T. O. Varghese, *et al.* State of the art and future prospectives of poly(lactic acid) based blends and composites, *Polym. Compos.*, 2018, **39**(1), 81–101.

20 Y. L. Cheng, S. B. Deng, P. Chen, *et al.* Polylactic acid (PLA) synthesis and modifications: a review, *Front. Chem. China*, 2009, **4**(3), 259–264.

21 H. Z. Liu and J. W. Zhang, Research progress in toughening modification of poly(lactic acid), *J. Polym. Sci., Part B: Polym. Phys.*, 2011, **49**(15), 1051–1083.

22 Y. Yang, L. S. Zhang, Z. Xiong, *et al.* Research progress in the heat resistance, toughening and filling modification of PLA, *Sci. China: Chem.*, 2016, **59**(11), 1355–1368.

23 C. M. Thurber, Y. Xu, J. C. Myers, *et al.* Accelerating reactive compatibilization of PE/PLA blends by an interfacially localized catalyst, *ACS Macro Lett.*, 2015, **4**(1), 30–33.

24 M. Y. Jo, Y. J. Ryu, J. H. Ko, *et al.* Effects of compatibilizers on the mechanical properties of ABS/PLA composites, *J. Appl. Polym. Sci.*, 2012, **125**(S2), E231–E238.

25 A. Rigoussen, P. Verge, J. M. Raquez, *et al.* In-depth investigation on the effect and role of cardanol in the compatibilization of PLA/ABS immiscible blends by reactive extrusion, *Eur. Polym. J.*, 2017, **93**, 272–283.

26 I. Balázs, B. Dániel, D. Attila, *et al.* Structure, properties and interfacial interactions in poly(lactic acid)/polyurethane blends prepared by reactive processing, *Eur. Polym. J.*, 2013, **49**(10), 3104–3113.

27 W. Y. Lin and J. P. Qu, Enhancing Impact Toughness of Renewable Poly(lactic acid)/Thermoplastic Polyurethane Blends via Constructing Co-continuous-like Phase Morphology Assisted by Ethylene-Methyl Acrylate-Glycidyl Methacrylate Copolymer, *Ind. Eng. Chem. Res.*, 2019, **58**(25), 10894–10907.

28 M. Wu, K. Wang, Q. Zhang, *et al.* Manipulation of multiphase morphology in the reactive blending system OBC/PLA/EGMA, *RSC Adv.*, 2015, **5**(117), 96353–96359.

29 G. P. Sui, K. Wang, S. M. Xu, *et al.* The combined effect of reactive and high-shear extrusion on the phase morphologies and properties of PLA/OBC/EGMA ternary blends, *Polymer*, 2019, **169**, 66–73.

30 U. Jon, G. E. Gonzalo and E. J. Ignacio, Melt processed PLA/PCL blends: effect of processing method on phase structure, morphology, and mechanical properties, *J. Appl. Polym. Sci.*, 2015, **132**(41), 42641.

31 A. Ostafinska, I. Fortelný, J. Hodan, *et al.* Strong synergistic effects in PLA/PCL blends: Impact of PLA matrix viscosity, *J. Mech. Behav. Biomed. Mater.*, 2017, **69**, 229–241.

32 A. Nuzzo, E. Bilotti, T. Peijs, *et al.* Nanoparticle-induced co-continuity in immiscible polymer blends-A comparative study on bio-based PLA-PA11 blends filled with organoclay, sepiolite, and carbon nanotubes, *Polymer*, 2014, **55**(19), 4908–4919.

33 D. Rasselet, A. S. Caro-Bretelle, A. Taguet, *et al.* Reactive Compatibilization of PLA/PA11 Blends and Their Application in Additive Manufacturing, *Materials*, 2019, **12**(3), 485.

34 R. Al-Ittry, K. Lamnawar and A. Maazouz, Reactive extrusion of PLA, PBAT with a multi-functional epoxide: Physico-chemical and rheological properties, *Eur. Polym. J.*, 2014, **58**, 90–102.

35 Z. Q. Sun, B. Zhang, X. C. Bian, *et al.* Synergistic effect of PLA-PBAT-PLA tri-block copolymers with two molecular weights as compatibilizers on the mechanical and rheological properties of PLA/PBAT blends, *RSC Adv.*, 2015, **5**(90), 73842–73849.

36 Y. Ding, B. Lu, P. L. Wang, *et al.* PLA-PBAT-PLA tri-block copolymers: Effective compatibilizers for promotion of the mechanical and rheological properties of PLA/PBAT blends, *Polym. Degrad. Stab.*, 2018, **147**, 41–48.

37 T. Yokohara and M. Yamaguchi, Structure and properties for biomass-based polyester blends of PLA and PBS, *Eur. Polym. J.*, 2008, **44**(3), 677–685.

38 S. Su, R. Kopitzky, S. Tolga, *et al.* Polylactide (PLA) and its blends with poly(butylene succinate) (PBS): a brief review, *Polymer*, 2019, **11**(7), 1193.



39 M. Akrami, I. Ghasemi, H. Azizi, *et al.* A new approach in compatibilization of the poly(lactic acid)/thermoplastic starch (PLA/TPS) blends, *Carbohydr. Polym.*, 2016, **144**, 254–262.

40 W. Yang, E. Fortunati, F. Dominici, *et al.* Synergic effect of cellulose and lignin nanostructures in PLA based systems for food antibacterial packaging, *Eur. Polym. J.*, 2016, **79**, 1–12.

41 C. A. P. Joziasse, M. D. C. Topp, H. Veenstra, *et al.* Supertough poly(lactide)s, *Polym. Bull.*, 1994, **33**(5), 599–605.

42 S. Wu, Chain structure and phase morphology, and toughness relationships in polymers and blends, *Polym. Eng. Sci.*, 1990, **30**(13), 753–761.

43 S. Wu, Predicting chain conformation and entanglement of polymers from chemical structure, *Polym. Eng. Sci.*, 1992, **32**(12), 823–830.

44 R. E. Drumright, P. R. Gruber and D. E. Henton, Polylactic acid technology, *Adv. Mater.*, 2000, **12**(23), 1841–1846.

45 L. T. Lim, R. Auras and M. Rubino, Processing technologies for poly(lactic acid), *Prog. Polym. Sci.*, 2008, **33**(8), 820–852.

46 K. M. Nampoothiri, N. R. Nair and R. P. John, An overview of the recent developments in polylactide (PLA) research, *Bioresour. Technol.*, 2010, **101**(22), 8493–8501.

47 G. Liu, X. Zhang and D. Wang, Tailoring Crystallization: Towards High-Performance Poly(lactic acid), *Adv. Mater.*, 2014, **26**(40), 6905–6911.

48 J. B. Zeng, K. A. Li and A. K. Du, Compatibilization strategies in poly(lactic acid)-based blends, *RSC Adv.*, 2015, **5**(41), 32546–32565.

49 S. Farah, D. G. Anderson and R. Langer, Physical and mechanical properties of PLA, and their functions in widespread applications-a comprehensive review, *Adv. Drug Delivery Rev.*, 2016, **107**, 367–392.

50 Z. Li, B. H. Tan, T. Lin, *et al.* Recent Advances in Stereocomplexation of Enantiomeric PLA-Based Copolymers and Applications, *Prog. Polym. Sci.*, 2016, **62**, 22–72.

51 V. Nagarajan, A. K. Mohanty and M. Misra, Perspective on polylactic acid (PLA) based sustainable materials for durable applications: focus on toughness and heat resistance, *ACS Sustainable Chem. Eng.*, 2016, **4**(6), 2899–2916.

52 M. Wang, Y. Wu, Y. D. Li, *et al.* Progress in toughening poly(Lactic Acid) with renewable polymers, *Polym. Rev.*, 2017, **57**(4), 1–37.

53 K. Hamad, M. Kaseem, M. Ayyoob, *et al.* Polylactic acid blends: the future of green, light and tough, *Prog. Polym. Sci.*, 2018, **85**, 83–127.

54 N. F. Alias and H. Ismail, An overview of toughening polylactic acid by an elastomer, *Polym.-Plast. Technol. Mater.*, 2019, **58**(13), 1–24.

55 M. Nofar, D. Sacligil, P. J. Carreau, *et al.* Poly (lactic acid) blends: processing, properties and applications, *Int. J. Biol. Macromol.*, 2018, **125**, 307–360.

56 L. I. Palade, H. J. Lehermeier and J. R. Dorgan, Melt rheology of high l-content poly(lactic acid), *Macromolecules*, 2001, **34**(5), 1384–1390.

57 V. Heshmati, A. M. Zolali and B. D. Favis, Morphology development in poly (lactic acid)/polyamide11 biobased blends: chain mobility and interfacial interactions, *Polymer*, 2017, **120**(30), 197–208.

58 V. Shah, *Handbook of plastics testing technology*, John Wiley and Sons, New York, 1998.

59 J. W. Gooch, *Encyclopedic Dictionary of Polymers*, Springer, New York, 2010.

60 S. Wu, Control of intrinsic brittleness and toughness of polymers and blends by chemical structure: a review, *Polym. Int.*, 1992, **29**(3), 229–247.

61 W. Brostow, H. E. Hagg Lobland and S. Khoja, Brittleness and toughness of polymers and other materials, *Mater. Lett.*, 2015, **159**, 478–480.

62 S. Wu and R. Beckerbauer, Effect of tacticity on chain entanglement in poly(methyl methacrylate), *Polym. J.*, 1992, **24**(12), 1437–1442.

63 S. Wu, A generalized criterion for rubber toughening: the critical matrix ligament thickness, *J. Appl. Polym. Sci.*, 1988, **35**(2), 549–561.

64 C. A. P. Joziasse, M. D. C. Topp, H. Veenstra, *et al.* Supertough poly(lactide)s, *Polym. Bull.*, 1994, **33**(5), 599–605.

65 A. Schindler and D. J. Harper, Polylactide. II. Viscosity-molecular weight relationships and unperturbed chain dimensions, *J. Polym. Sci., Polym. Chem. Ed.*, 1979, **17**(8), 2593–2599.

66 B. D. Favis, Polymer alloys and blends: recent advances, *Can. J. Chem. Eng.*, 1991, **69**(3), 619–625.

67 P. P. Lizymol and S. Thomas, Miscibility studies of polymer blends by viscometry methods, *J. Appl. Polym. Sci.*, 1994, **51**(4), 635–641.

68 D. J. David, N. A. Rotstein and T. F. Sincock, The application of miscibility parameter to the measurement of polymer-plasticizer compatibility, *Polym. Bull.*, 1994, **33**(6), 725–732.

69 Y. Y. Wang, S. C. Chen, Y. Z. Wang, *et al.* Transesterification and Miscibility of Polycarbonate/Polylactic Acid Blends, *Polym. Mater. Sci. Eng.*, 2009, **25**(11), 45–48.

70 C. Panayiotou, Polymer–polymer miscibility and partial solvation parameters, *Polymer*, 2013, **54**(6), 1621–1638.

71 C. Koning, M. V. Duin, C. Pagnoulle, *et al.* Strategies for Compatibilization of Polymer Blends, *Prog. Polym. Sci.*, 1998, **23**(4), 707–757.

72 W. N. Xiao, X. Huang, G. Z. Feng, *et al.* Research progress of toughening modification of polylactic acid, *Chem. Ind. Eng. Prog.*, 2011, **30**(3), 578–582.

73 B. Imre, Interactions, structure and properties in poly(lactic acid)/thermoplastic polymer blends, *eXPRESS Polym. Lett.*, 2013, **8**(1), 2–14.

74 B. Zhong and Z. Y. Al-Saigh, Characterization of biodegradable polymers by inverse gas chromatography. III. Blends of amylopectin and poly(l-lactide), *J. Appl. Polym. Sci.*, 2012, **123**(5), 2616–2627.



75 S. H. Li and E. M. Woo, Immiscibility-miscibility phase transitions in blends of poly(L-lactide) with poly(methyl methacrylate), *Polymer Int.*, 2008, **57**(11), 1242–1251.

76 S. H. Li and E. M. Woo, Effects of chain configuration on UCST behavior in blends of poly(L-lactic acid) with tactic poly(methyl methacrylate)s, *J. Polym. Sci., Part B: Polym. Phys.*, 2008, **46**(21), 2355–2369.

77 G. Stoclet, R. Seguela and J. M. Lefebvre, Morphology, thermal behavior and mechanical properties of binary blends of compatible biosourced polymers: Polylactide/polyamide11, *Polymer*, 2011, **52**(6), 1417–1425.

78 E. H. Merz, G. C. Claver and M. J. Baer, Studies on heterogeneous polymeric systems, *J. Polym. Sci.*, 1956, **22**(101), 325–341.

79 H. -J. Sue, Study of rubber-modified brittle epoxy systems. Part II: Toughening mechanisms under mode-I fracture, *Polym. Eng. Sci.*, 1991, **31**(4), 275–288.

80 H. S. Kim and P. Ma, Mode I and II fracture behaviour of rubber modified brittle epoxies, *Key Eng. Mater.*, 1998, **137**, 179–186.

81 S. Wu, Phase structure and adhesion in polymer blends: a criterion for rubber toughening, *Polymer*, 1985, **26**(12), 1855–1863.

82 N. C. Liu and W. E. Baker, The separate roles of phase structure and interfacial adhesion in toughening a brittle polymer, *Polym. Eng. Sci.*, 1992, **32**(22), 1695–1702.

83 H. J. Liang, W. Jiang, J. L. Zhang, *et al.* Toughening mechanism of polymer blends: Influence of voiding ability of dispersed-phase particles, *J. Appl. Polym. Sci.*, 1996, **59**(3), 505–509.

84 S. Kim, E. K. Hobbie, J. W. Yu, *et al.* Droplet breakup and shear-induced mixing in critical polymer blends, *Macromolecules*, 1997, **30**(26), 8245–8253.

85 R. P. Kambour, A review of crazing and fracture in termoplastics, *J. Polym. Sci., Macromol. Rev.*, 1973, **7**(1), 1–154.

86 C. J. G. Plummer and A. M. Donald, Crazing mechanisms and craze healing in glassy polymers, *J. Mater. Sci.*, 1989, **24**(4), 1399–1405.

87 Y. Okamoto, H. Miyagi and S. Mitsui, New cavitation mechanism of rubber dispersed polystyrene, *Macromolecules*, 1993, **26**(24), 6547–6551.

88 A. M. Donald, E. J. Kramer and R. A. Bubeck, The entanglement network and craze micromechanics in glassy polymers, *J. Polym. Sci., Polym. Phys. Ed.*, 1982, **20**(7), 1129–1141.

89 J. J. Han and H. X. Huang, Preparation and characterization of biodegradable polylactide/thermoplastic polyurethane elastomer blends, *J. Appl. Polym. Sci.*, 2011, **120**(6), 3217–3223.

90 T. Lebarb  , E. Grau, C. Alf  s and H. Cramail, Fatty acid-based thermoplastic poly(ester-amide) as toughening and crystallization improver of poly(L-lactide), *Eur. Polym. J.*, 2015, **65**, 276–285.

91 C. H. Ho, C. H. Wang, C. I. Lin, *et al.* Synthesis and characterization of TPO-PLA copolymer and its behavior as compatibilizer for PLA/TPO blends, *Polymer*, 2008, **49**(18), 3902–3910.

92 F. Feng and L. Ye, Morphologies and mechanical properties of polylactide/thermoplastic polyurethane elastomer blends, *J. Appl. Polym. Sci.*, 2011, **119**(5), 2778–2783.

93 N. Likittanaprasong, M. Seadan and S. Suttipruekpong, Impact property enhancement of poly (lactic acid) with different flexible copolymers, *IOP Conf. Ser.: Mater. Sci. Eng.*, 2015, **87**(1), 012069.

94 L. Han, C. Han and L. Dong, Morphology and properties of the biosourced poly(lactic acid)/poly(ethylene oxide-b-amide-12) blends, *Polym. Compos.*, 2013, **34**(1), 122–130.

95 L. J. Han, C. Y. Han and L. S. Dong, Effect of crystallization on microstructure and mechanical properties of poly [(ethylene oxide)-block-(amide-12)]-toughened poly(lactic acid) blend, *Polym. Int.*, 2013, **62**(2), 295–303.

96 J. Dai, H. Bai, Z. Liu, *et al.* Stereocomplex crystallites induce simultaneous enhancement in impact toughness and heat resistance of injection-molded polylactide/polyurethane blends, *RSC Adv.*, 2016, **6**(21), 17008–17015.

97 Z. Liu, Y. Luo, H. Bai, *et al.* Remarkably enhanced impact toughness and heat resistance of poly(L-lactide)/thermoplastic polyurethane blends by constructing stereocomplex crystallites in the matrix, *ACS Sustainable Chem. Eng.*, 2016, **4**(1), 111–120.

98 H. Xiu, H. W. Bai, C. M. Huang, *et al.* Selective localization of titanium dioxide nanoparticles at the interface and its effect on the impact toughness of poly(L-lactide)/poly(ether)urethane blends, *eXPRESS Polym. Lett.*, 2013, **7**(3), 261–271.

99 H. Xiu, C. Huang, H. Bai, *et al.* Improving impact toughness of polylactide/poly(ether)urethane blends via designing the phase morphology assisted by hydrophilic silica nanoparticles, *Polymer*, 2014, **55**(6), 1593–1600.

100 Y. Y. Shi, W. B. Zhang, J. H. Yang, *et al.* Super toughening of the poly(L-lactide)/thermoplastic polyurethane blends by carbon nanotubes, *RSC Adv.*, 2013, **3**(48), 26271–26282.

101 X. Zhang, E. Koranteng, Z. Wu, *et al.* Structure and properties of polylactide toughened by polyurethane prepolymer, *J. Appl. Polym. Sci.*, 2016, **133**(7), 42983.

102 S. K. Dogan, E. A. Reyes, S. Rastogi, *et al.* Reactive compatibilization of PLA/TPU blends with a diisocyanate, *J. Appl. Polym. Sci.*, 2014, **131**(10), 40251.

103 H. U. Zaman, J. C. Song, L. S. Park, *et al.* Poly(lactic acid) blends with desired end-use properties by addition of thermoplastic polyester elastomer and MDI, *Polym. Bull.*, 2011, **67**(1), 187–198.

104 X. Zhao, Z. Ding, Q. Lin, *et al.* Toughening of polylactide via in situ formation of polyurethane crosslinked elastomer during reactive blending, *J. Appl. Polym. Sci.*, 2017, **134**(2), 44383.

105 X. Zhao, M. Xu, Z. Ding, *et al.* Reactive blending toughened PLA by in situ formation of polyurethane crosslinked elastomer, *Polym. Sci., Ser. B*, 2017, **59**(4), 437–442.

106 X. Zhao, X. Yu, H. Chen, *et al.* Interfacial compatibility of super-tough poly(lactic acid)/polyurethane blends



investigated by positron annihilation lifetime spectroscopy, *J. Appl. Polym. Sci.*, 2018, **135**(31), 46596.

107 Y. S. He, J. B. Zeng, G. C. Liu, *et al.* Super-tough poly(*l*-lactide)/crosslinked polyurethane blends with tunable impact toughness, *RSC Adv.*, 2014, **4**(25), 12857–12866.

108 G. C. Liu, Y. S. He, J. B. Zeng, *et al.* In situ formed crosslinked polyurethane toughened polylactide, *Polym. Chem.*, 2014, **5**(7), 2530–2539.

109 X. Lu, X. Wei, J. Huang, *et al.* Supertoughened Poly(lactic acid)/Polyurethane Blend Material by in Situ Reactive Interfacial Compatibilization via Dynamic Vulcanization, *Ind. Eng. Chem. Res.*, 2014, **53**(44), 17386–17393.

110 X. Hu, Y. Li, M. Li, *et al.* Renewable and Super-Toughened Polylactide-based Composites: Morphology, Interfacial Compatibilization and Toughening Mechanism, *Ind. Eng. Chem. Res.*, 2016, **55**(34), 9195–9204.

111 R. L. Yu, L. S. Zhang, Y. H. Feng, *et al.* Improvement in toughness of polylactide by melt blending with bio-based poly(ester)urethane, *Chin. J. Polym. Sci.*, 2014, **32**(8), 1099–1110.

112 T. Lebarb  , E. Grau, B. Gadenne, *et al.* Synthesis of Fatty Acid-Based Polyesters and Their Blends with Poly(*l*-lactide) as a Way To Tailor PLLA Toughness, *ACS Sustainable Chem. Eng.*, 2015, **3**(2), 283–292.

113 L. Feng, X. Bian, G. Li, *et al.* Compatibility, mechanical properties and stability of blends of polylactide and polyurethane based on poly(ethylene glycol)-b-polylactide copolymers by chain extension with diisocyanate, *Polym. Degrad. Stab.*, 2016, **125**, 148–155.

114 L. Zhang, Z. Xiong, S. S. Shams, *et al.* Free radical competitions in polylactide/bio-based thermoplastic polyurethane/free radical initiator ternary blends and their final properties, *Polymer*, 2015, **64**, 69–75.

115 W. Zhang, L. Chen and Y. Zhang, Surprising shape-memory effect of polylactide resulted from toughening by polyamide elastomer, *Polymer*, 2009, **50**(5), 1311–1315.

116 Y. Li and H. Shimizu, Toughening of Polylactide by Melt Blending with a Biodegradable Poly(ether)urethane Elastomer, *Macromol. Biosci.*, 2007, **7**(7), 921–928.

117 T. Gurunathan, S. Mohanty and S. K. Nayak, Preparation and performance evaluation of castor oil-based polyurethane prepolymer/polylactide blends, *J. Mater. Sci.*, 2014, **49**(23), 8016–8030.

118 H. Kang, B. Qiao, R. Wang, *et al.* Employing a novel bioelastomer to toughen polylactide, *Polymer*, 2013, **54**(9), 2450–2458.

119 T. H. Zhao, Y. He, Y. D. Li, *et al.* Dynamic vulcanization of castor oil in a polylactide matrix for toughening, *RSC Adv.*, 2016, **6**(83), 79542–79553.

120 Y. He, T. H. Zhao, Y. D. Li, *et al.* Toughening polylactide by dynamic vulcanization with castor oil and different types of diisocyanates, *Polym. Test.*, 2017, **59**, 470–477.

121 G. C. Liu, Y. S. He, J. B. Zeng, *et al.* Fully Biobased and Supertough Polylactide-Based Thermoplastic Vulcanizates Fabricated by Peroxide-Induced Dynamic Vulcanization and Interfacial Compatibilization, *Biomacromolecules*, 2014, **15**(11), 4260–4271.

122 W. J. Si, X. P. An, J. B. Zeng, *et al.* Fully bio-based, highly toughened and heat-resistant poly(*l*-lactide) ternary blends via dynamic vulcanization with poly(*d*-lactide) and unsaturated bioelastomer, *Sci. China Mater.*, 2017, **60**(10), 1008–1022.

123 W. J. Si, L. Yang, J. Zhu, *et al.* Highly toughened and heat-resistant poly (*l*-lactide) materials through interfacial interaction control via chemical structure of biodegradable elastomer, *Appl. Surf. Sci.*, 2019, **483**, 1090–1100.

124 N. Zhang, Q. Wang, J. Ren, *et al.* Preparation and properties of biodegradable poly(lactic acid)/poly(butylene adipate-co-terephthalate) blend with glycidyl methacrylate as reactive processing agent, *J. Mater. Sci.*, 2009, **44**(1), 250–256.

125 H. Liu, W. Song, C. Feng, *et al.* Interaction of Microstructure and Interfacial Adhesion on Impact Performance of Polylactide (PLA) Ternary Blends, *Macromolecules*, 2011, **44**(6), 1513–1522.

126 M. Kumar, S. Mohanty, S. K. Nayak, *et al.* Effect of glycidyl methacrylate (GMA) on the thermal, mechanical and morphological property of biodegradable PLA/PBAT blend and its nanocomposites, *Bioresour. Technol.*, 2010, **101**(21), 8406–8415.

127 R. Al-Itry, K. Lamnawar and A. Maazouz, Rheological, morphological, and interfacial properties of compatibilized PLA/PBAT blends, *Rheol. Acta*, 2014, **53**(7), 501–517.

128 J. Wu, M. C. Kuo and C. Chen, Physical properties and crystallization behavior of poly(lactide)/poly(methyl methacrylate)/silica composites, *J. Appl. Polym. Sci.*, 2015, **132**(32), 42378.

129 T. Baouz, F. Rezgui and U. Yilmazer, Ethylene-methyl acrylate-glycidyl methacrylate toughened poly(lactic acid) nanocomposites, *J. Appl. Polym. Sci.*, 2013, **128**(5), 3193–3204.

130 Y. L. Feng, J. H. Yin, W. Jiang, *et al.* Properties of Poly(lactic acid) Toughened by Epoxy-functionalized Elastomer, *Chem. J. Chin. Univ.*, 2012, **33**(2), 400–403.

131 Y. Zhao, Y. Zhang, Z. L. Li, *et al.* Rheology, mechanical properties and crystallization behavior of glycidyl methacrylate grafted poly(ethylene octene) toughened poly(lactic acid) blends, *Korean J. Chem. Eng.*, 2016, **33**(3), 1104–1114.

132 X. Wang, J. Mi, J. Wang, *et al.* Multiple actions of poly(ethylene octene) grafted with glycidyl methacrylate on the performance of poly(lactic acid), *RSC Adv.*, 2018, **8**(60), 34418–34427.

133 F. Nie, R. Zhu, P. Zhang, *et al.* Infrared and Raman spectra analysis of PLA/PCL blend, *China Synth. Resin Plast.*, 2015, **32**(1), 59–62.

134 G. F. Brito, P. Agrawal and T. J. A. M  lo, Mechanical and Morphological Properties of PLA/BioPE Blend Compatibilized with E-GMA and EMA-GMA Copolymers, *Macromol. Symp.*, 2016, **367**(1), 176–182.

135 E. A. J. Al-Mulla, N. A. B. Ibrahim, K. Shameli, *et al.* Effect of epoxidized palm oil on the mechanical and morphological



properties of a PLA–PCL blend, *Res. Chem. Intermed.*, 2014, **40**(2), 689–698.

136 Q. Chen, Q. J. Shan, C. C. Tong, *et al.* Influence of reactive blending temperature on impact toughness and phase morphologies of PLA ternary blend system containing magnesium ionomer, *J. Appl. Polym. Sci.*, 2019, **136**, 47682.

137 V. Nagarajan, A. K. Mohanty and M. Misra, Blends of polylactic acid with thermoplastic copolyester elastomer: effect of functionalized terpolymer type on reactive toughening, *Polym. Eng. Sci.*, 2018, **58**(3), 280–290.

138 L. Zhao, J. Su, J. Han, *et al.* Optimizing the balance between stiffness and flexibility by tuning the compatibility of a poly(lactic acid)/ethylene copolymer, *RSC Adv.*, 2017, **7**(37), 23065–23072.

139 W. Dong, F. Jiang, L. Zhao, *et al.* PLLA microalloys versus PLLA nanoalloys: preparation, morphologies, and properties, *ACS Appl. Mater. Interfaces*, 2012, **4**(7), 3667–3675.

140 Y. P. Hao, H. H. Ge, L. J. Han, *et al.* Thermal and mechanical properties of polylactide toughened with a butyl acrylate-ethyl acrylate-glycidyl methacrylate copolymer, *Chin. J. Polym. Sci.*, 2013, **31**(11), 1519–1527.

141 Y. Feng, G. Zhao, J. Yin, *et al.* Reactive compatibilization of high-impact poly(lactic acid)/ethylene copolymer blends catalyzed by N,N-dimethylstearylamine, *Polym. Int.*, 2014, **63**(7), 1263–1269.

142 H. T. Oyama, Super-tough poly(lactic acid) materials: reactive blending with ethylene copolymer, *Polymer*, 2009, **50**(3), 747–751.

143 L. Deng, C. Xu, X. Wang, *et al.* Supertoughened polylactide binary blend with high heat deflection temperature achieved by thermal annealing above the glass transition temperature, *ACS Sustainable Chem. Eng.*, 2017, **6**(1), 480–490.

144 H. Liu, L. Guo, X. Guo, *et al.* Effects of reactive blending temperature on impact toughness of poly(lactic acid) ternary blends, *Polymer*, 2012, **53**(2), 272–276.

145 P. Martin, J. Devaux, R. Legras, *et al.* Competitive reactions during compatibilization of blends of polybutyleneterephthalate with epoxide-containing rubber, *Polymer*, 2001, **42**(6), 2463–2478.

146 P. Martin, C. Maquet, R. Legras, *et al.* Particle-in-particle morphology in reactively compatibilized poly(butylene terephthalate)/epoxide-containing rubber blends, *Polymer*, 2004, **45**(10), 3277–3284.

147 P. Martin, C. Maquet, R. Legras, *et al.* Conjugated effects of the compatibilization and the dynamic vulcanization on the phase inversion behavior in poly(butylene terephthalate)/epoxide-containing rubber reactive polymer blends, *Polymer*, 2004, **45**(15), 5111–5125.

148 Y. Yuryev, A. K. Mohanty and M. Misra, A New Approach to Supertough Poly(lactic acid): A High Temperature Reactive Blending, *Macromol. Mater. Eng.*, 2016, **301**(12), 1443–1453.

149 H. Liu, F. Chen, B. Liu, *et al.* Super Toughened Poly(lactic acid) Ternary Blends by Simultaneous Dynamic Vulcanization and Interfacial Compatibilization, *Macromolecules*, 2010, **43**(14), 6058–6066.

150 H. Liu, W. Song, F. Chen, *et al.* Interaction of Microstructure and Interfacial Adhesion on Impact Performance of Polylactide (PLA) Ternary Blends, *Macromolecules*, 2011, **44**(6), 1513–1522.

151 W. Song, H. Liu, C. Feng, *et al.* Effects of ionomer characteristics on reactions and properties of poly(lactic acid) ternary blends prepared by reactive blending, *Polymer*, 2012, **53**(12), 2476–2484.

152 H. Liu, X. Guo, W. Song, *et al.* Effects of Metal Ion Type on Ionomer-Assisted Reactive Toughening of Poly(lactic acid), *Ind. Eng. Chem. Res.*, 2013, **52**(13), 4787–4793.

153 T. H. Zhao, W. Q. Yuan, Y. D. Li, *et al.* Relating Chemical Structure to Toughness via Morphology Control in Fully Sustainable Sebatic Acid Cured Epoxidized Soybean Oil Toughened Polylactide Blends, *Macromolecules*, 2018, **51**(5), 2027–2037.

154 X. Zhang, Y. Li, L. Han, *et al.* Improvement in toughness and crystallization of poly(L-lactic acid) by melt blending with ethylene/methyl acrylate/glycidyl methacrylate terpolymer, *Polym. Eng. Sci.*, 2013, **53**(12), 2498–2508.

155 Y. L. Feng, Y. X. Hu, J. H. Yin, *et al.* High impact poly(lactic acid)/poly(ethylene octene) blends prepared by reactive blending, *Polym. Eng. Sci.*, 2013, **53**(2), 389–396.

156 L. Zhou, G. Zhao, Y. Feng, *et al.* Toughening polylactide with polyether-block-amide and thermoplastic starch acetate: influence of starch esterification degree, *Carbohydr. Polym.*, 2015, **127**, 79–85.

157 Z. Su, Q. Li, Y. Liu, *et al.* Compatibility and phase structure of binary blends of poly(lactic acid) and glycidyl methacrylate grafted poly(ethylene octane), *Eur. Polym. J.*, 2009, **45**(8), 2428–2433.

158 S. Sun, M. Zhang, H. Zhang, *et al.* Polylactide toughening with epoxy-functionalized grafted acrylonitrile–butadiene–styrene particles, *J. Appl. Polym. Sci.*, 2011, **122**(5), 2992–2999.

159 Y. Hao, H. Liang, J. Bian, *et al.* Toughening of polylactide with epoxy-functionalized methyl methacrylate–butadiene copolymer, *Polym. Int.*, 2014, **63**(4), 660–666.

160 N. Wu, H. Zhang and G. Fu, Super-tough Poly(lactide) Thermoplastic Vulcanizates Based on Modified Natural Rubber, *ACS Sustainable Chem. Eng.*, 2017, **5**(1), 78–84.

161 W. Dong, X. Cao and Y. Li, High-performance biosourced poly(lactic acid)/polyamide 11 blends with controlled salami structure, *Polym. Int.*, 2014, **63**(6), 1094–1100.

162 X. L. Yu, X. Wang, Z. Zhang, *et al.* High-performance fully bio-based poly(lactic acid)/polyamide11 (PLA/PA11) blends by reactive blending with multi-functionalized epoxy, *Polym. Test.*, 2019, **78**, 105980.

163 Y. Luo, Y. Ju, H. Bai, *et al.* Tailor-Made Dispersion and Distribution of Stereocomplex Crystallites in poly(L-lactide)/Elastomer Blends toward Largely Enhanced Crystallization Rate and Impact Toughness, *J. Phys. Chem. B*, 2017, **121**(25), 6271–6279.

164 K. Hashima, S. Nishitsuji and T. Inoue, Structure-properties of super-tough PLA alloy with excellent heat resistance, *Polymer*, 2010, **51**(17), 3934–3939.



165 W. Meng, Z. Wu, W. Ke, *et al.* Simultaneous the thermodynamics favorable compatibility and morphology to achieve excellent comprehensive mechanics in PLA/OBC blend, *Polymer*, 2014, **55**(24), 6409–6417.

166 N. Wu and H. Zhang, Mechanical properties and phase morphology of super-tough PLA/PBAT/EMA-GMA multicomponent blends, *Mater. Lett.*, 2017, **192**, 17–20.

167 X. Wang, S. Peng, H. Chen, *et al.* Mechanical properties, rheological behaviors, and phase morphologies of high-toughness PLA/PBAT blends by in situ reactive compatibilization, *Composites, Part B*, 2019, 107028.

168 K. Zhang, V. Nagarajan, M. Misra, *et al.* Supertoughened renewable PLA reactive multiphase blends system: phase morphology and performance, *ACS Appl. Mater. Interfaces*, 2014, **6**(15), 12436–12448.

169 D. Wang, Y. Li, X. M. Xie, *et al.* Compatibilization and morphology development of immiscible ternary polymer blends, *Polymer*, 2011, **52**(1), 191–200.

170 M. Asgari and M. Masoomi, Thermal and impact study of PP/PET fibre composites compatibilized with glycidyl methacrylate and maleic anhydride, *Composites, Part B*, 2012, **43**(3), 1164–1170.

171 K. S. Anderson, S. H. Lim and M. A. Hillmyer, Toughening of polylactide by melt blending with linear low-density polyethylene, *J. Appl. Polym. Sci.*, 2003, **89**(14), 3757–3768.

172 K. S. Anderson and M. A. Hillmyer, The influence of block copolymer microstructure on the toughness of compatibilized polylactide/polyethylene blends, *Polymer*, 2004, **45**(26), 8809–8823.

173 P. Maa, J. G. P. Goossens, A. B. Spoelstra, *et al.* Toughening of poly(lactic acid) by ethylene–vinyl acetate copolymer with different vinyl acetate contents, *Eur. Polym. J.*, 2012, **48**(1), 146–154.

174 P. Ma, P. Xu, W. Liu, *et al.* Bio-based poly(lactide)/ethylene-co-vinyl acetate thermoplastic vulcanizates by dynamic crosslinking: structure vs. property, *RSC Adv.*, 2015, **5**(21), 15962–15968.

175 P. Ma, P. Xu, Y. Zhai, *et al.* Biobased Poly(lactide)/ethylene-co-vinyl Acetate Thermoplastic Vulcanizates: Morphology Evolution, Superior Properties, and Partial Degradability, *ACS Sustainable Chem. Eng.*, 2015, **3**(9), 2211–2219.

176 R. K. Singla, S. N. Maiti and A. K. Ghosh, Fabrication of super tough poly(lactic acid)/ethylene-co-vinyl-acetate blends via a melt recirculation approach: static-short term mechanical and morphological interpretation, *RSC Adv.*, 2016, **6**(18), 14580–14588.

177 P. Ma, D. G. Hristova-Bogaerds, P. Schmit, *et al.* Tailoring the morphology and properties of poly(lactic acid)/poly(ethylene)-co-(vinyl acetate)/starch blends via reactive compatibilization, *Polym. Int.*, 2012, **61**(8), 1284–1293.

178 W. U. Li, Y. E. Zhang, D. Wu, *et al.* The Effect of Core–Shell Ratio of Acrylic Impact Modifier on Toughening PLA, *Adv. Polym. Technol.*, 2017, **36**(4), 491–501.

179 H. Liang, Y. Hao, J. Bian, *et al.* Assessment of miscibility, crystallization behaviors, and toughening mechanism of polylactide/acrylate copolymer blends, *Polym. Eng. Sci.*, 2015, **55**(2), 386–396.

180 X. G. Ge, S. George, S. Law, *et al.* Mechanical Properties and Morphology of Polylactide Composites with Acrylic Impact Modifier, *J. Macromol. Sci., Part B: Phys.*, 2011, **50**(11), 2070–2083.

181 H. Zhang, N. Liu, X. Ran, *et al.* Toughening of polylactide by melt blending with methyl methacrylate–butadiene–styrene copolymer, *J. Appl. Polym. Sci.*, 2012, **125**(S2), E550–E561.

182 H. Fang, F. Jiang, Q. Wu, *et al.* Supertough polylactide materials prepared through in situ reactive blending with PEG-based diacrylate monomer, *ACS Appl. Mater. Interfaces*, 2014, **6**(16), 13552–13563.

183 H. Zhang, J. Fang, H. Ge, *et al.* Thermal, mechanical, and rheological properties of polylactide/poly (1,2-propylene glycol adipate), *Polym. Eng. Sci.*, 2013, **53**(1), 112–118.

184 G. Kfouri, F. Hassouna, J. M. Raquez, *et al.* Tunable and Durable Toughening of Polylactide Materials Via Reactive Extrusion, *Macromol. Mater. Eng.*, 2014, **299**(5), 583–595.

185 G. Kfouri, J. Raquez, F. Hassouna, *et al.* Toughening of poly(lactide) using polyethylene glycol methyl ether acrylate: reactive versus physical blending, *Polym. Eng. Sci.*, 2015, **55**(6), 1408–1419.

186 S. R. Rathi, E. B. Coughlin, S. L. Hsu, *et al.* Effect of midblock on the morphology and properties of blends of ABA triblock copolymers of PDLA-mid-block-PDLA with PLLA, *Polymer*, 2012, **53**(14), 3008–3016.

187 M. Pluta and E. Piorkowska, Tough and transparent blends of polylactide with block copolymers of ethylene glycol and propylene glycol, *Polym. Test.*, 2015, **41**(1), 209–218.

188 R. Y. Bao, W. R. Jiang, Z. Y. Liu, *et al.* Balanced strength and ductility improvement of in situ crosslinked polylactide/poly(ethylene terephthalate glycol) blends, *RSC Adv.*, 2015, **5**(44), 34821–34830.

189 L. Lin, C. Deng, G. P. Lin, *et al.* Super Toughened and High Heat-Resistant Poly(Lactic Acid) (PLA)-Based Blends by Enhancing Interfacial Bonding and PLA Phase Crystallization, *Ind. Eng. Chem. Res.*, 2015, **54**(21), 5643–5655.

190 W. Dong, M. He, H. Wang, *et al.* PLLA/ABS Blends Compatibilized by Reactive Comb Polymers: Double Tg Depression and Significantly Improved Toughness, *ACS Sustainable Chem. Eng.*, 2015, **3**(10), 2542–2550.

191 P. Jariyasakoolroj, K. Tashiro, H. Wang, *et al.* Isotropically small crystalline lamellae induced by high biaxial-stretching rate as a key microstructure for super-tough polylactide film, *Polymer*, 2015, **68**, 234–245.

192 M. Bing, J. Deng, Q. Liu, *et al.* Transparent and ductile poly(lactic acid)/poly(butyl acrylate) (PBA) blends: structure and properties, *Eur. Polym. J.*, 2012, **48**(1), 127–135.

193 S. Ishida, R. Nagasaki, K. Chino, *et al.* Toughening of poly(L-lactide) by melt blending with rubbers, *J. Appl. Polym. Sci.*, 2009, **113**(1), 558–566.

194 P. Juntuek, C. Ruksakulpiwat, P. Chumsamrong, *et al.* Effect of glycidyl methacrylate-grafted natural rubber on physical properties of polylactic acid and natural rubber blends, *J. Appl. Polym. Sci.*, 2012, **125**(1), 745–754.



195 V. Tanrattanakul and P. Bunkaew, Effect of different plasticizers on the properties of bio-based thermoplastic elastomer containing poly(lactic acid) and natural rubber, *eXPRESS Polym. Lett.*, 2014, **8**(6), 387–396.

196 M. Maroufkhani, A. A. Katbab, W. Liu, *et al.* Polylactide (PLA) and acrylonitrile butadiene rubber (NBR) blends: the effect of ACN content on morphology, compatibility and mechanical properties, *Polymer*, 2017, **115**, 37–44.

197 U. Meekum and A. Khiansanoi, PLA and single component silicone rubber blends for sub-zero temperature blown film packaging applications, *Results Phys.*, 2018, **9**, 1127–1135.

198 Q. Zhao, D. Yu, B. Yang, *et al.* Highly efficient toughening effect of ultrafine full-vulcanized powdered rubber on poly(lactic acid)(PLA), *Polym. Test.*, 2013, **32**(2), 299–305.

199 C. Zhang, Y. Huang, C. Luo, *et al.* Enhanced ductility of polylactide materials: Reactive blending with pre-hot sheared natural rubber, *J. Polym. Res.*, 2013, **20**(4), 121–129.

200 N. Bitinis, R. Verdejo, P. Cassagnau, *et al.* Structure and properties of polylactide/natural rubber blends, *Mater. Chem. Phys.*, 2011, **129**(3), 823–831.

201 N. Bitinis, R. Verdejo, E. M. Maya, *et al.* Physicochemical properties of organoclay filled polylactic acid/natural rubber blend bionanocomposites, *Compos. Sci. Technol.*, 2012, **72**(2), 305–313.

202 N. Bitinis, A. Sanz, A. Nogales, *et al.* Deformation mechanisms in polylactic acid/natural rubber/organoclay bionanocomposites as revealed by synchrotron X-ray scattering, *Soft Matter*, 2012, **8**(34), 8990–8997.

203 Y. Chen, K. Chen, Y. Wang, *et al.* Biobased Heat-Triggered Shape-Memory Polymers Based on Polylactide/Epoxydized Natural Rubber Blend System Fabricated via Peroxide-Induced Dynamic Vulcanization: Co-continuous Phase Structure, Shape Memory Behavior, and Interfacial Compatibilization, *Ind. Eng. Chem. Res.*, 2015, **54**(35), 8723–8731.

204 Y. Chen, K. Chen, Y. Wang, *et al.* Biobased Heat-Triggered Shape-Memory Polymers Based on Polylactide/Epoxydized Natural Rubber Blend System Fabricated via Peroxide-Induced Dynamic Vulcanization: Co-continuous Phase Structure, Shape Memory Behavior, and Interfacial Compatibilization, *Ind. Eng. Chem. Res.*, 2015, **54**(35), 8723–8731.

205 Y. Chen, D. Yuan and C. Xu, Dynamically Vulcanized Biobased Polylactide/Natural Rubber Blend Material with Continuous Cross-Linked Rubber Phase, *ACS Appl. Mater. Interfaces*, 2014, **6**(6), 3811–3816.

206 D. Yuan, C. Xu, Z. Chen, *et al.* Crosslinked bicontinuous biobased polylactide/natural rubber materials: Super toughness, “net-like”-structure of NR phase and excellent interfacial adhesion, *Polym. Test.*, 2014, **38**, 73–80.

207 D. Yuan, K. Chen, C. Xu, *et al.* Crosslinked bicontinuous biobased PLA/NR blends via dynamic vulcanization using different curing systems, *Carbohydr. Polym.*, 2014, **113**, 438–445.

208 Y. Wang, K. Chen, C. Xu, *et al.* Supertoughened biobased poly(lactic acid)-epoxydized natural rubber thermoplastic vulcanizates: fabrication, co-continuous phase structure, interfacial in situ compatibilization, and toughening mechanism, *J. Phys. Chem. B*, 2015, **119**(36), 12138–12146.

209 L. Liu, J. Hou, L. Wang, *et al.* Role of Dicumyl Peroxide on Toughening PLLA via dynamic vulcanization, *Ind. Eng. Chem. Res.*, 2016, **55**(37), 9907–9914.

210 A. F. Yee and R. A. Pearson, Toughening mechanisms in elastomer-modified epoxies-part 1 mechanical studies, *J. Mater. Sci.*, 1986, **21**(7), 2462–2474.

211 M. E. J. Dekkers, S. Y. Hobbs and V. H. Watkins, Toughened blends of poly(butylene terephthalate) and BPA polycarbonate, part1 morphology, *J. Mater. Sci.*, 1988, **23**(4), 1219–1224.

212 R. Bagheri and R. A. Pearson, Role of particle cavitation in rubber-toughened epoxies: 1. Microvoid toughening, *Polymer*, 1996, **37**(20), 4529–4538.

213 D. Dompas, G. Groeninckx, M. Isogawa, *et al.* Toughening behaviour of rubber-modified thermoplastic polymers involving very small rubber particles: 2. Rubber cavitation behaviour in poly(vinyl chloride)/methyl methacrylate-butadiene-styrene graft copolymer blends, *Polymer*, 1994, **35**(22), 4750–4759.

214 J. Xu and B. H. Guo, Poly(butylene succinate) and its copolymers: research, development and industrialization, *Biotechnol. J.*, 2010, **5**(11), 1149–1163.

215 J. W. Rhim, H. M. Park and C. S. Ha, Bio-nanocomposites for food packaging applications, *Prog. Polym. Sci.*, 2013, **38**(10–11), 1629–1652.

216 F. Elena, P. Debora, I. Antonio, *et al.* Processing Conditions, Thermal and Mechanical Responses of Stretchable Poly(Lactic Acid)/Poly (Butylene Succinate) Films, *Materials*, 2017, **10**(7), 809.

217 W. Phetwarotai, H. Maneechot, E. Kalkornsurapranee, *et al.* Thermal behaviors and characteristics of polylactide/poly(butylene succinate) blend films via reactive compatibilization and plasticization, *Polym. Adv. Technol.*, 2018, **29**(7), 2121–2133.

218 X. Zhang and Y. Zhang, Reinforcement effect of poly(butylene succinate) (PBS)-grafted cellulose nanocrystal on toughened PBS/polylactic acid blends, *Carbohydr. Polym.*, 2016, **140**, 374–382.

219 R. Wang, S. Wang, Y. Zhang, *et al.* Toughening modification of PLLA/PBS blends via in situ compatibilization, *Polym. Eng. Sci.*, 2009, **49**(1), 26–33.

220 D. Ji, Z. Liu, X. Lan, *et al.* Morphology, rheology, crystallization behavior, and mechanical properties of poly(lactic acid)/poly(butylene succinate)/dicumyl peroxide reactive blends, *J. Appl. Polym. Sci.*, 2014, **131**(3), 39580.

221 M. Harada, T. Ohya, K. Iida, *et al.* Increased impact strength of biodegradable poly(lactic acid)/poly(butylene succinate) blend composites by using isocyanate as a reactive processing agent, *J. Appl. Polym. Sci.*, 2007, **106**(3), 1813–1820.

222 O. Persenaire, R. Quintana, Y. Lemmouchi, *et al.* Reactive compatibilization of poly(l-lactide)/poly(butylene succinate) blends through polyester maleation: from materials to properties, *Polym. Int.*, 2014, **63**(9), 1724–1731.



223 M. Shibata, Y. Inoue and M. Miyoshi, Mechanical properties, morphology, and crystallization behavior of blends of poly(*l*-lactide) with poly(butylene succinate-co-lactate) and poly (butylene succinate), *Polymer*, 2006, **47**(10), 3557–3564.

224 M. Shibata, N. Teramoto and Y. Inoue, Mechanical properties, morphologies, and crystallization behavior of plasticized poly(*l*-lactide)/poly(butylene succinate-co-L-lactate) blends, *Polymer*, 2007, **48**(9), 2768–2777.

225 P. A. Palsikowski, C. N. Kuchnir, I. F. Pinheiro, *et al.* Biodegradation in Soil of PLA/PBAT Blends Compatibilized with Chain Extender, *J. Polym. Environ.*, 2018, **26**(1), 330–341.

226 S. Zhou, H. Huang, X. Ji, *et al.* Super-Robust Polylactide Barrier Films by Building Densely Oriented Lamellae Incorporated with Ductile *in Situ* Nanofibrils of Poly(butylene adipate-co-terephthalate), *ACS Appl. Mater. Interfaces*, 2016, **8**(12), 8096–8109.

227 L. Jiang, M. P. Wolcott and J. Zhang, Study of Biodegradable Polylactide/Poly(butylene adipate-co-terephthalate) Blends, *Biomacromolecules*, 2006, **7**(1), 199–207.

228 S. Lin, W. Guo, C. Chen, *et al.* Mechanical properties and morphology of biodegradable poly(lactic acid)/poly(butylene adipate-co-terephthalate) blends compatibilized by transesterification, *Mater. Des.*, 2012, **36**, 604–608.

229 K. Li, J. Peng, L. S. Turng, *et al.* Dynamic rheological behavior and morphology of polylactide/poly(butylene adipate-co-terephthalate) blends with various composition ratios, *Adv. Polym. Technol.*, 2011, **30**(2), 150–157.

230 L. Jiang, M. P. Wolcott and J. Zhang, Study of Biodegradable Polylactide/Poly(butylene adipate-co-terephthalate) Blends, *Biomacromolecules*, 2006, **7**(1), 199–207.

231 W. Dong, B. Zou, P. Ma, *et al.* Influence of phthalic anhydride and bioxazoline on the mechanical and morphological properties of biodegradable poly(lactic acid)/poly[(butylene adipate)-co-terephthalate] blends, *Polym. Int.*, 2013, **62**(12), 1783–1790.

232 W. Dong, B. Zou, Y. Yan, *et al.* Effect of Chain-Extenders on the Properties and Hydrolytic Degradation Behavior of the Poly(lactide)/Poly(butylene adipate-co-terephthalate) Blends, *Int. J. Mol. Sci.*, 2013, **14**(10), 20189–20203.

233 R. Al-Ittry, K. Lamnawar and A. Maazouz, Improvement of thermal stability, rheological and mechanical properties of PLA, PBAT and their blends by reactive extrusion with functionalized epoxy, *Polym. Degrad. Stab.*, 2012, **97**(10), 1898–1914.

234 S. Lin, W. Guo, C. Chen, *et al.* Mechanical properties and morphology of biodegradable poly (lactic acid)/poly (butylene adipate-co-terephthalate) blends compatibilized by transesterification, *Mater. Des.*, 2012, **36**, 604–608.

235 P. Ma, X. Cai, Y. Zhang, *et al.* In-situ compatibilization of poly(lactic acid) and poly(butylene adipate-co-terephthalate) blends by using dicumyl peroxide as a free-radical initiator, *Polym. Degrad. Stab.*, 2014, **102**, 145–151.

236 N. Zhang, C. Zeng, L. Wang, *et al.* Preparation and Properties of Biodegradable Poly(lactic acid)/Poly(butylene adipate-co-terephthalate) Blend with Epoxy-Functional Styrene Acrylic Copolymer as Reactive Agent, *J. Polym. Environ.*, 2013, **21**(1), 286–292.

237 M. Labet and W. Thielemans, Synthesis of polycaprolactone: a review, *Chem. Soc. Rev.*, 2009, **38**(12), 3484–3504.

238 I. Fortelny, A. Ujčić, L. Fambri, *et al.* Phase structure, compatibility and toughness of PLA/PCL blends: a review, *Frontiers in Materials*, 2019, **6**, 206.

239 J. Urquijo, G. Guerrica-Echevarria and EguiazaabalJI, Melt processed PLA/PCL blends: Effect of processing method on phase structure, morphology, and mechanical properties, *J. Appl. Polym. Sci.*, 2015, **132**(41), 42641.

240 M. Decol, W. M. Pachekoski and D. Becker, Compatibilization and ultraviolet blocking of PLA/PCL blends via interfacial localization of titanium dioxide nanoparticles, *J. Appl. Polym. Sci.*, 2018, **135**(6), 44849.

241 H. Bai, H. Xiu, J. Gao, *et al.* Tailoring impact toughness of poly(*l*-lactide)/poly( $\epsilon$ -caprolactone) (PLLA/PCL) blends by controlling crystallization of PLLA matrix, *ACS Appl. Mater. Interfaces*, 2012, **4**(2), 897–905.

242 H. Bai, C. Huang, H. Xiu, *et al.* Toughening of poly(*l*-lactide) with poly( $\epsilon$ -caprolactone): Combined effects of matrix crystallization and impact modifier particle size, *Polymer*, 2013, **54**(19), 5257–5266.

243 M. Harada, K. Iida, K. Okamoto, *et al.* Reactive compatibilization of biodegradable poly(lactic acid)/poly( $\epsilon$ -caprolactone) blends with reactive processing agents, *Polym. Eng. Sci.*, 2008, **48**(7), 1359–1368.

244 YuX. ChenH, W. Zhou, *et al.* Highly toughened polylactide (PLA) by reactive blending with novel polycaprolactone-based polyurethane (PCLU) blends, *Polym. Test.*, 2018, **70**, 275–280.

245 Y. Xi, J. Clénet, H. Xu, *et al.* Two Step Extrusion Process: From Thermal Recycling of PHB to Plasticized PLA by Reactive Extrusion Grafting of PHB Degradation Products onto PLA Chains, *Macromolecules*, 2015, **48**(8), 2509–2518.

246 P. Ma, A. B. Spoelstra, P. Schmit, *et al.* Toughening of poly (lactic acid) by poly ( $\beta$ -hydroxybutyrate-co- $\beta$ -hydroxyvalerate) with high  $\beta$ -hydroxyvalerate content, *Eur. Polym. J.*, 2013, **49**(6), 1523–1531.

247 Y. Bian, Toughening mechanism behind intriguing stress-strain curves in tensile tests of highly enhanced compatibilization of biodegradable poly(lactic acid)/poly(3-hydroxybutyrate- co-4-hydroxybutyrate) blends, *RSC Adv.*, 2014, **4**(79), 41722–41733.

248 V. Ojijo and S. S. Ray, Super toughened biodegradable polylactide blends with non-linear copolymer interfacial architecture obtained via facile *in situ* reactive compatibilization, *Polymer*, 2015, **80**, 1–17.

249 V. Ojijo, S. S. Ray and R. Sadiku, Toughening of biodegradable polylactide/poly(butylene succinate-co-adipate) blends via *in situ* reactive compatibilization, *ACS Appl. Mater. Interfaces*, 2013, **5**(10), 4266–4276.



250 V. Ojijo, S. S. Ray and R. Sadiku, Concurrent Enhancement of Multiple Properties in Reactively Processed Nanocomposites of Polylactide/Poly[(butylene succinate)-co-adipate] Blend and Organoclay, *Macromol. Mater. Eng.*, 2014, **299**(5), 596–608.

251 R. Wang, S. Wang and Y. Zhang, Morphology, mechanical properties, and thermal stability of poly(L-lactic acid)/poly(butylene succinate-co-adipate)/silicon dioxide composites, *J. Appl. Polym. Sci.*, 2010, **113**(6), 3630–3637.

252 S. Jacobsen and H. G. Fritz, Filling of poly(lactic acid) with native starch, *Polym. Eng. Sci.*, 1996, **36**(22), 2799–2804.

253 X. Wang, Y. Hu, L. Song, *et al.* Flame retardancy and thermal degradation of intumescence flame retardant poly(lactic acid)/starch biocomposites, *Ind. Eng. Chem. Res.*, 2011, **50**(2), 713–720.

254 P. Jariyasakoolroj and S. Chirachanchai, Silane modified starch for compatible reactive blend with poly(lactic acid), *Carbohydr. Polym.*, 2014, **106**, 255–263.

255 S. Li, J. Xia, Y. Xu, *et al.* Preparation and characterization of Acorn starch/Poly(lactic acid) composites modified with functionalized vegetable oil derivates, *Carbohydr. Polym.*, 2016, **142**, 250–258.

256 N. F. Zaaba and H. Ismail, A review on tensile and morphological properties of poly (lactic acid) (PLA)/thermoplastic starch (TPS) blends, *Polym.-Plast. Technol. Mater.*, 2019, 1–20.

257 Z. Xiong, Y. Yang, J. Feng, *et al.* Preparation and characterization of poly (lactic acid)/starch composites toughened with epoxidized soybean oil, *Carbohydr. Polym.*, 2013, **92**(1), 810–816.

258 C. Xu, X. Luo, X. Lin, *et al.* Preparation and characterization of polylactide/thermoplastic konjac glucomannan blends, *Polymer*, 2009, **50**(15), 3698–3705.

259 O. Jeremy, L. Philippe, R. Jean-Marie, *et al.* Toughening of polylactide by tailoring phase-morphology with P[CL-co-LA] random copolymers as biodegradable impact modifiers, *Eur. Polym. J.*, 2013, **49**(4), 914–922.

260 J. Odent, Y. Habibi, J. M. Raquez, *et al.* Ultra-tough polylactide-based materials synergistically designed in the presence of rubbery  $\epsilon$ -caprolactone-based copolyester and silica nanoparticles, *Compos. Sci. Technol.*, 2013, **84**, 86–91.

261 S. Huang, H. Sun, J. Sun, *et al.* Biodegradable tough blends of poly(L-lactide) and poly(castor oil)-poly(L-lactide) copolymer, *Mater. Lett.*, 2014, **133**, 87–90.

262 X. Li, H. Kang, J. Shen, *et al.* Highly toughened polylactide with novel sliding graft copolymer by in situ reactive compatibilization, crosslinking and chain extension, *Polymer*, 2014, **55**(16), 4313–4323.

263 G. Theryo, F. Jing, L. M. Pitet, *et al.* Tough Polylactide Graft Copolymers, *Macromolecules*, 2010, **43**(18), 7394–7397.

264 J. Karger-Kocsis, O. Gryshchuk and N. Jost, Toughness response of vinyl ester/epoxy-based thermosets of interpenetrating network structure as a function of the epoxy resin formulation: Effects of the cyclohexylene linkage, *J. Appl. Polym. Sci.*, 2003, **88**(8), 2124–2131.

265 L. Zhang, Y. Jiang, Z. Xiong, *et al.* Highly recoverable rosin-based shape memory polyurethanes, *J. Mater. Chem. A*, 2013, **1**(10), 3263–3267.

266 B. Zhang and S. R. Turner, New poly(arylene ether sulfone)s based on 4,4'-(trans-1,4-cyclohexanediylibis(methylene)] bisphenol, *Polymer*, 2013, **54**(17), 4493–4500.

267 W. J. Yoon, S. Y. Hwang, J. M. Koo, *et al.* Synthesis and characteristics of a biobased high-Tg terpolyester of isosorbide, ethylene glycol, and 1,4-cyclohexane dimethanol: effect of ethylene glycol as a chain linker on polymerization, *Macromolecules*, 2013, **46**(18), 7219–7231.

268 L. Zhang, S. S. Shams, Y. Wei, *et al.* Origin of highly recoverable shape memory polyurethanes (SMPUs) with non-planar ring structures: a single molecule force spectroscopy investigation, *J. Mater. Chem. A*, 2014, **2**(47), 20010–20016.

269 J. Qiu, F. Liu, J. Zhang, *et al.* Non-planar ring contained polyester modifying polylactide to pursue high toughness, *Compos. Sci. Technol.*, 2016, **128**, 41–48.

